DEFORMATION AND CRACKING OF PARTIALLY PRESTRESSED CONCRETE BEAMS UNDER STATIC AND CYCLIC FATIGUE LOADING

BY
Muhamed H. Harajli
and
Antoine E. Naaman

August 1984 Report No. UMEE 84R1

Department of Civil Engineering
The University of Michigan
College of Engineering

Ann Arbor, Michigan 48109

Department of Civil Engineering
The University of Michigan

DEFORMATION AND CRACKING OF PARTIALLY PRESTRESSED CONCRETE BEAMS UNDER STATIC AND CYCLIC FATIGUE LOADING

BY
Muhamed H. Harajli
and
Antoine E. Naaman

August 1984 Report No. UMEE 84R1

A Report on a Research Project Sponsored by
The NATIONAL SCIENCE FOUNDATION Grant
CEE-82 11563 and CEE-84 02194

Ann Arbor, Michigan

ABSTRACT

This study was conducted to evaluate the fatigue resistance of partially prestressed concrete beams. All beams were 9in x 4.5in (229x114 mm^2) cross section, 10 ft (3.05 m) long, simply supported, 9 ft (2.74 m) span and loaded in four point bending. Twelve different sets of beams were tested. Each set consisted of 2 identical specimens designed with the same input parameters. One control beam was tested under static load to determine the ultimate load resistance. The second beam was tested under cyclic fatigue loading at a constant load range fluctuating between 40% and 60% of the observed ultimate load capacity of the static specimen. The main input variables were the partial prestressing ratio (PPR) and the reinforcing index ($\bar{\omega}$). Four different levels of PPR and three different levels of $\bar{\omega}$ covering both fully prestressed and fully reinforced were explored.

The six partially prestressed and the three fully reinforced beams survived 5 million cycles without suffering fatigue failure. The three fully prestressed beams which were loaded beyond cracking failed respectively at 1.21, 2.17 and 1.94 million cycles by fracturing of the prestressing strands in the constant moment region. The stress ranges from strain measurements in the strands observed in the early cycles were 10 ksi (68.95 Mpa), 16 ksi (110 Mpa) and 19 ksi (131 Mpa) respectively. Throughout the

test, measurements of deflections, crack widths, curvatures and reinforcement strains were systematically recorded. A comprehensive set of data was obtained in these tests and could be used as a data base for any future studies. A qualitative analysis of these data is also provided.

ACKNOWLEDGEMENT

This research was supported by the National Science Foundation under grants No. CEE 82-11563 and CEE 84-02194 respectively to the University of Illinois at Chicago and to the University of Michigan, with Dr. Michael P. Gaus as program director. The writers are very grateful for that support.

Sincere thanks are due to professor A. Andonian for his advise and constructive comments on all aspects of the data gathering phase.

Also the help of D. Fanella and S. Watcharaumnuay in casting the beam specimens, J. Gramsas in fabricating the various fixtures for the experiment, and L. Jhonson in calibrating the electronic instrumentation is greatly appreciated.

LIST OF FIGURES

Figure		Page
1.1	S-N Curves For Reinforcing Steel	11
1.2	S-N curve For Prestressing Strands	12
2.1	Planned Experimental Program For The Two Working Phases	23
2.2	Beam Dimensions And Steel Lay-Out	24
2.3	Beam Cross Sections	26
2.4	Beam Preparation: (a) Strain Gages Instrumentation, b) Reinforcing Cages, (c) Wood Mold And Prestressing bed	34
2.5	Beam Preparation: (a) Prestressing Operation, (b) Torch Cutting For Strand Release, (c) Cast Beams	38
2.6	Strain Gages 1 Used On The Prestressing Strand 2 Used On The Reinforcing Bars	39
2.7	Typical Strain Gage Mounting On The Prestressing Strands And Reinforcing Bars	39
2.8	Instrumentation: Deflection And Crack Width Measurement	44
2.9	Crack Width Measuring Device	44
2.10	Dial Gage Mounting For Strand Slip Measurement .	45
2.11	Close Up View Of Instrumentation: Deflection, Crack Width and Curvature	46
2.12	Beam Setting In Testing Machine	48
2.13	General Test Setup: Loading Machine And Data Acquisition System	50
2.14	Close Up View Of Test Setup	51
3.1	Typical Beam Failures : PS3, PD1	61
3.2	Typical Beam Failures : PP1D3, PP1S1	62
3.3	Typical Beam Failures : PP2D3	63
3.4	Crack Width Variation With Load At Different PPR:	

(a) $\bar{\omega} = 2/3\omega_{max}$, (b) $\bar{\omega} = \omega_{max}$ 65

3.5 Crack Width Variation Versus Reinforcing Steel Stress At Different PPR: (a) $\bar{\omega} = 1/3\ \omega_{max}$, (b) $\bar{\omega} = 2/3\ \omega_{max}$, (c) $\bar{\omega} = \omega_{max}$ 66

3.6 Effect Of $\bar{\omega}$ On Load-Curvature Relationships: (a) PPR Close to 0.33, (b) PPR Close To 0.67 67

3.7 Comparison Of Observed Fatigue Life With Existing Data 74

3.8 Load-Deflection Curves For Beams: (a) PS2 (Static) (b) PD2 (Cyclic) 75

3.9 Load-Deflection Curves For Beams PS3 (Static) And PD3 (Cyclic) 76

3.10 Load-Deflection Curves For Beams: (a) PP2S2 (Static), (b) PP2D2 (Cyclic) 77

3.11 Load-Deflection Curves For Beams: (a) PP1S2 (Static), (b) PP1D2 (Cyclic) 78

3.12 Load-Deflection Curves For Beams: (a) RS2 (Static) (b) RD2 (Cyclic) 79

3.13 Observed Deflection Versus Number Of Cycles ($\bar{\omega} = 1/3\omega_{max}$) 81

3.14 Observed Deflection Versus Number Of Cycles ($\bar{\omega} = 2/3\omega_{max}$) 82

3.15 Observed Deflection Versus Number Of Cycles ($\bar{\omega} = \omega_{max}$) 83

3.16 Observed Crack Width Versus Number Of Cycles ($\bar{\omega} = 1/3\omega_{max}$) 86

3.17 Observed Crack Width Versus Number Of Cycles ($\bar{\omega} = 2/3\omega_{max}$) 87

3.18 Observed Crack Width Versus Number Of Cycles ($\bar{\omega} = \omega_{max}$) 88

3.19 Variation of Curvature Versus Number Of Cycles For Various Beam Specimens 90

APPENDIX A

A1 Load-Deflection Curves For Beams: (a) PS1 (Static) (b) PD1 (Cyclic) 109

A2 Load-Deflection Curves For Beams: (a) PP2S1 (Static)

(b) PP2D1 (Cyclic) 110

A3 Load-Deflection Curves For Beams: (a) PP2S3 (Static) (b) PP2D3 (Cyclic) 111

A4 Load-Deflection Curves For Beams: (a) PP1S1 (Static) (b) PP1D1 (Cyclic) 112

A5 Load-Deflection Curves For Beams: (a) PP1S3 (Static) (b) PP1D3 (Cyclic) 113

A6 Load-Deflection Curves For Beams: (a) RS1 (static) (b) RD1 (Cyclic) 114

A7 Load-Deflection Curves For Beams: (a) RS3 (Static) (b) RD3 (Cyclic) 115

A8 Load-Deflection Curve Of Beam PP2D1 After 5 Million Cycles In Comparison With Its Control Static Beam (PP2S1) 116

A9 Load-Deflection Curve Of Beam PP2D2 After 5 Million Cycles In Comparison With Its Control Static Beam (PP2S2) 117

A10 Load-Deflection Curve Of Beam PP2D3 After 5 Million Cycles In Comparison With Its Control Static Beam (PP2S3) 118

A11 Load-Deflection Curve Of Beam PP1D1 After 5 Million Cycles In Comparison With Its Control Static Beam (PP1S1) 119

A12 Load-Deflection Curve Of Beam PP1D2 After 5 Million Cycles In Comparison With Its Control Static Beam (PP1S2) 120

A13 Load-Deflection Curve Of Beam PP1D3 After 5 Million Cycles In Comparison With Its Control Static Beam (PP1S3) 121

A14 Load-Deflection Curve Of Beam RD2 After 5 Million Cycles In Comparison With Its Control Static Beam (RS2) 122

A15 Load-Deflection Curve Of Beam RD3 After 5 Million Cycles In Comparison With Its Control Static Beam (RS3) 123

LIST OF TABLES

Table		Page
1.1	Proposed S-N Equations For Prestressing Strands ..	12
2.1	Summary Of Reinforcing Parameters	27
2.2	Concrete Mix Proportions	30
2.3	Stress-Strain Characteristics Of Prestressing Strands	31
3.1	Stresses In the Reinforcement At Time Of Loading .	56
3.2	Comparison Of Observed And Computed Ultimate Moments For All Test Beams	58
3.3	Calculated Concrete Nominal Tensile Stresses and Observed Stress Ranges In The Reinforcement	73
3.4	Measured Crack Spacing And Number Of Cracks	85
3.5	Stresses In The Prestressing And Reinforcing Steel At P_{min} and P_{max}, Cycle No. 1	93
3.6	Stresses In The Prestressing And Reinforcing Steel At P_{min} And P_{max}, Cycle No. 3	94
3.7	Stresses In The Prestressing And Reinforcing Steel At Two Load Levels P_{min} And P_{max} (Static Beams) ..	95
3.8	Deflection And Load Characteristics Of Beams Loaded To Failure After 5 million Cycles	97

APPENDIX B

B1	Ultimate Load Cycle For Beam PP2D1	125
B2	Ultimate Load Cycle For Beam PP2D2	126
B3	Ultimate Load Cycle For Beam PP2D3	127
B4	Ultimate Load Cycle For Beam PP1D1	128
B5	Ultimate Load Cycle For Beam PP1D2	129
B6	Ultimate Load Cycle For Beam PP1D3	130
B7	Ultimate Load Cycle For Beam RD2	131
B8	Ultimate Load Cycle For Beam RD3	132

1S Data For Beam PS1 133
2S Data For Beam PS2 135
3S Data For Beam PS3 137
4S Data For Beam PP2S1 139
5S Data For Beam PP2S2 141
6S Data For Beam PP2S3 143
7S Data For Beam PP1S1 145
8S Data For Beam PP1S2 147
9S Data For Beam PP1S3 149
10S Data For Beam RS1 151
11S Data For Beam RS2 153
12S Data For Beam RS3 155
1D Data For Beam PD1 157
2D Data For Beam PD2 158
3D Data For Beam PD3 160
4D Data For Beam PP2D1 162
5D Data For Beam PP2D2 164
6D Data For Beam PP2D3 166
7D Data For Beam PP1D1 168
8D Data For Beam PP1D2 170
9D Data For Beam PP1D3 172
10D Data For Beam RD1 174
11D Data For Beam RD2 176
12D Data For Beam RD3 178

LIST OF NOTATIONS

A_{ps} = area of prestressing steel

A_s = area of tension reinforcing steel

A'_s = area of compression reinforcing steel

b = width of beam cross section

d = depth of reinforcement

d_{ps} = depth of prestressing steel

d_s = depth of reinforcing steel

f_{ps} = prestressing steel stress

f_{pu} = ultimate strength of prestressing steel

f_s = reinforcing steel stress

f_y = yield stress of reinforcing steel

f'_c = concrete strength

f_{cr} = stress range in the concrete

f_{max} = maximum stress level

f_{min} = minimum stress level

M_u = ultimate moment

M_n = nominal moment

M_L = live load service moment

M_d = dead load service moment

N = number of cycles

PPR = partial prestress ratio

P_{max} = maximum load level in the fatigue load range

P_{min} = minimum load level in the fatigue load range

P_u = ultimate load

S = safe stress range

$\bar{\omega}$ = reinforcing index

ω_{max} = maximum reinforcing index

Δf_{ps} = stress range in the prestressing steel

Δf_s = stress range in the reinforcing steel

$\underline{\Delta} f_{ps}$ = increase in stress in the prestressing steel above zero load level

Δ_u = ultimate deflection

TABLE OF CONTENTS

INTRODUCTION 1

1.1 General 1

1.2 Fatigue in Partially Prestressed Beams 3

1.3 Literature Background 6

1.3.1 Concrete 6

1.3.2 Reinforcing bars 7

1.3.3 Prestressing strands 9

1.3.4 Prestressed and partially prestressed beams . 13

1.4 Objectives and Summary 18

EXPERIMENTAL PROGRAM 21

2.1 Beam Parameters 21

2.1.1 Input variables 21

2.2 Materials 29

2.2.1 Concrete 29

2.2.2 Prestressing steel 30

2.2.3 Reinforcing steel 31

2.3 Beam Fabrication 32

2.3.1 Preparation of reinforcing cages 32

2.3.2 Tensioning procedure 33

2.3.3 Concrete casting 35

2.4 Instrumentation 37

2.4.2 Deflection 40

2.4.3 Crack width 41

2.4.4 Curvature 42

2.4.5 Slip 42

2.4.6 Data acquisition system 43

2.5 Test Setup 47
2.6 Test Procedure 49
2.6.1 Static test 49
2.6.2 Fatigue test 52
TEST RESULTS 54
3.1 Calculation of Effective Prestress 54
3.2 Static Load Test 54
3.2.1 Cracking load 54
3.2.2 Ultimate load 55
3.3 Behavior of Static Test Specimens 57
3.3.1 Load-deflection 57
3.3.2 Crack width 60
3.3.3 Load-curvature 64
3.4 Fatigue Test 69
3.4.1 Fatigue life 69
3.5 Behavior of Fatigue Test Specimens 72
3.5.1 Deflection 72
3.5.2 Cracks and crack width 84
3.5.3 Average curvature 89
3.6 Reinforcement Stresses 91
3.7 Ultimate Load After Cycling 92
OBSERVATIONS AND CONCLUSIONS 98
4.1 Observations 98
4.2 Conclusions 100
LIST OF REFERENCES 102
APPENDIX A 108
APPENDIX B 124

CHAPTER I

INTRODUCTION

1.1 General

Due to the widespread use of concrete structures in different types of applications, fatigue is becoming increasingly an important aspect in design. Fatigue is a process of progressive and irreversible deterioration in the material subjected to repetitive loads. There are several reasons given by the ACI committee 215 (1) to indicate that the fatigue strength of concrete might be an important design consideration; these include:

1. Use of concrete members in different types of applications which undergo continuous repetition of load, such as prestressed concrete in railway and highway bridges, reinforced concrete pavements, marine structures and the like.
2. Widespread use of ultimate strength design procedures and higher strength materials.
3. New recognition of the effects of repeated load on a member, which lead to increase in the crack widths and deflections in comparison to identical static load.

In addition to the reasons mentioned above, the continuously increasing traffiç volume and heavy loads, specially on highway and railway bridges, requires a special attention for and better understanding of the fatigue characteristics of these structures.

Fatigue strength is rarely properly considered in the current design codes and this is also the case for prestressed concrete. Little guidance is given to engineers concerning the design of prestressed concrete members for fatigue. Numerous tests conducted on prestressed strands and reinforcing bars tested freely in air have shown that 1) the stress range, 2) the minimum stress level and 3) the length of the specimen are all factors that influence fatigue life. The stress range was observed to be one of the most important factors in the fatigue life of prestressing strands and reinforcing bars. Every thing else being equal, the higher the stress range the lower is the fatigue life. Most of the experimental tests conducted on structural concrete beams (22-25,29,31,32,34) showed that their fatigue life is mainly governed by the fatigue fracture of the tension reinforcement. Fatigue fracture of the concrete in compression,when the concrete is part of a flexural concrete beam is very rare and not likely to occur. Many of these tests have also indicated that the stress range in the reinforcement resulting from repetitive application of live loads is one of the main factors that dictate the fatigue life of the beam element.

Most of the earlier fatigue tests available in literature on prestressed concrete flexural beams refered to the fictitous nominal tensile stress in the concrete calculated by assuming uncracked section as being an important index for fatigue studies. However it is becoming

increasingly evident that the stress range in the steel is the basic influencing factor to be considered and also the most important factor in controlling the fatigue resistance of structural concrete beams. This is particularly true in the case of partial prestressing.

1.2 Fatigue in Partially Prestressed Beams

Partially prestressed concrete beams are defined here as concrete beams reinforced with a combination of prestressed and non prestressed reinforcement intended to resist flexure. Such beams are generally designed to crack under full service load (dead plus live load). Partially prestressed concrete can offer some advantages over fully reinforced or fully prestressed concrete. Compared to fully reinforced concrete, partial prestressing offer better cracking and deflection control (short and long term) and lesser use of materials; compared to fully prestressed concrete, partial prestressing offers better camber and a higher ductility and energy absorption to failure (54). Improved ductility is an important factor in earthquake resistance design.

Today it is possible to design partially prestressed beams following the same ACI code design philosophy prescribed for reinforced or prestressed concrete, namely: design to satisfy ultimate strength as well as serviceability criteria. Serviceability criteria includes

allowable stresses, cracking, deflection, corrosion and fatigue.

Although a reasonable number of investigations has dealt with the fatigue behavior of reinforcing bars and prestressing strands tested freely in air, little information exists on the fatigue behavior of partially prestressed beams and experimental data are greatly needed. It is generally agreed that a different fatigue life may be observed for a prestressing strand tested freely or as a part of a concrete member. Some of the reasons were summarized in (28) :

a) In a free test the effect of gripping and the effect of strand untwisting may substantially influence the observed fatigue life.

b) Fretting action between the concrete and the strand might reduce the net sectional area of the strand. This effect increases the stress range of the prestressed strand and therefore reduces its fatigue life.

c) Extensive slippage of tendons in pretensioned members due to a possible bond failure will result not only in a higher stress range in the strands but also in excessive crack widths and deflections. This condition will lead to unserviceable conditions hence failure for all practical purposes.

Partially prestressed beams are generally more susceptible to fatigue failure than equivalent reinforced

concrete beams. Naaman (28) explains this characteristics as follows. In fully reinforced and fully prestressed concrete members the stress changes in the concrete and in the steel under the effect of repetitive loads are not critical. This is particularly the case in fully prestressed concrete where the stress change in the prestressing strand is of the order of few ksi. However, in partially prestressed concrete beams, the section is generally uncracked under the sole effect of the dead load and will crack due to first application of live load. Subsequent applications of live loads will lead to cracks opening at the decompression stress which is lesser than the cracking stress. First cracking or subsequent crack opening will shift upward the location of the neutral axis of bending of the section leading to a higher rate of increase in the steel stress and correspondingly in the concrete extreme fiber compression stress (to maintain equilibrium of forces and moments in the section). These repetitive changes in stresses create fatigue damage in the corresponding materials, reduce bond properties at the interface between steel an concrete and lead to substantial increase in crack widths and deflections under service loads.

Because the stress range generated by live loads are believed to be higher for partially prestressed than for fully prestressed or fully reinforced beams, it is expected that the effect of fatigue loading on the corresponding

increase in crack widths and deflections will be more pronounced, hence deserve careful investigation.

1.3 Literature Background

1.3.1 Concrete

Fatigue of concrete is generally influenced by many factors such as range and rate of loading, load history, material properties and environmental conditions (1). The failure of concrete under cyclic fatigue loading results from progressive microcracking which leads to progressive damage in the concrete indicated by the increase in the level of strain at f_{min} and f_{max}. The fatigue failure of concrete, when part of a concrete flexural member, is very unlikely to occur. Computerized analysis on more than 200 partially prestressed beams (27) indicated only 3 possible cases of slabs and hollow core slabs where fatigue of concrete may have been critical.

Tests conducted on plain concrete specimens (4-7) have shown that concrete could sustain about 10 million cycles for a stress range between 0 and 50% of its static strength. The fatigue strength of concrete (stress range) decreases almost linearly with increasing number of cycles when plotted on a semi-log scale. The relation between f_{min}, f_{max}, and N is often expressed in terms of an S-N diagram. However, for the purpose of design, the relation suggested by ACI committee 215 on fatigue of concrete to

achieve at least 10 million cycles (modified Goodman diagram) could be used:

$$f_{cr} = 0.4f'_c - f_{min}/2 \qquad (1.1)$$

where f_{cr} and f'_c are the stress range and the static strength of concrete respectively while f_{min} is the minimum stress level of the concrete in compression.

1.3.2 Reinforcing bars

Reinforcing steel exhibit a good resistance to fatigue. Although fatigue failure of reinforcing bars has not been a controlling factor in the fatigue life of reinforced concrete flexural members, the trend in the concrete structure toward using ultimate strength design approach and higher yield strength reinforcement makes fatigue characteristics of reinforcing bars of more concern to designers.

The most important parameters that influence the fatigue life of reinforcing bars are summarized in a study conducted by the Portland Cement Association (PCA) in 1975 (10). The study was sponsored in part by NCHRP to investigate the fatigue strength of deformed reinforcing steel bars. A total of 353 deformed bars from 5 United states manufacturer were tested. The following important observations were obtained (10) :

1) Stress range, minimum stress, bar diameter, bar grade and bar geometry are all factors that influence the fatigue life of reinforcing bars.

2) The stress range in the reinforcing bar is the primary factor in determining its fatigue life.

3) The lowest stress range at which fatigue fracture occurred in No. 11 bar grade 60 was 21.3 ksi at a minimum stress level equal to 17.5 ksi.

4) Increasing the minimum stress level by 3 ksi was found to be equivalent to changing the stress range by 1 ksi.

5) Every thing else being equal, the fatigue strength of reinforcing bars increases with decreasing bar grade and with increasing yield strength.

6) Transverse lugs and manufacture bar identification marks cause stress concentration at the intersection of the base of transverse lugs and longitudenal ribs induced during the deformation process. The magnitude of this stress concentration depends primarily on the ratio of the lug radius at the base of deformation to its height (r/h). All fatigue fractures in the test were initiated at the base of transverse lug or bar mark.

Based on these test results, the following equation was recommended for design for straight hot-rolled reinforcing bar with no welds and no stress raisers (more severe than deformation meeting ASTM standards (A615)) :

$$f_r = 21 - f_{min}/3 + 8r/h \qquad (1.2)$$

where

f_r = stress range in ksi

f_{min} = minimum stress level in ksi (tension positive)

r/h = ratio of transverse lug base radius to lug height (a value equal to 0.3 is suggested in the absence of any information)

This last formula was adopted by ACI committee 343, 1977 report (11) and currently adopted in AASHTO specifications (3). Typical S-N curves from the PCA test (10) are shown in figure 1.1.

1.3.3 Prestressing strands

ACI committee 215 (1) pointed out that fatigue of prestressing steel and anchorages is generally unlikely to be a critical design factor in uncracked prestressed concret beams. However, fatigue should be considered in prestressed concrete structures to 1) allow provisions for design of cracked sections under service loads and 2) permit the use of prestressing in structures that undergo significant load repetitions and overloads (such as bridges, vibrating equipments and the like).

Based on fatigue studies (13,14,20,21,45), many mathematical equations have been proposed in the technical literature to describe the fatigue characteristics of prestressing strands. A summary of the proposed equations is shown in table 1.1. It could be observed from this table that these equations are expressed in terms of stress range, number of cycles N and minimum stress level f_{min} as being

the most important parameters that influence the fatigue life of the strands. Some other factors might also be important such as type of prestressing steel, steel treatment, anchorage type and degree of bond .

A fatigue life of 2 million cycles for stress relieved strands is considered normal for most applications. A typical stress range versus number of cycles of prestressing strands tested in air collected from various investigations (13,14,15,47) are shown in figure 1.2. Best fit line of data given as a function of stress range versus number of cycles to failure was expressed as follows (60):

$$(S/f_{pu}) = -0.123\log N + 0.87 \qquad (1.3)$$

where

S = maximum safe stress range for a fatigue life of N cycles

f_{pu} = ultimate strength of the prestressing strand

N = number of cycles to failure

It is important to indicate that most fatigue failures in these test data occurred at the grips or occurred because of fretting between a failed wire and adjacent wires in the strands.

Based on a fatigue study of prestressed beams Irwin (19) pointed out that prestressing strands might exhibit an endurance limit at a stress range of about 0.13 f_{pu} at a mean stress level equal to $0.66f_{pu}$. Such values seem quite optimistic in view of more recent results.

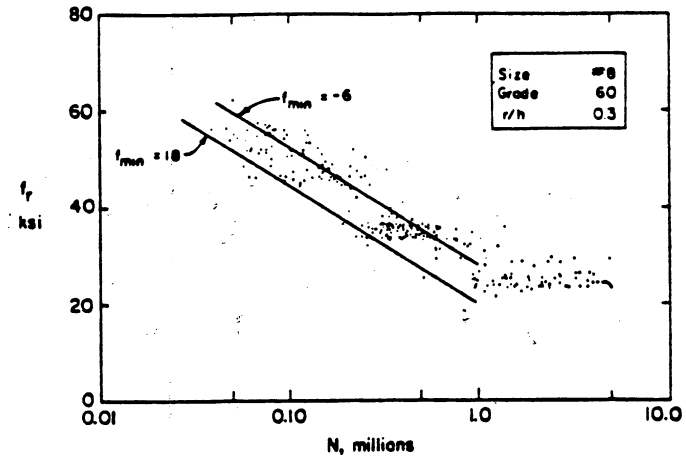

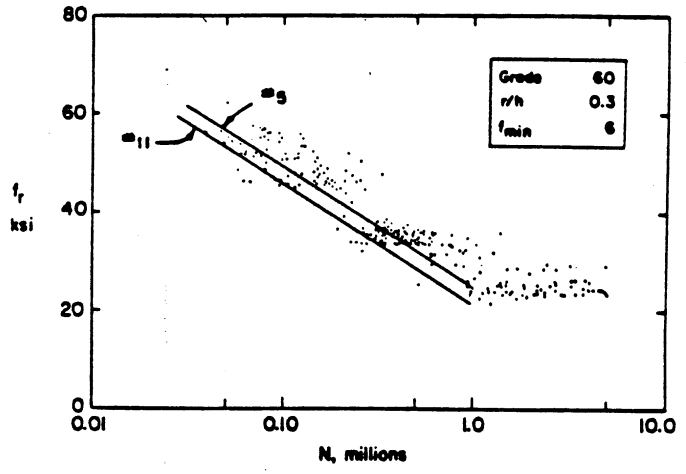

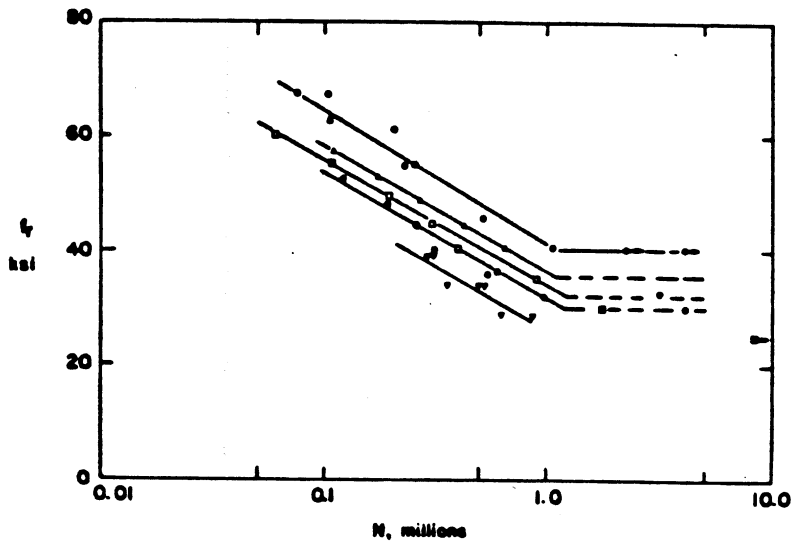

Fig.1.1 S-N Curves For Reinforcing Steel Bars (Ref. 10)

Table 1.1 Proposed S-N Equations For Prestressing Strands

Fisher and Viest (21)	$\text{Log}_{10}N = 9.354 - 00.0423f_r - 0.0102f_{s,min}$ $f_r = f_{s,max} - f_{s,min}$
Warner and Hulsbos (1445)	$\text{Log}_{10}N = 1.4332/R + 5.5212 - 0.0486R$ $R = S_{max} - (0.83S_{min} + 23)$ valid for $40\% < S_{min} < 60\%$, $0 < R < 15\%$
Hilmes and Ekberg (20)	$S_r = (1640 - 11.5S_{min})N^{-0.320}$ for $40{,}000 < N < 400{,}000$ $S_r = (115.5 - 0.78S_{min})N^{-0.1154}$ for $400{,}000 < N < 4{,}000{,}000$
Van Horn (13)	$\text{Log}_{10}N = 6.356 - 0.1373R_s + 0.00303R_s^2$ $R_s = S_{max} - (1.05S_{min} + 8.0)$ valid for $40\% < S_{min} < 60\%$, $0 < R_s < 20\%$

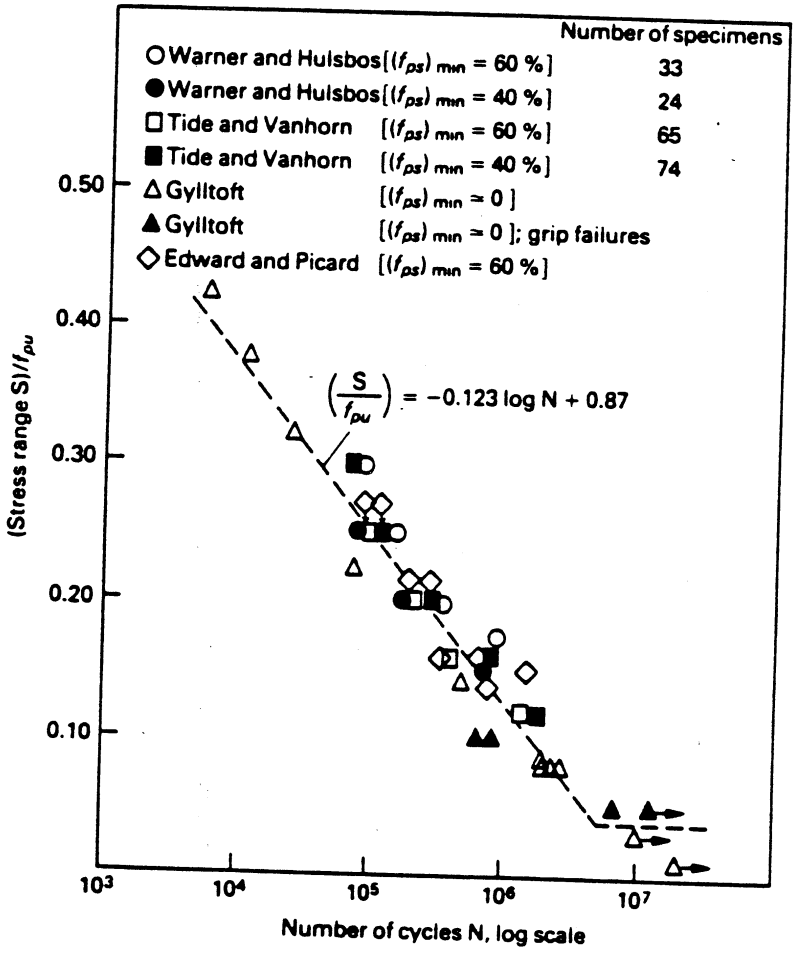

Fig. 1.2 S-N Curve For Prestressing Strands (Ref. 60)

For design purposes, the fatigue requirement in prestressed concrete structures is accounted for by limiting the stress range in the prestressing strands and/or limiting the nominal tensile stress in the concrete under service load. The 1971 FIP (39) suggested a maximum stress range in the prestressing strands equal to $0.15f_{pu}$ at a minimum stress level equal to $0.75f_{pu}$ for a 2 million cycles fatigue life (based on Smith diagram). Recent tests however have shown that the above stress range is on the unsafe side (23). In 1974, ACI committee 215 (1) limited the stress range in prestressing strands to $0.1f_{pu}$. However, recently, the ACI committee suggested that this stress range be lowered.

1.3.4 Prestressed and partially prestressed beams

Ozel and Anderman (24), tested eight 6in x 8in x 20' long beams prestressed with 7/16" strands. Six of the beams were subjected to a constant fatigue load range producing a different nominal tensile stresses in the bottom tension fiber. Five of the beams failed in fatigue by fatigue failure of the prestressing strands. The rate of deflection increase with cyclic load was slightly reduced for the first 30,000 cycles but showed a significant increase prior to failure. Bond failure of the prestressing strand was observed to be insignificant in these tests.

Hanson, Hulsbos and Vanhorn (22), conducted fatigue tests on 6 concrete I beams with 18" overall height and 3" web width prestressed with 270 ksi grade strands. The beams

were simply supported and subjected to a symmetrical two point load. All the six beams were initially overloaded to about 80% of their calculated ultimate load resistance for studying the effect of precracking on the fatigue performance of fully prestressed beams. After overloading, the beams were cycled under fatigue load fluctuating between 19% and 45% up to 2 million cycles producing a nominal tensile stress in the concrete of $5\text{-}6\sqrt{f'_c}$. At the end of 2 million cycles, little structural damage was observed. The maximum fatigue loads were increased to between 48% and 54% to produce a nominal tensile stress varying between $8\sqrt{f'_c}$ and $10\sqrt{f'_c}$ until failure. Failure in the beams was partly due to strand fracturing and partly due to failure of shear stirrups. Based on the result of their test they suggested that the nominal tensile stress in the concrete be limited to $6\sqrt{f'_c}$. Also they indicated that the fatigue life of the beams were less than expected from available data on the fatigue life of the strands.

Abeles, Brown and Hu (25), tested 33 fully prestressed small scale flexural beams under different load ranges varying between a minimum load level equal to 30% and a maximum load level equal to 50-90% of the ultimate load capacity of the beams. Slippage of the strands contributed significantly to failure of the beams in these tests. They concluded that strand fatigue life for beams with good bond between the concrete and the strand exceed the fatigue life of strands tested freely in air. However, specimens that

suffered strand slippage showed a tremendous reduction in the fatigue life of the strands. This was attributed to the increase in stress range that result from a decrease in the effective prestress due to slippage.

Rabbat, Kar, Russel and Bruce (23), tested 6 composite full-size type II AASHTO beam specimens, 50' long, with blanketed and draped tendons. The main purpose was to study and compare the behavior of blanketed and draped tendons in prestressed beams under fatigue loading. All specimens were precracked statically prior to fatigue loading. Three beams were cycled under load producing zero tensile stress while the remaining beams were cycled under a load producing $6\sqrt{f'_c}$. Crack former were used for all test specimens. They observed that fatigue life of the beams designed under $6\sqrt{f'_c}$ nominal tensile stress were significantly less than those designed at zero tensile stress. Specimens cycled at zero tensile load survived 5 million cycles while those at $6\sqrt{f'_c}$ failed between 3.2 and 3.7 million cycles by fracturing of the prestressing strands. They concluded that beams designed for $6\sqrt{f'_c}$ nominal tensile stress under full service load could be vulnerable to fatigue failure. The maximum stress range in the strands observed in the 3rd cycle was 12.8 ksi and increased to 20.1 ksi in subsequent cycles before failure. In this test the strands in the beams suffered slippage of different magnitudes for the various test beams.

Dave and Garwood (30), tested 9 I section beams three of which were tested under cyclic fatigue loading. The beams were partially prestressed bonded post tensioned class "3". The fluctuating test load varied between 29% and 58% of the design ultimate load. All beams survived 3 million cycles.

Bennet and dave (29), tested 9 partially prestressed beams under repeated two point loading. The load range varied between around 25% and 50% of the ultimate design moment. All beams survived 3 million cycles except one beam which failed at 2.6 million cycles by fatigue fracturing of the prestressing strand.

Fauchart, Kavyrchine and Trinh (31,32), tested a number of partially prestressed rectangular and T beams from fully prestressed to fully reinforced. All beams were tested under a constant cycle load range with minimum load equal 15% and maximum load equal to 45%-75% of the beam ultimate load capacity. Stresses in the reinforcement were measured by extensometers. Measured and calculated stresses were comparable to within 10% difference. The most important conclusion from their test is that the failure of the test beams by fatigue can be fairly well predicted from the fatigue life of the prestressing strand alone.

Foo and Warner (34), tested 6 pretensioned partially prestressed concrete beams under constant load cycle. All test units were identical and prestressed with 7-wire

strands. Beams were simply supported and loaded at two point load. Deflection and curvature were mostly marked in the early load phase, and became progressively less with increasing number of cycles. Five beams failed in fatigue by successive fracturing of the reinforcing bars and wires in the prestressing strands. They observed that cyclic loading helps in 1) destroying local bond specially around the prestressing strand, 2) extending and widening existing cracks, and 3) initiating new cracks locally. They also concluded that fatigue failure in the prestressed strands or reinforcing bars are equally likely in partially prestressed beams. Also the fatigue performance of reinforcing and prestressing steel is not significantly different from that observed in specimens tested freely in the air.

Mansur (41), tested 12 partially prestressed beams having 12x6 in cross section. All beams were loaded at two point load and were designed to have identical load capacity. The purpose of this test was to examine the effect of post fatigue loading on the ultimate load capacity and deformation of partially prestressed beams. Three different levels of partial prestressing ratio equal to 0, 0.41 and 0.67 respectively were explored. For each level of partial prestressing ratio, 4 beams were tested. One beam was tested under static load to determine its ultimate load capacity, while the remaining three beams were subjected respectively to 11,000, 33,000, and 100,000 cycles prior to the static cycle to failure. Every beam in the fatigue test

was cycled between 10% and 60% of the ultimate load capacity of the static specimen. In these tests, all beams that were preloaded in fatigue were observed to gain strength. The increase in strength was higher for higher values of partial prestressing ratio. Also it was observed that most of the beam deformation (crack width, deflection and curvature) occured in the early stage of cyclic loading.

One of the main drawback of many of the investigations available in the technical literature is the lack of some technical information related to the experiment. Although the observed fatigue life is generally given in all studies, very few investigations give simultaneously information on measured and/or calculated stresses in the reinforcement, basic material properties, crack widths, deflections, and their variation under fatigue. None gives a complete set of data related to the above variables or obtained under the same conditions.

1.4 Objectives and Summary

The objective of this study is to investigate the behavior of partially prestressed concrete rectangular members under cyclic fatigue loading. The particular feature of this study is that a special emphasis was devoted to instrument the beams under load hence providing a complete set of data related to a number of input and output variables. This include materials properties, loads, stresses and strains, curvatures, crack widths, and

deflections under static and cyclic loads. This report describes the first set of tests on rectangular beams. It is expected that the study will be extended to include T beams and hollow core slabs. This report concentrates on providing a complete data base. Analytic models to predict crack width, deflection and fatigue life based on the tests and data described herein are in progress.

A total of 12 sets of beams were tested. The main parameters utilized in this investigation are the reinforcing index $\bar{\omega}$ and the partial prestressing ratio PPR. The reinforcing index is representative of the total tensile force (and/or moment) taken by the steel at ultimate. The partial prestressing ratio is representative of the amount of tensile force or moment taken by the total steel. Four levels of partial prestressing ratios were selected, namely, 0, about 0.33, about 0.67 and 1. The value of PPR, 0 and 1, represent respectively fully reinforced and fully prestressed concrete, while the values of 0.33 and 0.67 represent two different levels of partial prestressing. For every level of partial prestressing ratio, 3 levels of reinforcing index were utilized, namely, about 0.1, 0.2 and 0.3. Two beams were designed for each set of variables. One beam was tested under monotonically increasing load up to failure as a control specimen, while the second beam was tested under high cycle fatigue with a constant load range between 40 and 60% of the ultimate load capacity of the beam tested under static loading. Each beam

in the dynamic series was cycled up to 5 million cycles, or failure, whichever occurred first.

Chapter 2 of this report includes extensive details of the experimental program and the input variables. Chapter 3 present the results of all the static and cyclic tests. This include data on the fatigue life of the members, the variation of deflection, crack width, curvature and stresses in the tension reinforcement under static and fatigue loading. Chapter 4 provides a brief summary of the observations and conclusions.

CHAPTER II

EXPERIMENTAL PROGRAM

2.1 Beam Parameters

2.1.1 Input variables

A flow chart of the planned experimental program is shown in figure 2.1. A rectangular beam cross section was used throughout. Its dimension and span length are shown in figure 2.2. The major variables included the reinforcing index $\bar{\omega}$ and the partial prestressing ratio PPR. For each combination of reinforcing index and partial prestressing ratio, two beams were tested; one beam was tested under static load as a control specimen and the other was tested under fatigue load.

The reinforcing index and partial prestressing ratio were defined as follows :

$$\bar{\omega} = (A_{ps}f_{ps} + A_s f_y - A'_s f_y)/bdf'_c \qquad (2.1)$$

$$PPR = (M_u)_p/(M_u)_{p+s} \qquad (2.2)$$

where

A_{ps}, A_s, A'_s = area of prestressing steel, tension and compression non prestressed steel respectively.

f_{ps}, f_y = stress in the prestressing steel and yield stress of non prestressed stell respectively.

$(M_u)_p$, $(M_u)_{p+s}$ = ultimate moment contribution of the prestressing steel and total steel respectively.

The values of f_{ps} was estimated from prior non-linear analysis. The three target reinforcement indices were respectively $1/3\omega_{max}$, $2/3\omega_{max}$ and ω_{max}, where ω_{max} correspond to the limit between under-reinforced and over reinforced sections. ω_{max} is equal to 0.3 for purely prestressed rectangular section and corresponds approximately to the maximum reinforcement ratio $0.75\rho_{bal}$ for purely reinforced sections (16). The target values of the partial prestressing ratio were 1, 0.33, 0.67 and 0. However, it is not possible to achieve simultaneously, an exact level of reinforcing index, an exact level of partial prestressing ratio and an exactly specified nominal moment resistance. Moreover once theoretical values are arrived at, they can not be achieved exactly in practice because of non continuous sizes in reinforcing bars and strands. Hence trial and error was used for selecting reinforcement areas as close as possible to the theoretical values.

The beams were designed using a specially written computer program for non-linear analysis to calculate the "exact" input variables of the test specimens, namely, $\bar{\omega}$ and PPR, as well as the nominal moment resistance of the beam. The computer program also allowed evaluating the deflection and curvature of the beams under monotonically increasing load thus facilitated planning for the test in advance. The design was also checked using ACI 318-83 (2) approach for designing concrete sections. Beam cross section and steel reinforcement for all beam specimens are shown in

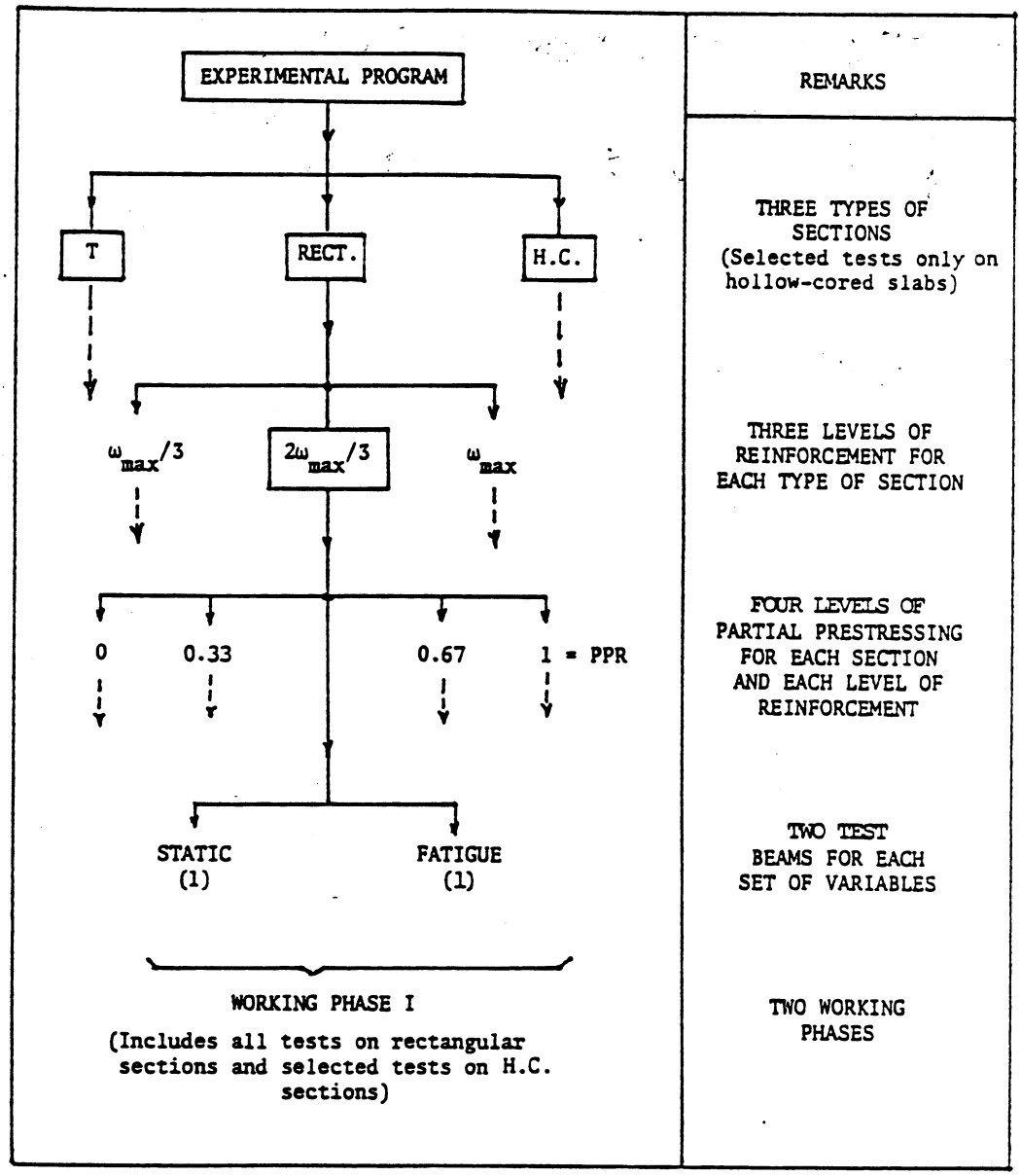

Fig. 2.1 Planned Experimental Program For The Two Working Phases

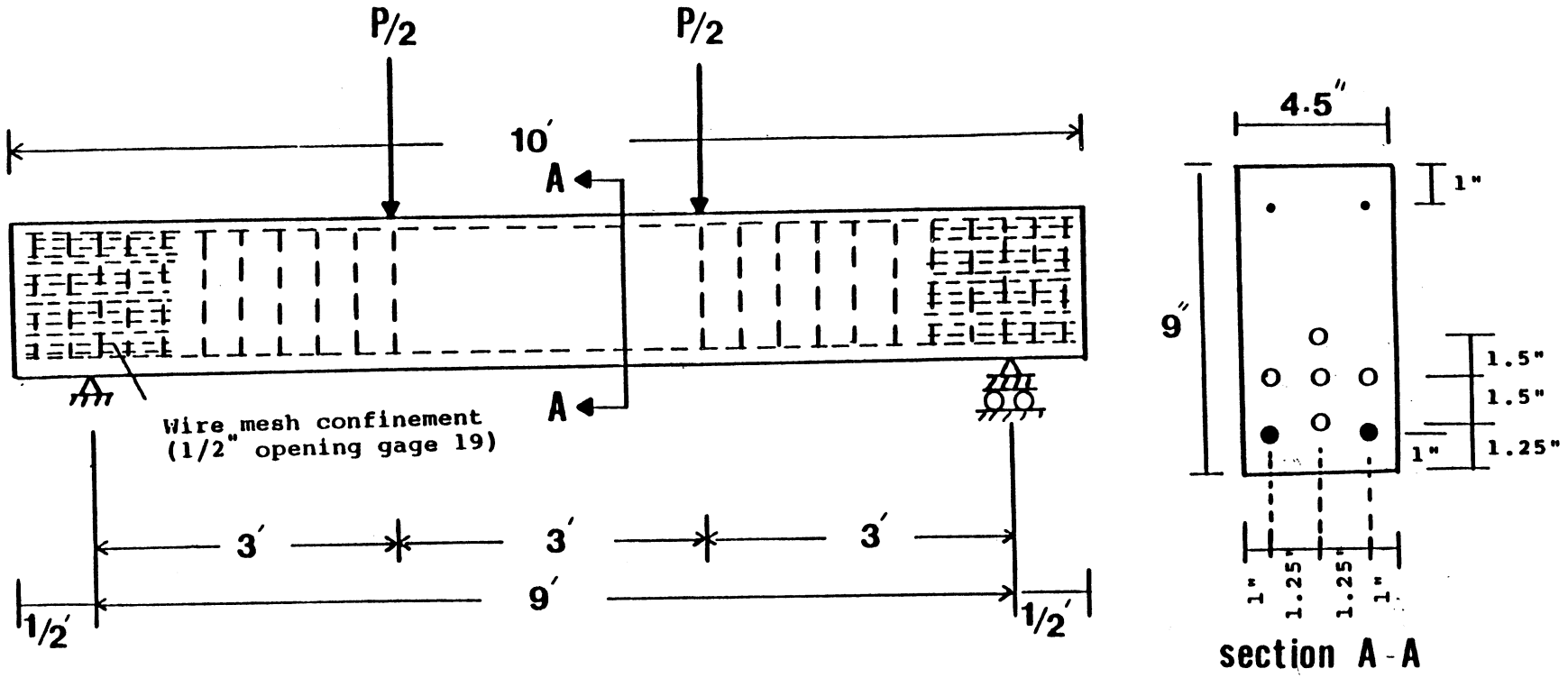

Shear reinforcement : D1 (high yield), A_v = 0.01 in^2/leg
f_y = 140 ksi

Stirrup spacing = 4" for beams with $\bar{\omega}$ = 0.1, 0.2
= 2" for beams with $\bar{\omega}$ = 0.3

O Prestressing strand location

● Reinforcing bar location

Fig. 2.2 Beam Dimensions And Steel Lay-out

figure 2.3. Beams designation with their reinforcement and their corresponding reinforcing indices and partial prestressing ratios are shown in table 2.1.

2.1.2 Cyclic load range

For each beam, two design criteria were used to determine the level of cyclic loading. In all cases the maximum load was selected to generate a maximum moment M_{max}: 1) less than 60% of the predicted nominal moment resistance and 2) less than the moment which would induce a predicted stress in the prestressing strand equal to 95% of its proportional limit stress and a predicted stress in the reinforcing steel less than 90% of its yield strength. Non-linear analysis of the designed specimens in addition to experimental measurement of the tension reinforcement stresses of the static test beams had shown that the first criteria governs for all the beams considered in the experimental program.

Keeping the maximum moment less than 60% of the nominal moment resistance leads to a safety factor against flexural failure of about 1.67, which compares well with the current safety provisions implied in the ACI code, as shown next. Let us Define:

$$M_u = \phi M_n = 1.4M_D + 1.7M_L \qquad (2.3)$$

where the subscripts u,n,D and L refer, respectively, to required strength, nominal strength, dead load and live

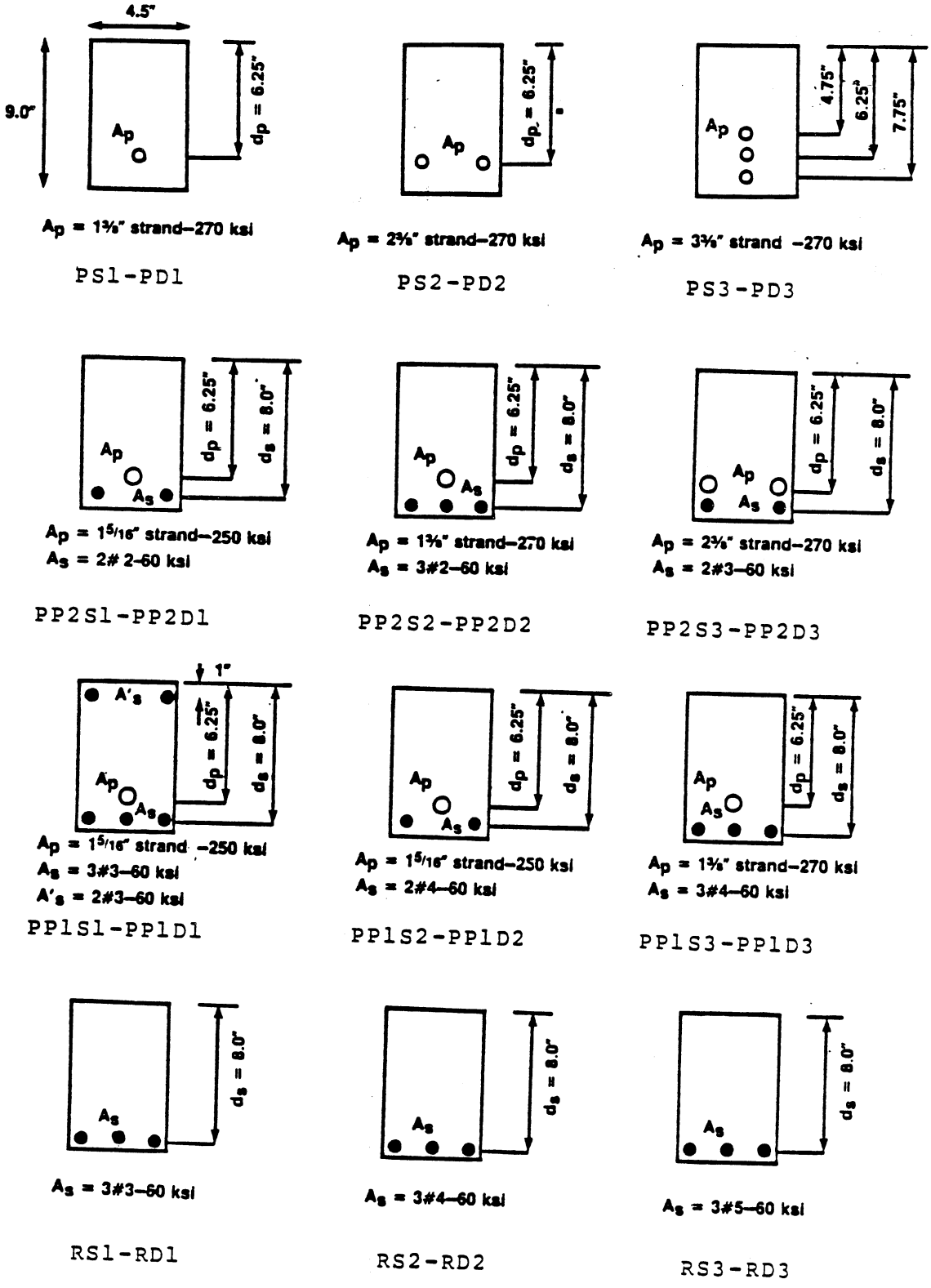

Fig. 2.3 Beam Cross Sections

Table 2.1 Summary Of Reinforcing Parameters

Beam	Prestressing Steel (A_{ps}), in^2	Reinforcing Steel (A_s), in^2	Compressive Steel (A'_s), in^2	f'_c (psi)	$\bar{\omega}$	PPR
PS1	1($\frac{3}{8}$" strand)	0	2 # D1	5570	0.14	1.0
PD1	(0.085)		(0.017)			
PS2	2($\frac{3}{8}$" strand)	0	2 # D1	5300	0.28	1.0
PD2	(0.170)		(0.017)	5660	0.26	
PS3	3($\frac{3}{8}$" strand)	0	2 # D1	5730	0.37	1.0
PD3	(0.255)		(0.017)			
PP2S1	1($\frac{5}{16}$" strand)	2 # 2	2 # D1	6576	0.10	0.62
PP2D1	(0.058)	(0.10)	(0.017)			
PP2S2	1($\frac{3}{8}$" strand)	3 # 2	2 # D1	5290	0.20	0.68
PP2D2	(0.085)	(0.15)	(0.017)			
PP2S3	2($\frac{3}{8}$" strand)	2 # 3	2 # D1	6200	0.30	0.74
PP2D3	(0.170)	(0.22)	(0.017)			
PP1S1	1($\frac{5}{16}$" strand)	3 # 3	2 # 3	6040	0.13	0.33
PP1D1	(0.058)	(0.33)	(0.22)			
PP1S2	1($\frac{5}{16}$" strand)	2 # 4	2 # D1	5806	0.20	0.33
PP1D2	(0.058)	(0.40)	(0.017)			

Table 2.1 (Continue)

Beam	Prestressing Steel (A_{ps}), in^2	Reinforcing Steel (A_s), in^2	Compressive Steel (A'_s), in^2	f'_c (psi)	$\bar{\omega}$	PPR
PP1S3	1($\frac{3}{8}$" strand)	3 # 4	2 # D1	5998	0.30	0.34
PP1D3	(0.085)	(0.60)	(0.017)			
RS1	0	3 # 3	2 # D1	5940	0.12	0
RD1		(0.33)	(0.017)			
RS2	0	3 # 4	2 # D1	7000	0.17	0
RD2		(0.60)	(0.017)	5870	0.20	
RS3	0	3 # 5	2 # D1	7000	0.23	0
RD3		(0.93)	(0.017)	5553	0.29	

Note: P — Fully Prestressed R — Fully Reinforced

PP1 — Partially Prestressed(PPR=0.33) PP2 — Partially Prestressed(PPR=0.67)

S — Static Load D — Dynamic (Cyclic) Load

1,2,3 after S and D represent the level of Reinforcing Index at 0.1,0.2,0.3

f_{pu} = 270 ksi.($\frac{3}{8}$" strand) E_{ps} = 28600 ksi.

f_{pu} = 250 ksi.($\frac{5}{16}$" strand) E_{ps} = 28000ksi

load. The value of ϕ is taken equal to 0.9 for flexure. In equation (2.3), the safety factor on the average is equal to (1.4+1.7)/2x0.9 = 1.72, which is close to the above 1.67.

The minimum load was selected so as the difference between the maximum load and the minimum load is about equal to the full design live load. This leads to a minimum moment of the order of 0.4 M_n as shown next:

Assume:

$$M_{max} = M_D + M_L = M_{min} + M_L = 0.60\ M_n \qquad (2.4)$$

and

$$\phi M_n = 1.4M_D + 1.7M_L = 1.4M_{min} + 1.7M_L \qquad (2.5)$$

in which the minimum moment M_{min}, simulates the dead load moment in a full size member. Using ϕ = 0.9 and replacing M_L by its value from (2.5) into (2.4) leads to M_{min} = 0.4 M_n

Note that for the same magnitude of the fluctuating load, the stress change in the steel depends on the value of the partial prestressing ratio and other design parameters.

2.2 Materials

2.2.1 Concrete

Normal weight concrete was used throughout. The cement used was ASTM type III high-early strength. The aggregate was P stone of maximum size 3/8 inch (10 mm). The sand was masonry type sand. A superplasticizer (Melment) was added in about 0.6% by weight of cement to increase the workability

of the concrete. The mix proportions per cubic yard are shown in table 2.2.

Table 2.2 Concrete Mix Proportions

Cement	795 lbs
Aggregate	1840 lbs
Sand	1358 lbs
Water	36 gallons
Super plasticizer	0.6% of the weight of cement

The mix were designed to achieve a 6000 psi (41.4 Mpa) concrete strength (Actual concrete strengths for the various test specimens obtained at the time of loading are shown in table 2.1).

2.2.2 Prestressing steel

Two types of prestressing steel 7 wire strands was used : 3/8 and 5/16 inch (9.53 and 7.94 mm) in diameter with 270 and 250 ksi (1862 and 1724 Mpa) specified ultimate strength respectively. The reason for using two different types of strands was due to the difficulty in obtaining the desired input variables with one strand size. The strands were supplied by (Florida Wire and Cable Company) and their properties as supplied by the manufacturer are described in table 2.3.

The apparent modulus of elasticity measured in this study from strain gages attached to a single wire of the strand was 33500 and 32850 ksi for the 3/8 and 5/16 inch strands respectively.* These high values are attributed to the fact that the strain gages were attached to one wire which is spirally oriented relative to the longitudinal axis of the strand. Actual moduli are of the order of 28600 ksi (197.2 KN/mm^2) and 28000 ksi (193 KN/mm^2) for the 3/8 and 5/16 inch strand respectively.

Table 2.3 Stress-Strain Proporties of Strands

	3/8" strands	5/16" strands
Ultimate breaking strength (lbs)	23500	14900
Ultimate extension (in/in)	0.0495	0.0495
Force at 1% extension (lb)	21600	13100
Elongation at $0.7f_{pu}$ (in/in)	0.00662	0.00625
Modulus of elasticity (ksi)	28600	28000
Cross sectional area (in^2)	0.085	0.058

2.2.3 Reinforcing steel

The longitudinal bars in the test beams were grade 60 deformed bars with size No.2, No.3, No.4, and No.5. The actual yield stress of the reinforcement varied between 63 ksi (434.4 Mpa) and 77 ksi (531 Mpa) depending on the size

* In converting the prestressing steel apparent strains (obtained from strain gages reading) into real stresses, the apparent strains were first multiplied by a factor equal to 1.171 and 1.173 for the 3/8" and 5/16" respectively, then used in the actual stress-strain curves of the prestressing steel (provided by the Manufacturer) to get the stresses. These factors (1.171 and 1.173) were obtained by dividing the observed apparent modulus of elasticity of the prestressing strands by the modulus of elasticity supplied by the Manufacturer

of the bar. The modulus of elasticity was of the order of 29000 ksi (200 KN/mm^2). Special high strength deformed steel wires (D1 type) supplied by Portland Cement Association (PCA) was used for shear reinforcement. This wire was 0.12 inch (3 mm) in diameter, 0.01 in2 (6.45 mm2) in cross section and had an approximate yield strength of 140 ksi (965 Mpa). A low yield strength wire, (also type D1) of 40 ksi (276 Mpa) yield strength was used in the top and bottom of the beam (where and whenever no longitudinal reinforcement was provided) in order to support the shear reinforcement. This steel was not considered in designing the beam specimens, nor in the analysis of the test data.

2.3 Beam Fabrication

2.3.1 Preparation of reinforcing cages

The reinforcing bars were cut in the laboratory to the required size. Their middle section was prepared for strain gage installation. Shear reinforcement was bent using a special bender and then spot welded, forming a closed type stirrup. The shear and longitudinal steel reinforcement were assembled and tied together. A one foot long wire mesh cage (mesh gauge 19 with 1/2 inch opening) was added at each end to strengthen and stiffen the reinforcing cage. Then strain gages were attached. Additional stirrups were also provided at both ends of the beam to account for any possible bursting or spalling due to overstresses at release of the

pretensioned strands. A photograph of the cages is shown in figure 2.4 b.

Before casting, the cages were placed in an oil coated wood mold inside a prestressing bed. The wood mold was made of 3/4 inch (19 mm) thick ply wood and designed to accommodate 2 beams side by side at one time. The prestressing bed was 12 foot long (3.66 m) clear length, with a capacity to prestress up to 32 strands and 4 beams of the size used in this test. The prestressing bed was specially designed for the purpose of this test and was fabricated by Smedberg Machine and Tool, Inc. Chicago, Illinois. A photograph of the wood mold and prestressing bed is shown in figure 2.4 c. Strand pieces in 16 foot (4.9 m) length, were then inserted into the reinforcement cage, anchored at one end of the prestressing bed and positioned for prestressing. Note that the strands were already instrumented (strain gages attached). (Fig. 2.4 a).

2.3.2 Tensioning procedure

The tension was applied by a 20 ton capacity, 2 inch stroke center hole hydraulic ram, driven by a hand pump. The hydraulic ram was calibrated with a proofing ring before use in order to make correlation between the pressure in the pump, the force transmitted at the head of the ram and into the strand, and also to check the calibration provided by the manufacturer for the pressure gauge. Each strand was pretensioned individually in increments of 2 kips (8.9 KN)

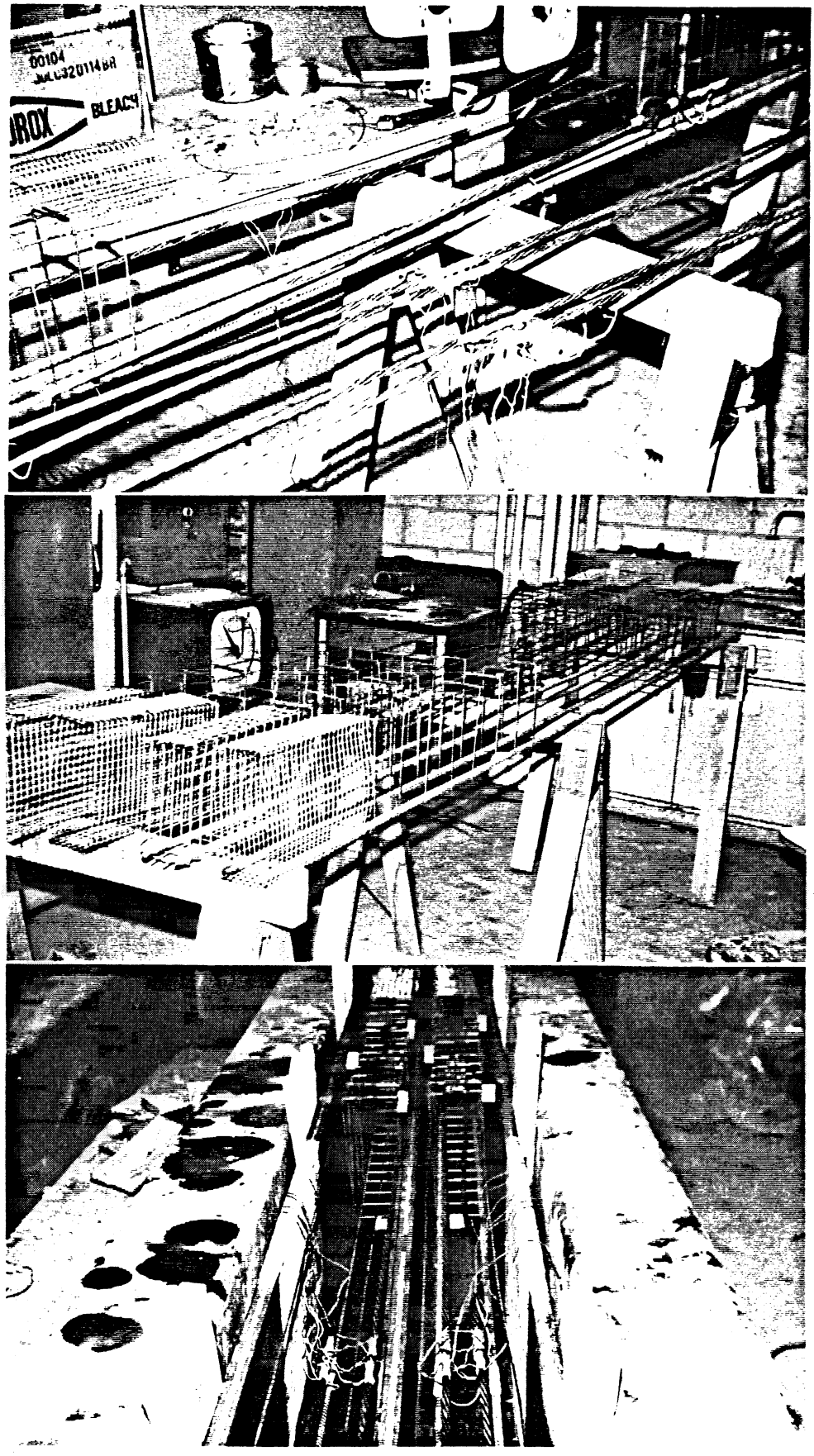

Fig.2.4 Beam Preparation: (a) Strain Gages Instrumentation, (b) Reinforcing Cages, (c) Wood Mold And Prestressing Bed

and strain gages readings monitored by a strain gage indicator was recorded. The tension force was increased until the desired force (70% of strand ultimate strength) on the strand was reached (16100 lbs (71.6 KN) and 10100 lbs (44.9 KN) for the 3/8 and 5/16 inch strand respectively), and the readings from the strain gages were recorded. Then the force was increased by about 750 lbs (3.34 KN) to account for estimated strand seating loss upon anchorage. After anchoring, the strains given by the strain gages were also measured. The initial force in the strand after anchorage was then obtained from the final strain gage reading using the average apparent modulus of elasticity of the two or three strain gages attached to this particular strand. Due to the short length of the prestressed strands (12.7'), the loss of prestress due to strand seating during the anchorage process was substantially high, thus resulting in a low initial prestress for some beam specimens. This problem was minimized for some beams by repeating the prestressing operation twice. A picture of the prestressing operation is shown in figure 2.5 a.

2.3.3 Concrete casting

Concrete was poured depending on the case after a period of 1 or 24 hours from the time of pretensioning. Each two beams in the static and dynamic series were generally cast together. Concrete was mixed in the laboratory using a small rotary mixer. A laboratory size needle vibrator was

used for internal vibration of the concrete; care was taken not to damage the strain gage installations or disturb the position of the reinforcement cage. The concrete surface was then levelled, trowel finished and covered with burlap and plastic sheets.

An average of nine 3x6 inch concrete cylinders were taken for each two beams cast in order to determine the concrete strength. Three of the concrete cylinders were tested to determine the concrete strength just before releasing the prestressing strands; while the remaining 6 cylinders were used to determine the concrete strength just before starting the flexural load test. Forms were removed after 1 day of casting and the beams were moist cured (hosed) occasionally every 6 hours together with the concrete cylinders. The resistance of the strain gages were checked after removing the molds for any possible damage during casting; no such damage was encountered in this phase of testing.

The prestressing strands were released 2 to 3 days after casting and also after the concrete strength had reached at least 3000 - 4000 psi (21- 28 Mpa) as obtained from cyclinder tests. The release was accomplished by cutting the strand with an oxygen torch, (Fig. 2.5 b).

The beams were then lifted from the prestressing bed by two hooks inserted at the two ends before casting using a

specially designed laboratory crane. A photograph of some of the cast beams is shown in figure 2.5 c.

2.4 Instrumentation

2.4.1 Strain gages

Strain gages were attached to the reinforcing bars and the prestressed strands at their mid span location. Two types of electrical strain gages supplied by Micromeasurement Group were used. One type EA-06-125BT (gage factor equal 2.05, transverse sentivity equal 0.2%, gage length equal 0.125 inch and matrix size 0.35Lx0.15W in2) were used on the reinforcing bars; the other type EA-06-230DS (gage factor equal 2.055, transverse sensitivity equal -0.1%, gage length equal 0.23 inch, matrix size 0.5Lx0.12W in2), being thinner, was used on the prestressing strands. Both types of gages had 120 ohms electrical resistance. A photograph of the type of strain gages used is shown in figure 2.6. Typical strain gage attachement to the prestressing strands and reinforcing bars is shown in figure 2.7.

Before attaching the strain gages, the surface of the reinforcing bars and the prestressing strand was cleaned and treated with "Freon TF" degreaser, conditioned with "M-Prep" conditioner and neutralized with "M-Prep" neutralizer (all supplied by Measurement Group). Adhesive type "M-Bond AE-10 EA-10/15" was applied, then the strain gages were clamped to

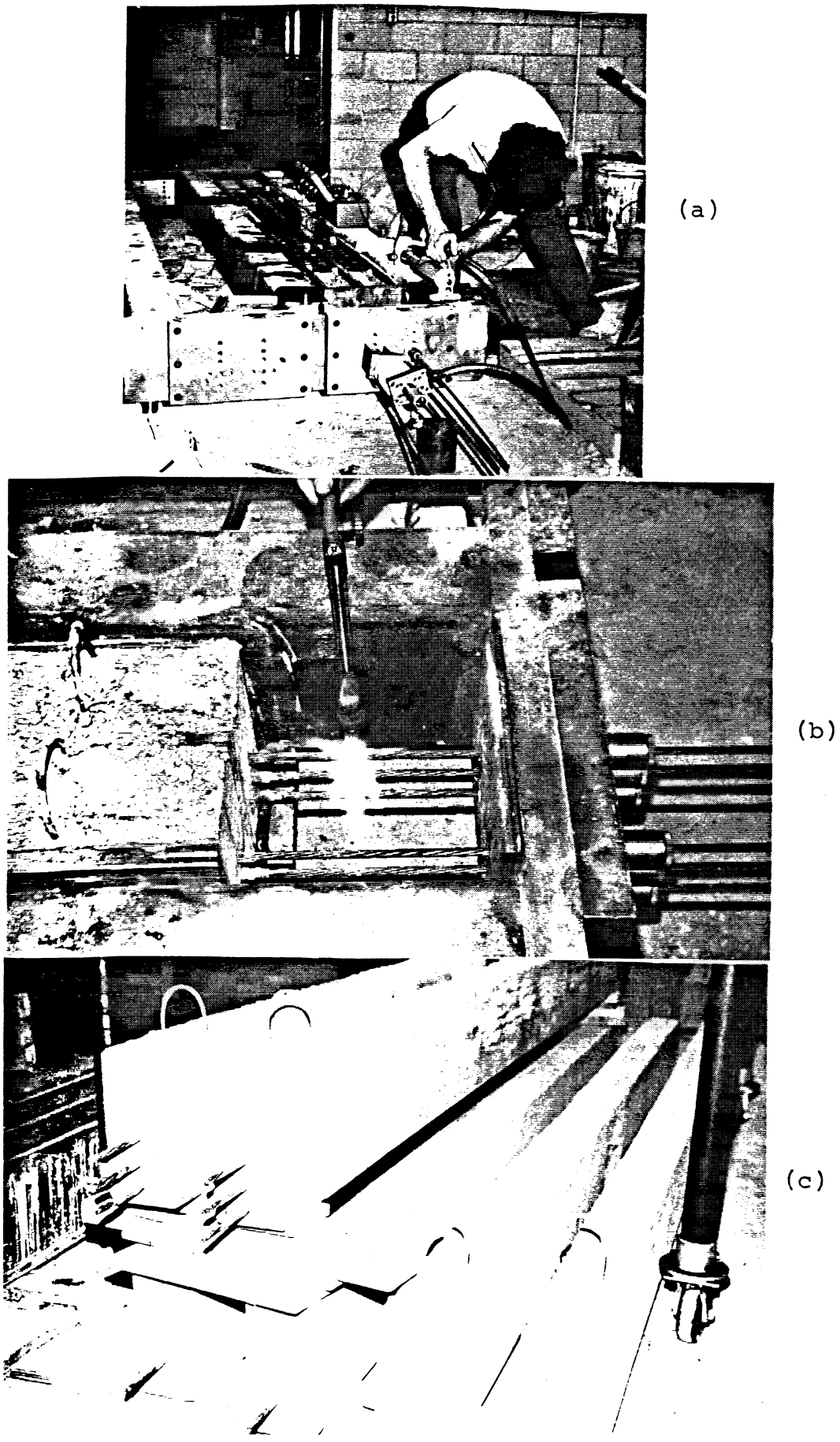

Fig.2.5 Beam Preparation: (a) Prestressing Operation, (b) Torch Cutting For Strand Release, (c) Cast Beams

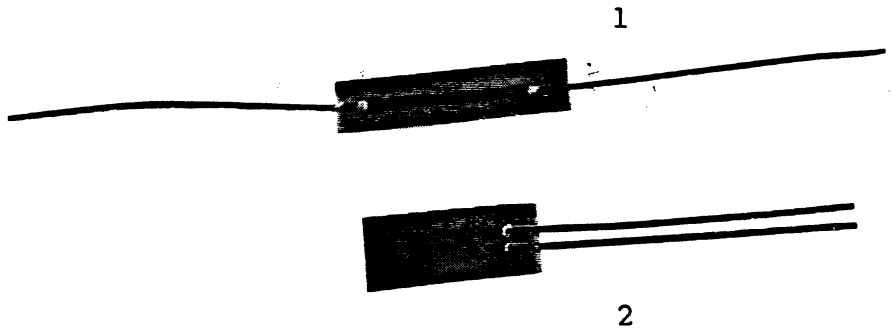

Fig. 2.6 Strain Gages : 1 Used on The Prestressing Strands,
2 Used on The Reinforcing Bars

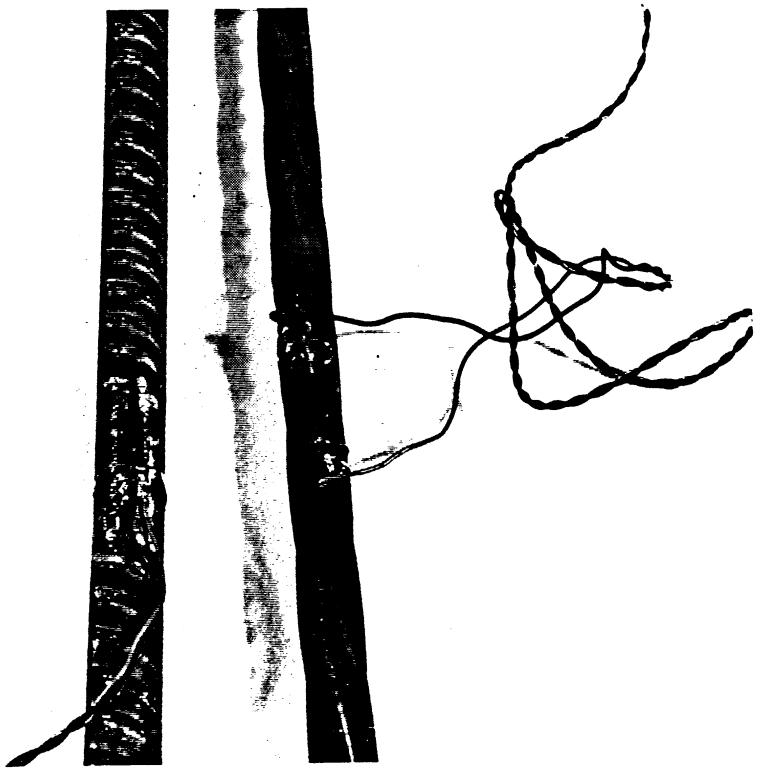

Fig. 2.7 Typical Strain Gage Mounting On The Prestressing Strands And Reinforcing Bars

the bar reinforcement surface using a rubber band (wrapped several times), and to the prestressing strand using a specially designed clamp. Clamping pressure was maintained for at least 6 hours required for the adhesive to cure. Occasionally, some of the strain gages were damaged during the installation procedure. These gages were removed and replaced using "M-bond 200" adhesive (curing time 2 minutes) which performed similarly to the "AE-10/15" adhesive. The lead wires were then soldered and the resistance of the strain gages were checked before applying any coating material. "M coat A" was then applied to insulate the strain gages, followed by "M-coat G" to waterproof and protect the strain gages from the fluid concrete.

Two strain gages were attached to the reinforcing steel, one on each exterior bar. Two or three strain gages were attached to each prestressing strand at the same section depending on the number of strands used in any one beam. Each strain gage was located on every 2nd or 3rd wire in the strand depending respectively on whether 3 or 2 strain gages were attached.

2.4.2 Deflection

Deflection of the beam specimens during the test was measured at 5 inches away from mid span by two linear voltage differential transformers (LVDT) placed on either side of the beam at symetrical distances relative to midspan (Fig. 2.8). The two LVDT's were Shaevitz 1000 DC-D having

± 1" stroke limit. During the test, both LVDT's were supported by two magnetic bases attached to the testing bed of the loading machine. Two dial gages were used to measure the deflection of the testing bed at the location of the end supports during one of the static test in order to account for any possible differential deflection between the supporting bed and the beam specimen. The measured deflection at maximum load was found negligible in all cases. An HP X - Y recorder was also used to trace the load-deflection curve at the 1/3 loading points transmitted through the load ram.

2.4.3 Crack width

During the test, crack width was measured at the location of a crack former at midspan. Two Schaevitz AC-500 MHR LVDT's (stroke limit equal ± 0.5") were used for this purpose. Both LVDT's were attached on either side of the beam by a special device and located at 1" distance from the bottom tension fiber along the centroid of the reinforcing steel. Photographs of the crack width measurement in the beam and crack width measuring device are shown in figures 2.8 and 2.9 respectively. The crack width was also measured occasionally during the testing using a telescope mounted with a scale reticle to check and examine the readings of the LVDT; both readings were generally in good agreement.

2.4.4 Curvature

For some beams (PS2,PP2S3,PP1S3,RS2), curvature obtained during test was measured by two dial gages placed along the constant moment region at midspan. For the remaining beams these dial gages were replaced by two Schaevitz AC-125 HPA (stroke limit equal ± 0.125"). The gage length was 10" (254 mm) and the height between the centerline of the two LVDT was 11.5" (292 mm). Curvature increase with load was measured for all beam specimens in the static test series (except beam RS1). Also Curvature variation with increasing number of cycles was measured for 7 beams in the dynamic series.

2.4.5 Slip

Slip of the prestressed strand due to any possible bond failure was measured during the static and cyclic test. One dial gage was attached to a stretch of one of the prestressed strands extending outside the beam ends. The dial gage was secured to the strand by a C-clamp and oriented in horizontal direction along the axis of the strand with its sensing bar supported directly on the vertical end faces of the beam. A photograph of the dial gage is shown in figure 2.10. As explained later, in no case was any significant reading observed indicating that no slippage has occured during testing.

A photograph of some of the various measuring instruments and their location in the beam is shown in figure 2.11.

2.4.6 Data acquisition system

To simplify the systematic acquisition of the data, a computarized data acquisition system (trade name system 4000) supplied by Micromeasurement Groups was used. The system is composed of the data acquisition control unit itself, an HP 86 microcomputer, a video screen, a printer, and disk drive. The data acquisition system included a strain gage scanner capable of scanning up to 20 strain gage channels and a universal scanner capable of scanning up to 10 LVDT channels. A software program was supplied with the system. A data disk allows entering all the information related to the measuring instruments such as gage factor, transverse sensitivity, LVDT stroke, excitation voltage and the like. The program disk reads the information given by the data acquisition system and translates it into useful engineering units (michrostrain, mm, inch etc ...). The use of this data acquisition system allowed full automization of the data . The program disk also allowed for direct plots of observed results as one channel versus another channel.

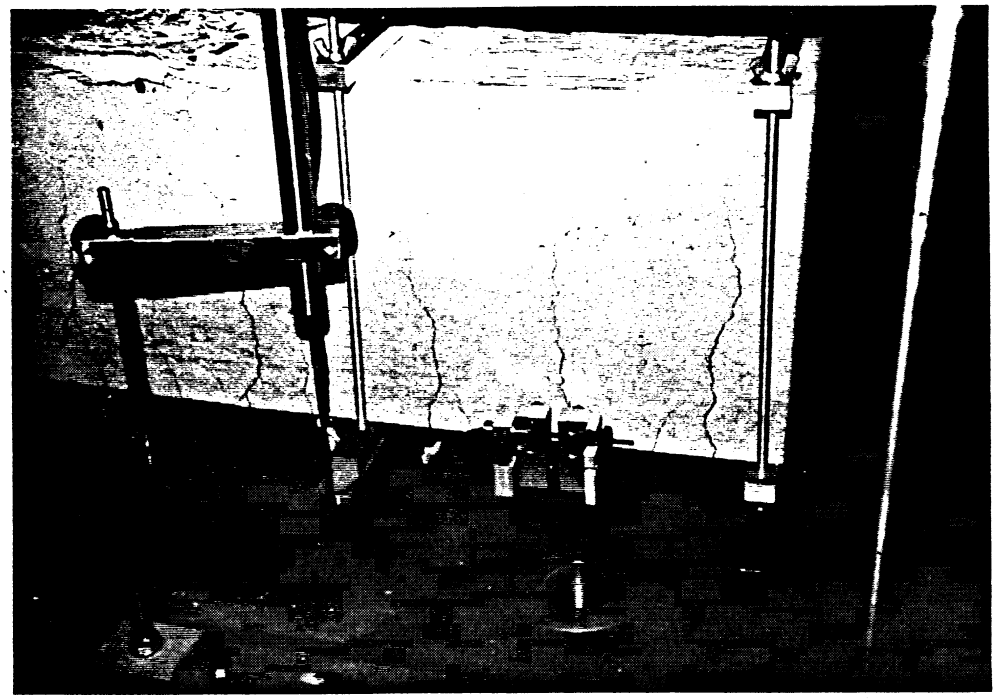

Fig. 2.8 Instrumentation: Deflection And Crack Width Measurement

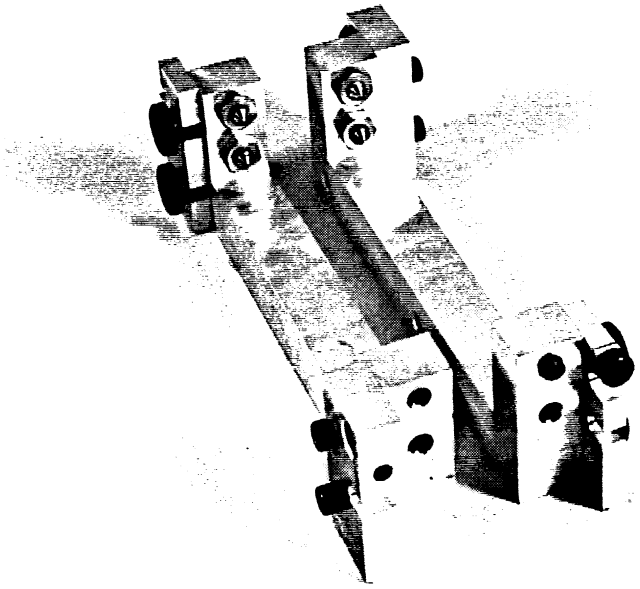

Fig. 2.9 Crack Width Measuring Device

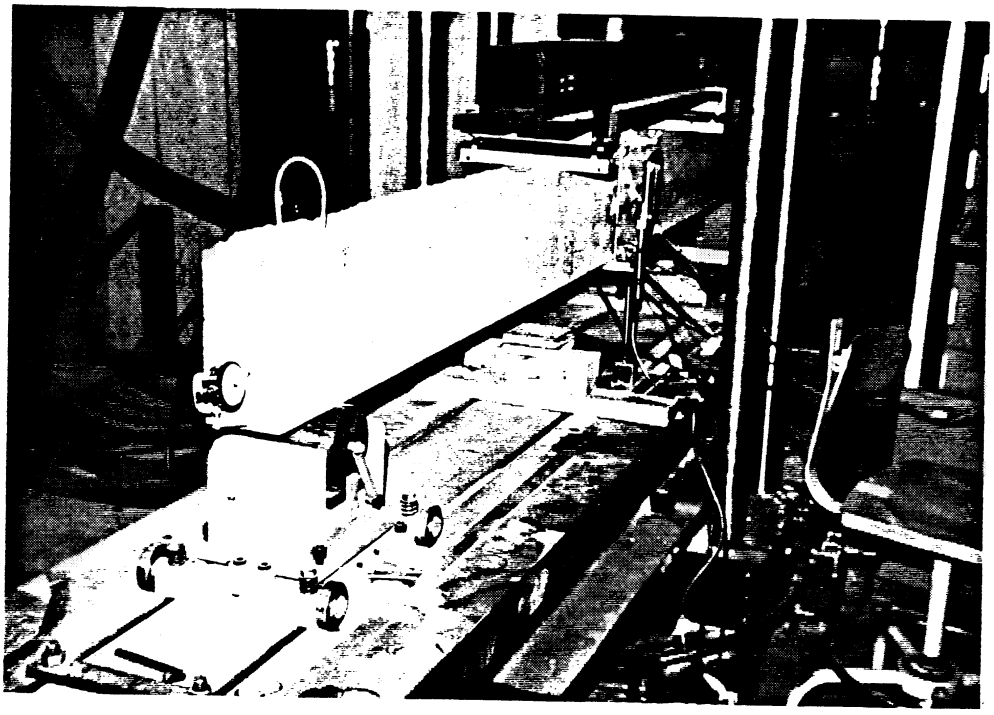

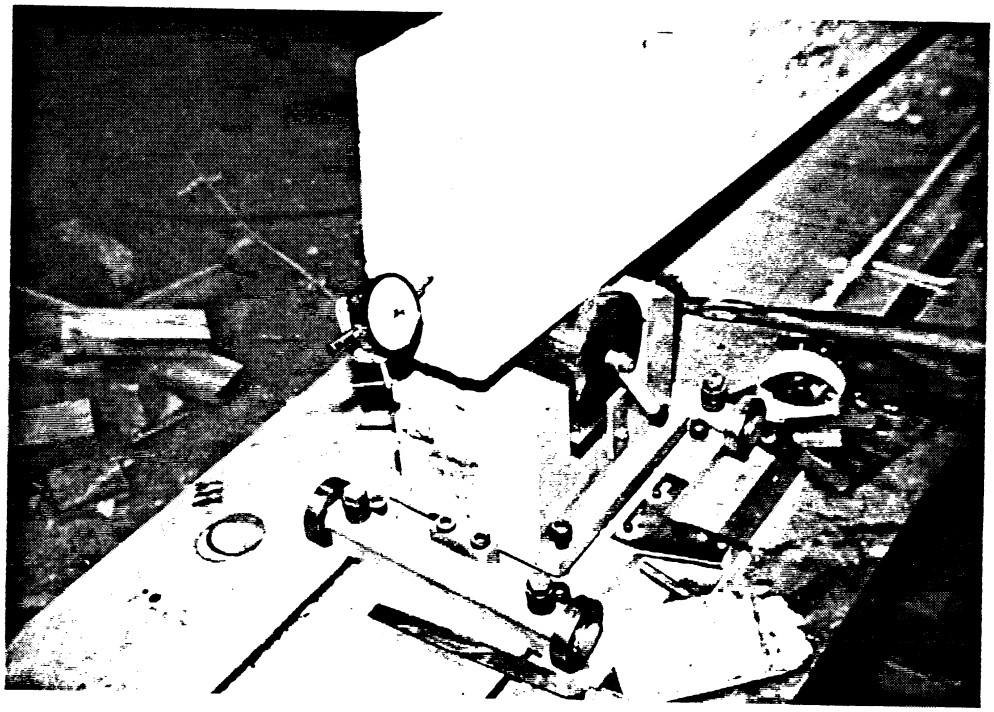

Fig. 2.10 Dial Gage Mounting For Strand Slip Measurement

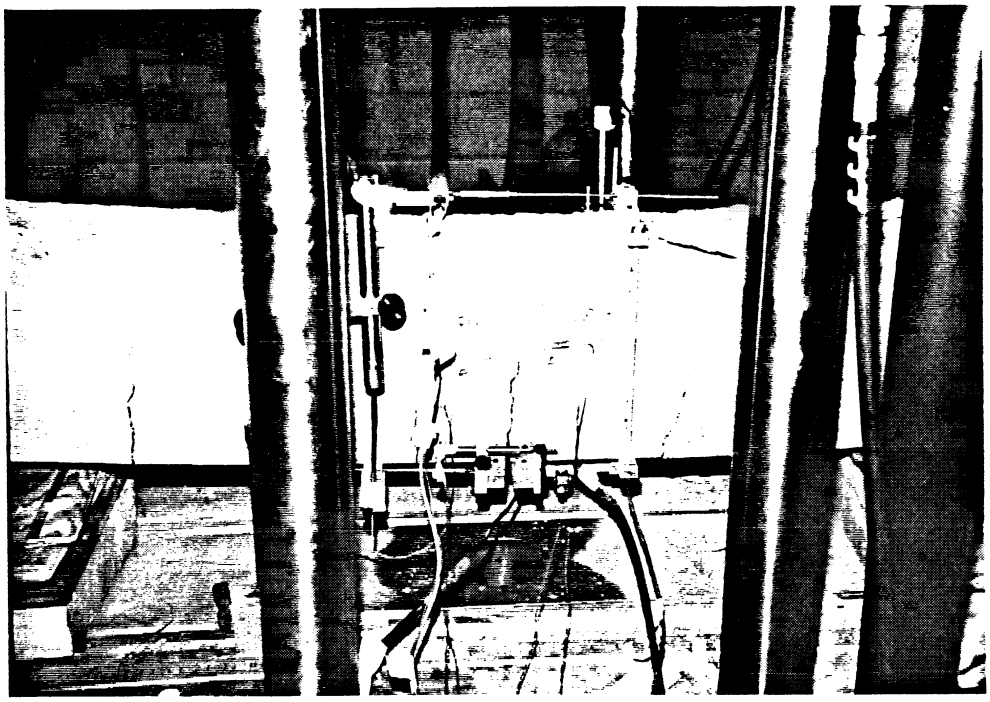

Fig. 2.11 Close Up View Of Instrumentation: Deflection, Crack Width And Curvature

2.5 Test Setup

The beams were supported on two sliding rollers designed to allow rotational twisting between the two ends of the test beams. Both rollers were mounted on a 12 foot long and 2 foot wide steel testing bed. The rollers were adjusted to 9' (2.74 m) span and centered relative to the loading ram by a graduated tape fixed on the testing bed. They were then properly tightened by 4 bolts to prevent any lateral sway during the test. A photograph of beam setting is shown in figure 2.12.

The load was transmitted to the concrete specimen through a steel beam with two adjustable loading pads. The steel beam was connected to a steel swivelhead bolted to the loading cell. The load pads were adjusted to a 1/3 load points, thus creating a constant moment region over 3' length (0.915 m), then tightened properly to the steel beam to prevent any possible movement during the test.

The testing machine was an Instron's specially modified closed - loop servo controlled hydraulic machine with load and stroke control capability. It comprised a 110 kip dynamic capacity frame, a 55 kip dynamic actuator with 6 inch stroke, a 60 gpm hydraulic service manifold and a 40 gpm pump. The machine had a load and stroke digital voltmeter readout and was capable of high loading frequency

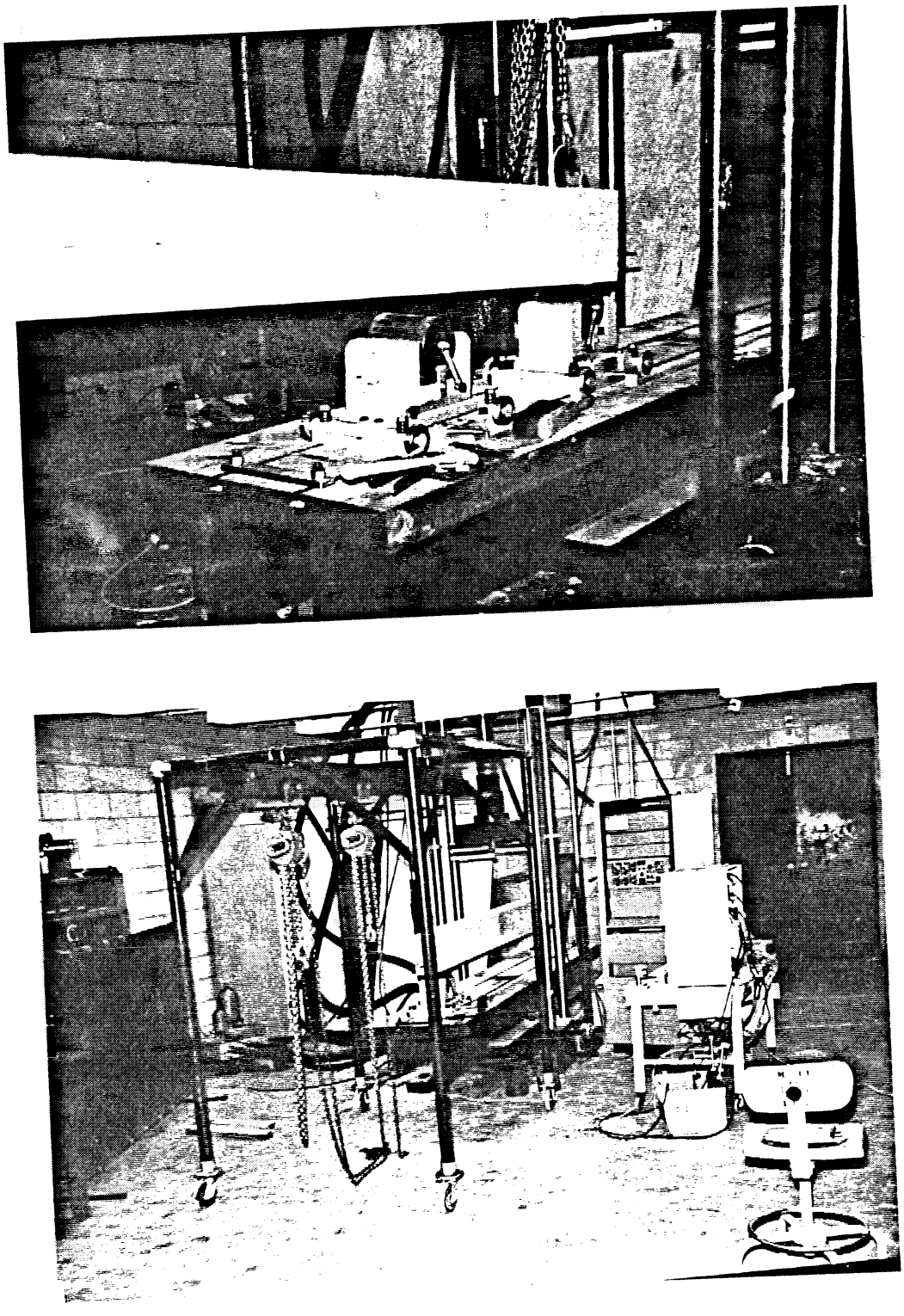

Fig. 2.12 Beam Setting In Testing Machine

for different cyclic wave functions. The sine wave is believed to best represent the live load cycle application on actual structures and therefore was adopted in this experiment. The testing machine was equipped with a load cell calibrated for 50 kips full capacity.

A photograph of the test setup is shown in figures 2.13 and 2.14.

2.6 Test Procedure

2.6.1 Static test

Prior to the actual test, the beams were loaded initially to a small fraction (about 5%) of the ultimate load then unloaded so as to stabilize the beam and also to prevent any possible twisting. The strain gages and LVDT's connected to the data acquisition system were then zeroed and calibrated. The static load was applied at an approximate rate of 1 kip/min. At every load increment which ranged from 2.5 to 5% of ultimate load, the data from the various measuring devices were scanned by the data acquisition system and printed automatically by the printer without interrupting the loading sequence (the data aquisition system was capable of reading up to 30 channels per second). In addition, the load deflection history of the beam at the loading points was also monitored by an HP X - Y recorder. The overall testing time of one beam under static load took, on the average, 15 to 25 minutes depending

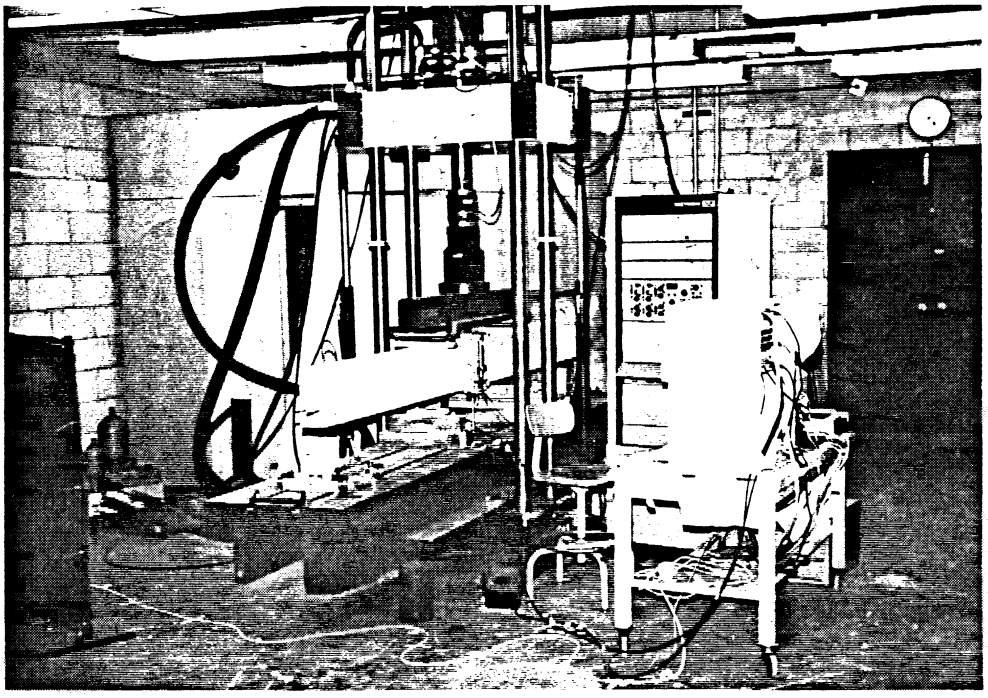

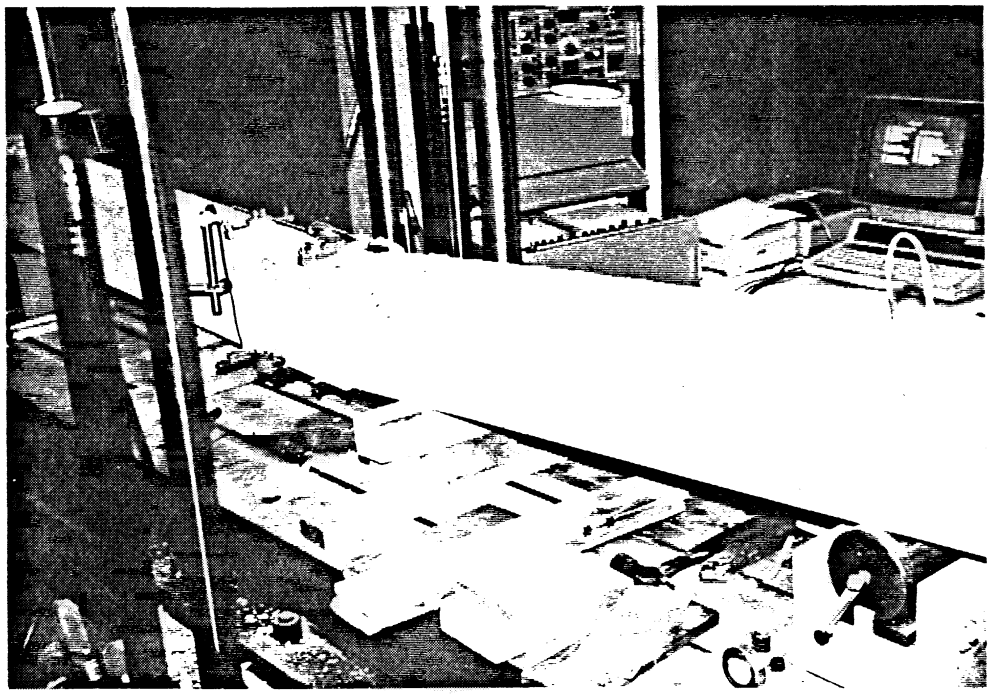

Fig. 2.13 General Test Setup: Loading Machine And Data Acquisition System

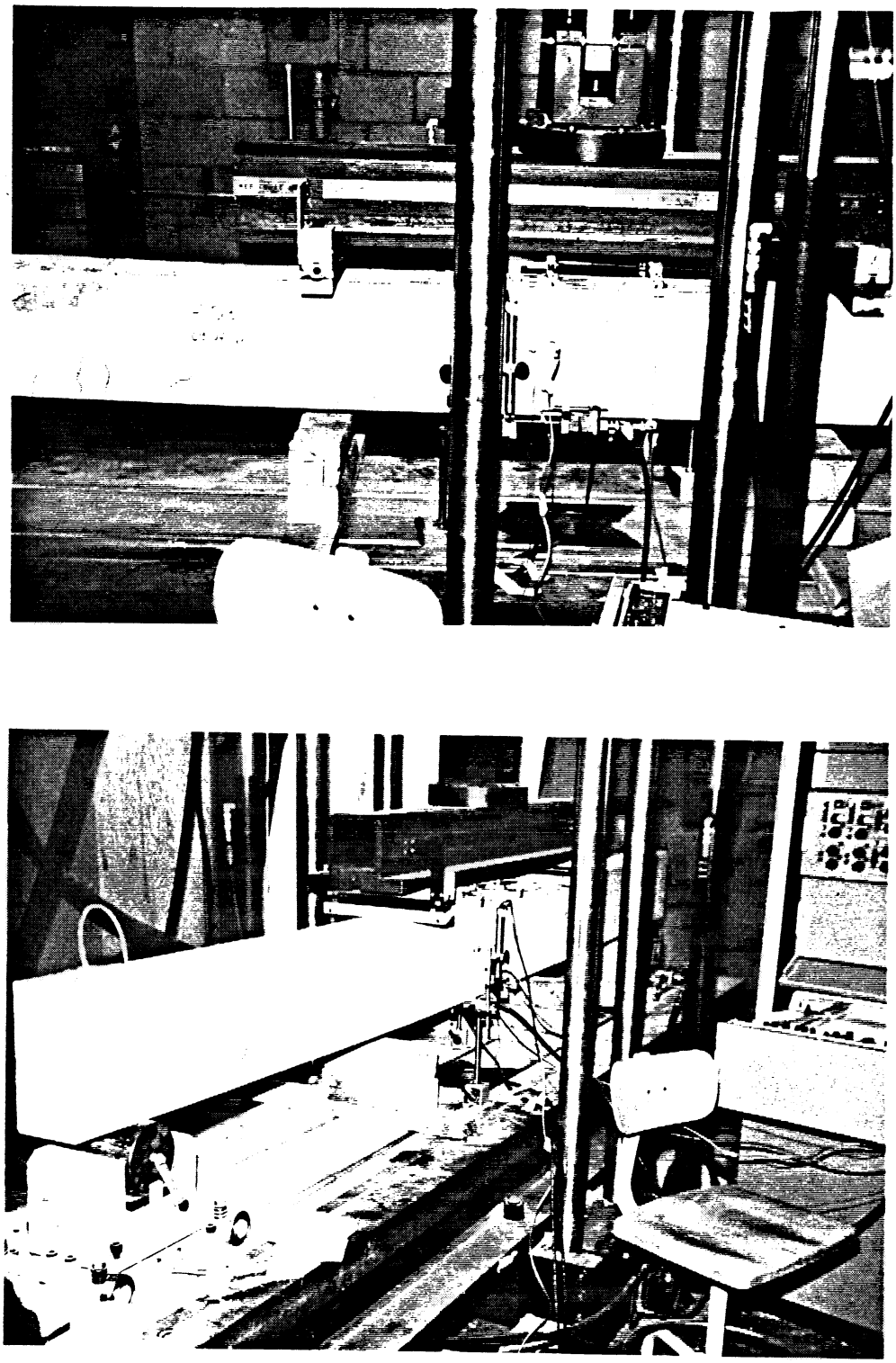

Fig. 2.14 Close Up View Of Test Setup

on the maximum load capacity of the beam tested. At the end of every test, the ultimate load capacity of the beam was recorded on the print out and some remarks about the test were taken. The beam was then dismanteled for further inspection.

2.6.2 Fatigue test

The static test was in general followed immediately by a fatigue test of the sister beam (having the same design variables). The maximum and minimum cyclic loads P_{max} and P_{min} were taken as 60 and 40% of the ultimate load capacity as observed from the statically tested beams. The instruments were initialized following the same procedure as in the static test. Then the load was applied statically to P_{max} then unloaded to P_{min}. In order to stabilize the beam for fatigue measurements, three subsequent static cycles at a rate of 1 kip/minute were applied between P_{min} and P_{max} and for each, strains, deflections, crack widths and curvatures were recorded. The cyclic test between P_{min} and P_{max} was then started at a cyclic frequency ranging from 6 to 7 cycles/sec depending on the compliance of the beam specimen considered.

Throughout the test, readings were taken at a number of cycle intervals. Those readings were taken at a small cycle interval during the early stages of the test, then the intervals were increased at a later stage depending on the fatigue damage observed. For every reading, the cyclic load

was interrupted and a static cycle was applied between P_{min} and P_{max}. During the static cycle, measurements were taken by the data acquisition system for 10 to 12 equally spaced load increments on the loading and unloading portions of the cycle including P_{min} and P_{max}.

Each fatigue test took on the average 8 to 10 days of continuous cycling. At the end of the test (5 million cycles) and if fatigue failure did not occur, the beam was unloaded to zero load and a static test was conducted up to destruction to examine the effect of prior cyclic fatigue on the ultimate load capacity and deformation of the beam.

CHAPTER III

TEST RESULTS

3.1 Calculation of Effective Prestress

A special computer program was written to determine the loss of prestressing force in the strands for the fully and partially prestressed units due to elastic shortening at transfer, shrinkage and creep in the concrete. The time step method was used. The detail of this method and its formulation are given elsewhere (60). The precompression force in the reinforcing steel at the time of testing due to shrinkage and prestressing force was also accounted for. Table 3.1, includes a description of the approximate time between tensioning and casting, age at loading, total prestress losses (computed as mentioned above), reinforcing steel precompression stress, and effective prestress in the prestressing strands at the time of testing.

3.2 Static Load Test

3.2.1 Cracking load

A crack was initiated at the location of a crack former at midspan. In the fully reinforced and partially prestressed units, the crack former extended up to the nonprestressed reinforcement. The cover to the centroid of the nonprestressed reinforcement was kept constant and equal 1" (25.4 mm) in all cases. For fully prestressed specimens, the crack former was 0.25" (6.35 mm) high.

Under increasing load or moment, the precompression stress in the concrete bottom fiber due to the prestressing force decreases. Cracking develops when the tension stress exceeds the tensile strength of the concrete. For all beam specimens, cracking was initiated at the location of the crack former at midspan. However, visible tensile cracks spread along the length of the beam mostly in the constant moment region. These cracks developed shortly after initiation of the midspan crack. Cracking caused a noticeable change in stress increase in the tension steel and in the measured crack widths.

The cracking load as well as other relevant data for each beam specimen in the static test series are given in Appendix B (tables 1S - 12S).

3.2.2 Ultimate load

The ultimate load was taken in this test as the load corresponding to the maximum load on the load-deflection curves beyond which the beam suffered a reduction in strength and collapsed. The magnitude of the ultimate load varied depending on the level of the reinforcing index.

The ACI 318-83 approach for calculating the ultimate moment capacity of flexural concrete section was used in calculating the theoretical moment capacity of the beams. However, the yield strength of the non prestressed reinforcement was taken equal to 70 ksi (483 Mpa) which

Table 3.1 Stresses In The Reinforcement At Time Of Loading

Beam	Initial strand stress (ksi)	Time between tensioning and casting(hours)	Age at loading (days)	At time of testing		
				Prestress losses (ksi)	Reinforcing steel stress* (ksi)	Effective prestress, f_{pe} (ksi)
PS1	185	24	28	15.8	---	169.0
PD1	189			16.1	---	173.0
PS2	154	2	20	16.8	---	137.0
PD2	162			18.8	---	143.0
PS3	159	24	26	22.7	---	136.0
PD3	170			24.1	---	146.0
PP2S1	175	24	15	10.0	6.0	165.0
PP2D1	175			10.0	6.0	165.0
PP2S2	189	2	30	21.6	10.7	167.0
PP2D2	179			19.0	10.4	160.0
PP2S3	149	2	25	16.1	13.3	133.0
PP2D3	146			15.4	13.0	131.0
PP1S1	175	24	20	11.1	6.4	164.0
PP1D1	175			11.1	6.4	164.0
PP1S2	175	2	20	15.3	6.2	160.0
PP1D2	148			9.8	5.7	138.0
PP1S3	160	2	22	12.9	7.3	147.0
PP1D3	163			13.5	7.4	150.0
RS1	--	--	19	--	2.2	--
RD1	--		31	--	3.2	--
RS2	--	--	12	--	1.3	--
RD2	--		26	--	2.4	--
RS3	--	--	13	--	1.3	--
RD3	--		81	--	3.3	--

Note : Prestressed strands were released 2 to 3 days after casting

* Precompression stress in the nonprestressed reinforcement (-ve)

represent the average observed from test. Comparison between the ACI predicted and observed ultimate moments are shown in table 3.2. The high ratio of test to calculated moment observed in the fully prestressed beams is due in part to the conservative equation specified by the ACI code for calculating the stress in the prestressing steel f_{ps}, at ultimate.

3.3 Behavior of Static Test Specimens

3.3.1 Load-deflection

The load-deflection curves for some of the test beams are shown in figures 3.8a,3.9,3.10a-3.12a along with some relevant plots from the fatigue test. Load-deflection curves for remaining beams are shown in figures A1-A7 of Appendix A. Numerical results are summarized in tables 1S-12S of Appendix B.

It could be observed from these figures that for most reinforced and partially prestressed beams, the load-deflection curve comprises 4 portions: 1) from zero load up to cracking, 2) from cracking up to yield , 3) from yield up to strain hardening if any and finally 4) from strain hardening up to ultimate. However, for under-reinforced fully prestressed beams only three stages generally exists. Note that for beam PS3 which was over-reinforced, a brittle failure was observed (Phot. is shown in figure 3.1).

Beam designation	Ultimate moment (k-inch)		Test/Calc.
	Calculated ACI(318-83) (2)	Test results	
PS1	122.0	147.2	1.21
PS2	205.0	250.6	1.22
PS3	275.7	342.0	1.24
PP2S1	132.4	151.2	1.14
PP2S2	187.5	208.8	1.11
PP2S3	297.2	360.0	1.21
PP1S1	242.4	293.0	1.21
PP1S2	265.3	283.5	1.07
PP1S3	370.9	384.1	1.04
RS1	173.1	204.1	1.18
RS2	303.1	324.0	1.07
RS3	441.7	444.1	1.01

Mean = 1.14
S.D = 0.08

Table 3.2 Comparison Of Observed And Computed Ultimate Moments For All Test Beams

Prior to cracking all beams behaved essentially in an elastic manner. After cracking, fully reinforced concrete beams and beams with low PPR developed a relatively linear load-deflection response in comparison to beams fully prestressed or with high partial prestressing ratio. Reduction in stiffness resulted in all the test beams after cracking as expected, depending on the level of the reinforcing index and the partial prestressing ratio. For equal partial prestressing ratio, increasing the level of reinforcing index implies increasing the area of tension reinforcement, this in effect result in a stiffer beam and therefore in a low rate of deflection versus applied load. Also, for equal $\bar{\omega}$, increasing the level of partial prestressing ratio results in a high pecentage of prestressing steel relative to the total steel and hence a small overall area of tension reinforcement. This leads to a larger deflection rate with increasing load. Although the fully prestressed beams had the highest stiffness before cracking, these beams suffered the highest stiffness reduction after cracking, (specially beam PS1).

Yielding of the reinforcing steel occurred prior to that of the prestressing steel for all partially prestressed units because of the physical location of the reinforcing steel relative to the prestressing steel. Beam PS1 in the fully prestressed series yielded at a load of about 7 kips (31 KN) and showed substantial reduction in stiffness up to failure. Beam PS2 and PS3, because of their high reinforcing

index, did not show a clear yielding pattern. After yielding, fully reinforced beams RS1 and RS2 developed a well defined yield plateau followed by a strain hardening stage up to failure. However, Beam RS3 failed before reaching the strain hardening stage. Strain hardening of the reinforcing steel is also evident in some partially prestressed units. Its effect however decreases with an increase in the reinforcing index and PPR.

All beams in the static series failed in flexural compression (concrete crushing) at the top concrete fiber in the constant moment zone except beam PS3 where failure was due to spalling of the concrete cover surrounding the prestressed strands. Typical photographs of beam failure in both the static and fatigue beam specimens are shown in figures 3.1-3.3. The prestressing strand of beam PS1 broke shortly after reaching the peak of the load deflection curve.

3.3.2 Crack width

Throughout the test, crack width was measured at the location of the crack former at mid span. Data results are summarized in table 1S-12S. Typical plots of crack width versus applied load is shown in figure 3.4. It could be seen that the rate of crack width increase, as described by the slope of the curves, depends on the partial prestressing ratio. It was generally observed that the higher the partial prestressing ratio, the higher is the slope of the crack

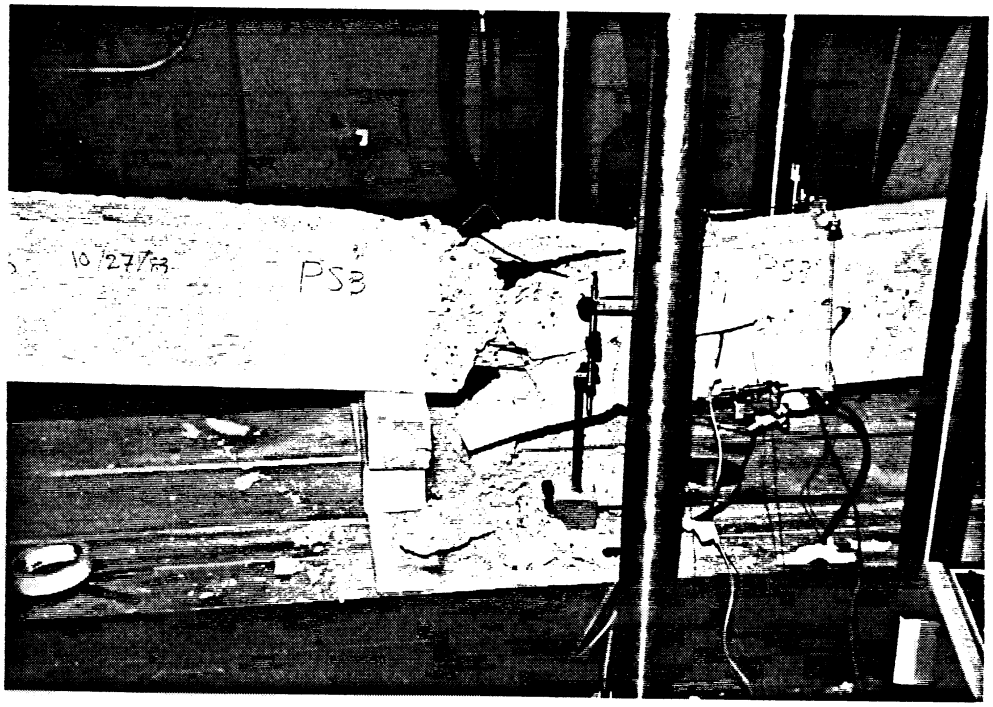

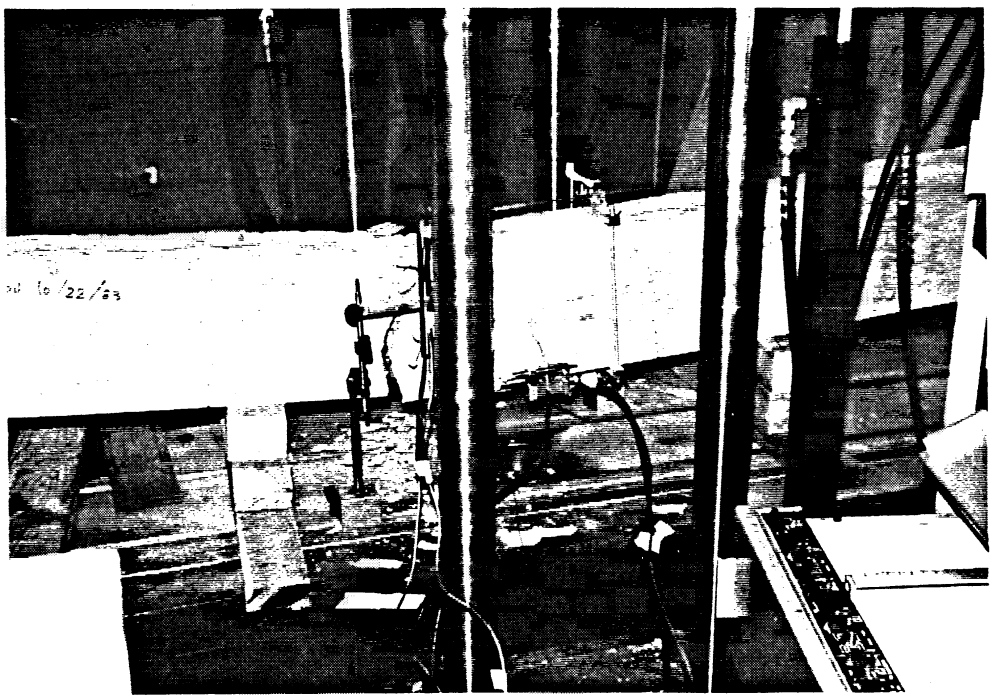

Fig. 3.1 Typical Beam Failures: PS3, PD1

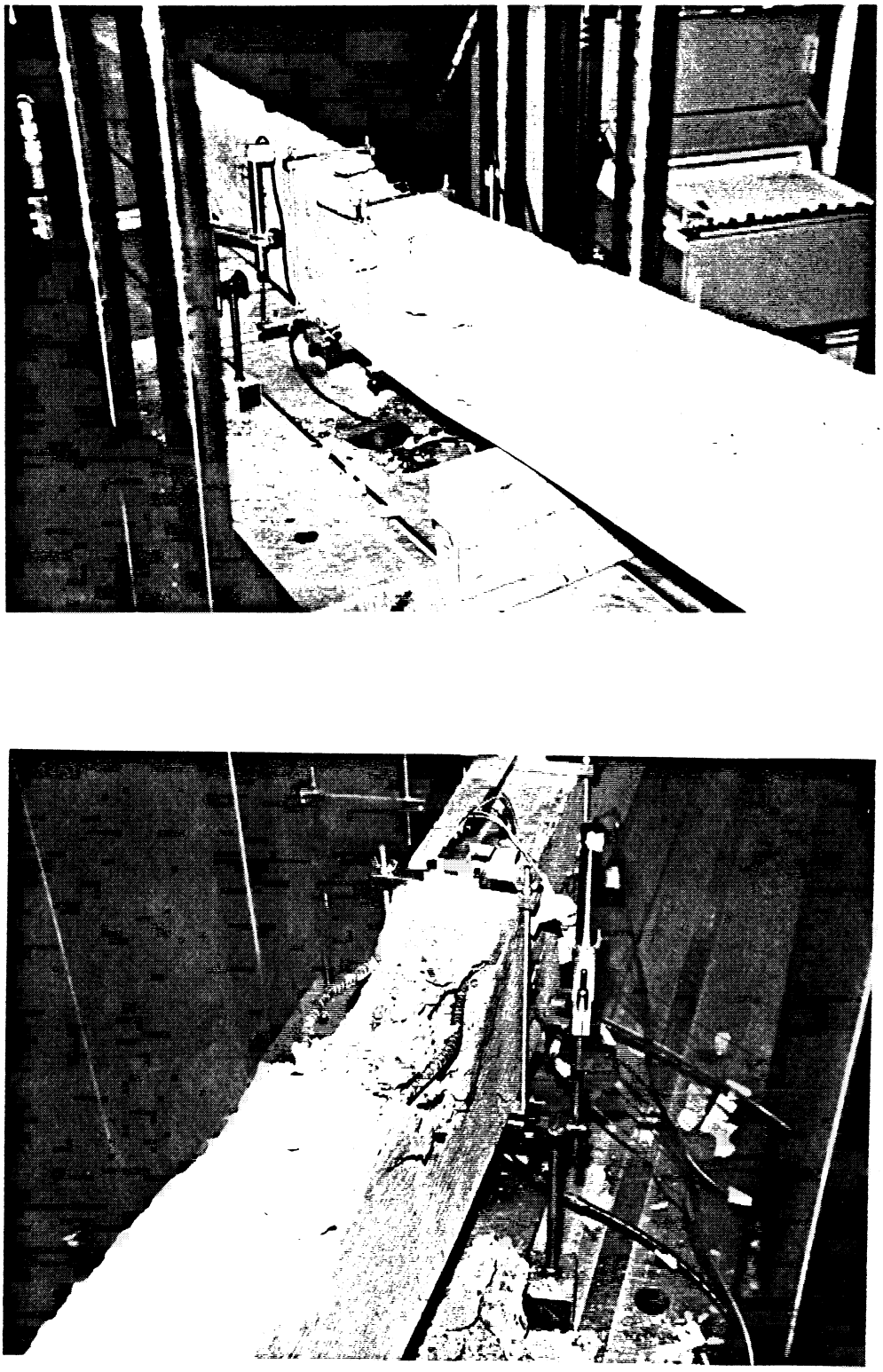

Fig. 3.2 Typical Beam Failures: PP1D3, PP1S1

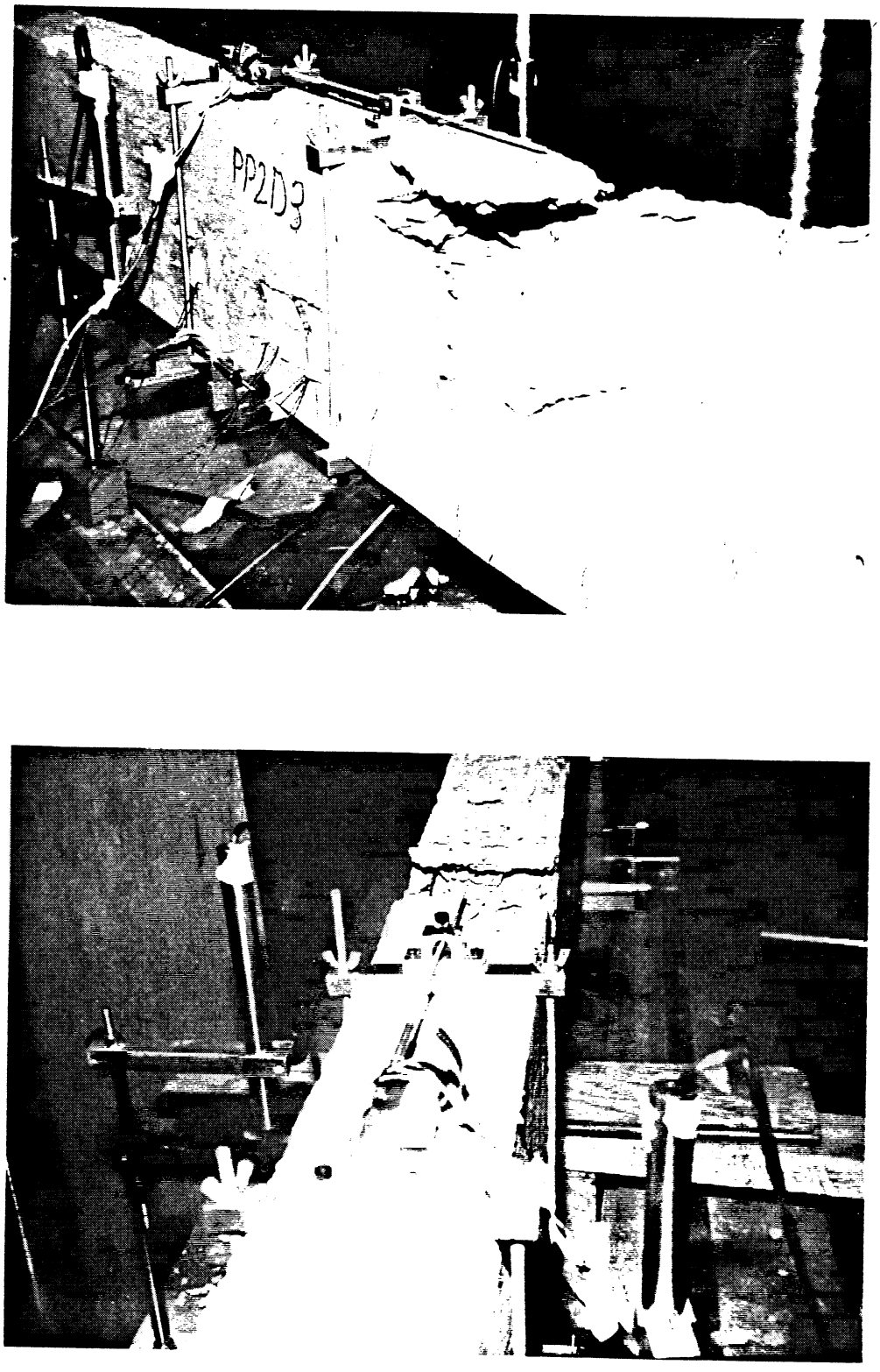

Fig. 3.3 Typical Beam Failure: PP2D3

width versus load curve. Although the crack initiation in the fully prestressed beams was delayed due to prestressing, these beams suffered the highest rate of crack width increase with load after cracking. Beams with reinforcing steel placed close to the bottom concrete tension fiber or beams with a high area of reinforcing steel (low level of PPR) showed more evenly distributed cracks, and less crack spacings. This may be due to the better overall bond characteristics of the tension reinforcement with the surrounding concrete.

It has been shown (50,51,53) that crack widths can be expressed as a direct function of the average strain in the reinforcement and crack spacing. For a given reinforcement parameters, the crack spacing generally remains constant within the elastic range of loading. Hence for a linear increase in load, a linear increase in stress in the reinforcement thus in crack width is observed. Figure 3.5 show the variation of crack width versus reinforcing steel stress. The sudden decrease in the crack width rate in some curves is due to the formation of extra cracks with increasing load.

3.3.3 Load-curvature

Curvature was measured at midspan over a gage length equal 10". Figure 3.6 shows the variation of curvature with the applied load for some of the test specimens. The curvature obtained was in general in a region where at least

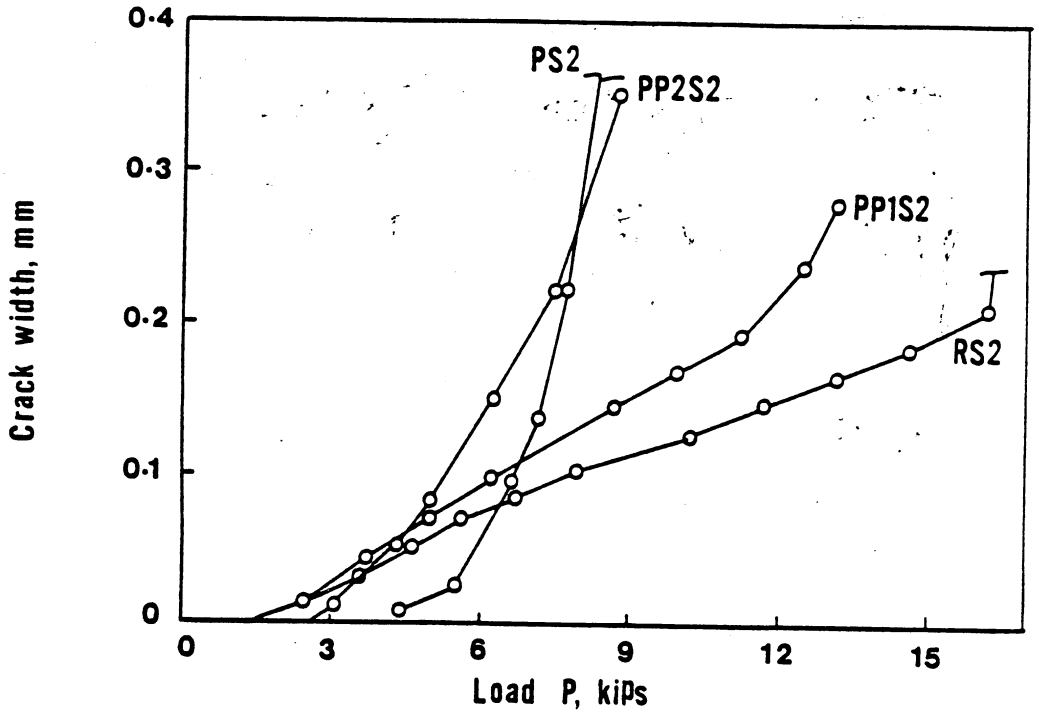

(a)

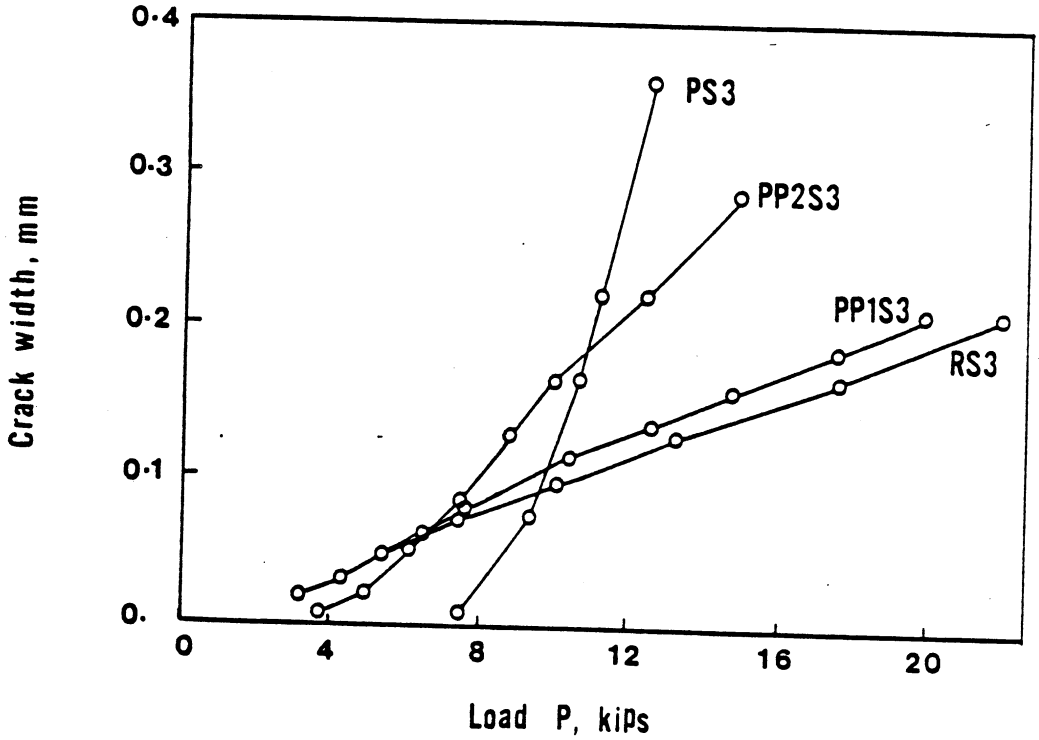

(b)

Fig. 3.4 Crack Width Variation With Load At Different PPR: (a) $\bar{\omega} = 2/3\ \omega_{max}$, (b) $\bar{\omega} = \omega_{max}$

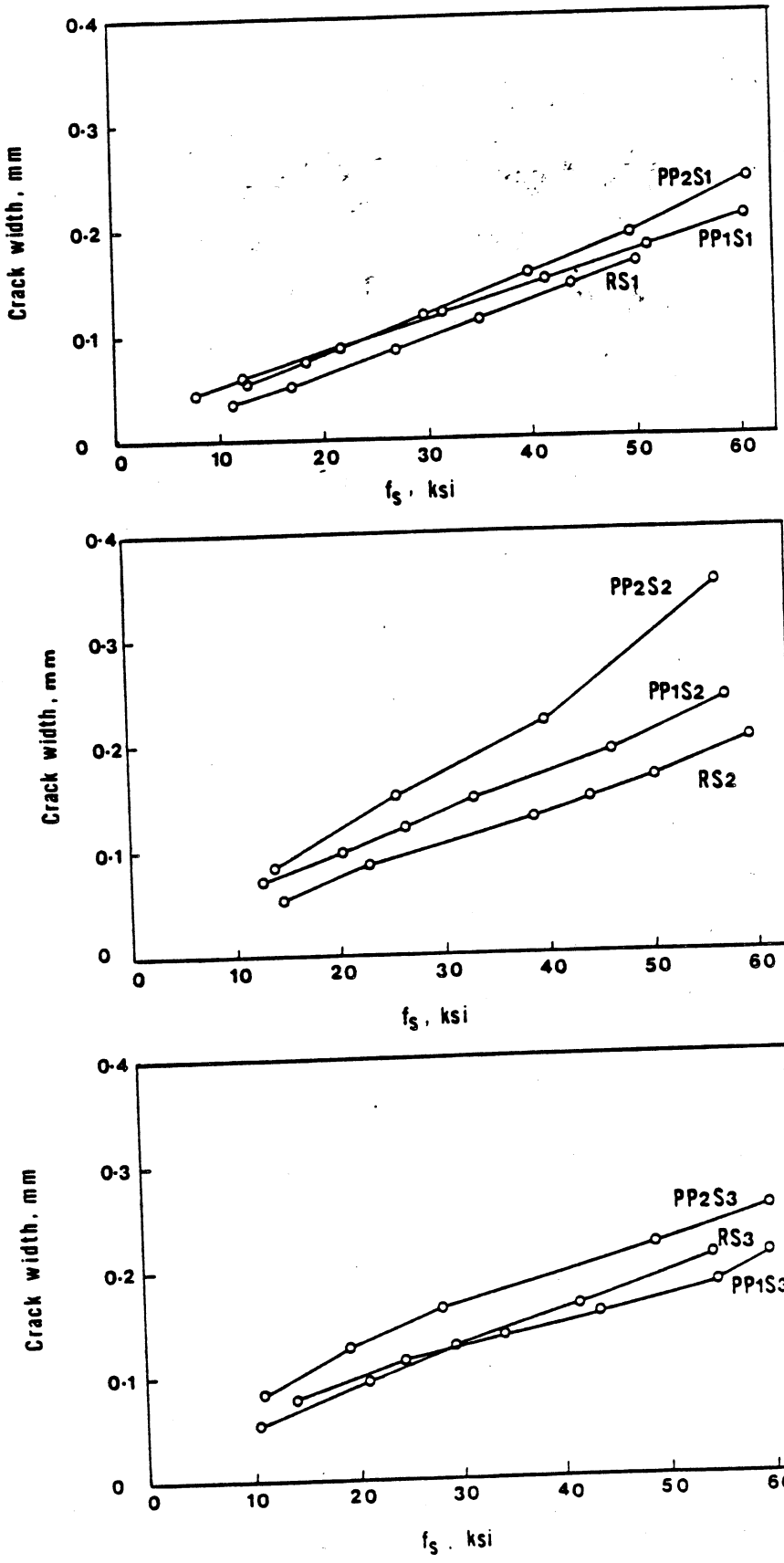

Fig. 3.5 Crack Width Variation Versus Reinforcing Steel Stress At Different PPR: (a) $\bar{\omega} = 1/3\ \omega_{max}$, (b) $\bar{\omega} = 2/3\ \omega_{max}$ (c) $\bar{\omega} = \omega_{max}$

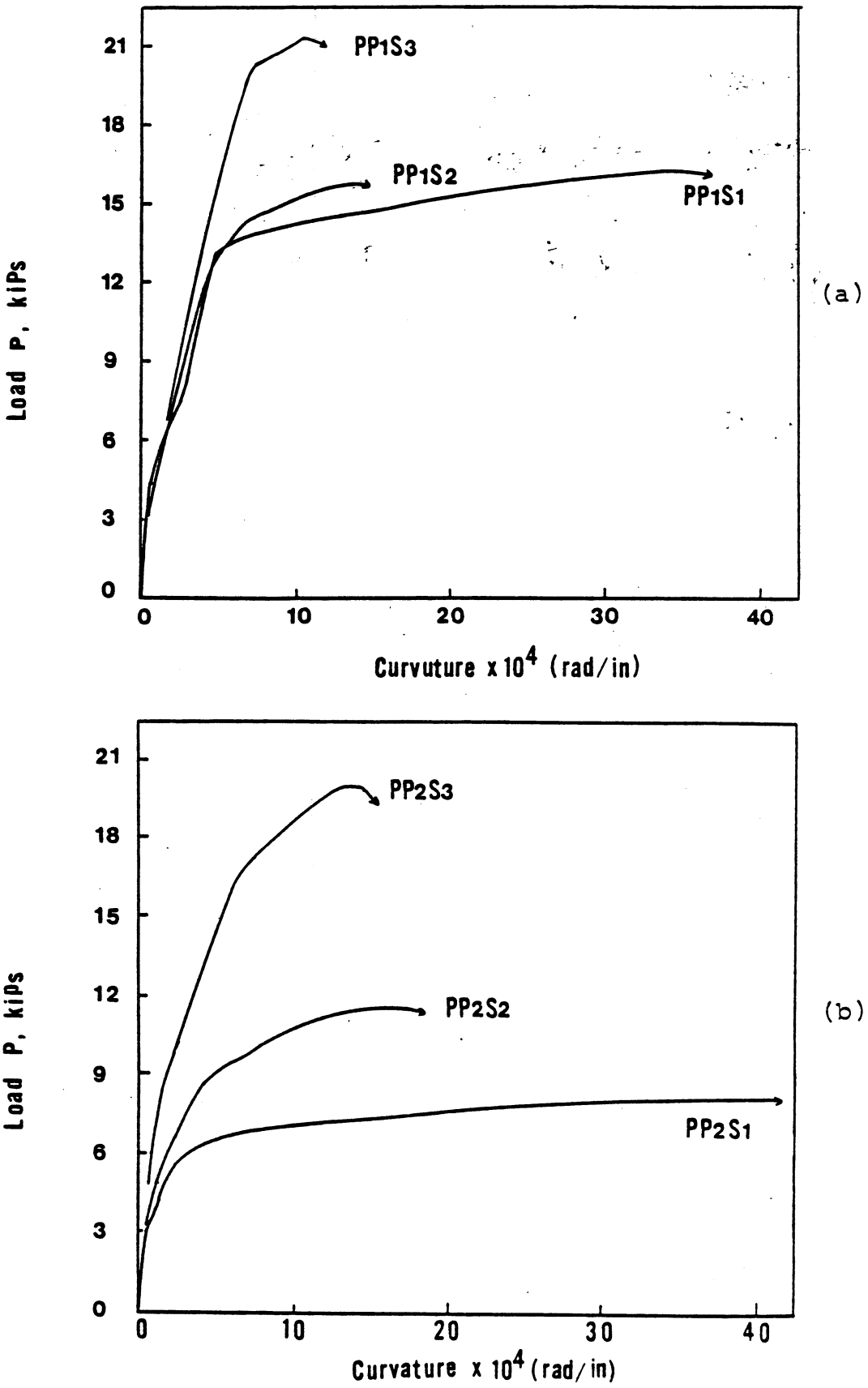

Fig. 3.6 Effect Of $\bar{\omega}$ On Load-Curvature Relationships: (a) PPR Close To 0.33, (b) PPR Close To 0.67

two or three cracks were formed. Therefore it represents the average curvature over 10" length in the constant moment region of the beam. It is clear from these figures that the load-curvature curves show the same trends as the load-deflection curves.

The load-curvature curves and the load-deflection curves mentioned before reveal an important aspect of the behavior of concrete beams under monotonically increasing load, namely, ultimate deformation or ductility. It can be observed that the level of maximum curvature and/or deflection is most importantly related to the level of reinforcing index. Increasing the level of reinforcing index results in a larger neutral axis depth at ultimate and therefore less deformation capacity. The ductility of concrete beams depends globaly on the ductility of the reinforcement; prestressing steel is less ductile than reinforcing steel. Therefore, beams reinforced with prestressing steel are expected to be less ductile than beams reinforced with reinforcing steel. Fully prestressed beams showed the least ductility in comparison with the remaining beams in this test. However, partially prestressed beams (for both levels of partial prestresing) were observed to have the same order of maximum deformation as fully reinforced beams of approximately similar levels of reinforcing index. This increase in ductility is in favor of partial prestressing which also combines the advantages of both full prstressing and full reinforcing.

The effect of compression reinforcement in increasing the ductility of concrete beams is evident in figure 3.6a. It can be seen from this figure that the maximum curvature in beam PP1S1 is substantially larger than that of beam PP1S2 although both beams were of approximately equal observed strength (both beams have approximately equal tension reinforcing index). Compression reinforcement in beam PP1S1 resulted in decreasing its total reinforcing index (see equation 2.1) and therefore in a dramatic increase in its maximum deformation compared to beam PP1S2.

3.4 Fatigue Test

All specimens were tested under constant load range varying between 40 and 60% of the ultimate load capacity of the control specimen having the same input variables in the static test series. The average cycle frequency was equal 6.0-7.0 cycles/sec depending on the compliance of the test specimens and the frequency response of the actuator. Fatigue test datas for all beam specimens are summarized in tables 1D-12D of Appendix B.

3.4.1 Fatigue life

All the 6 partially prestressed and the 3 fully reinforced beams survived 5 million cycles (beam RD1 was cycled only up to 3 million cycles) without suffering a major fatigue damage. Fully reinforced beams encountered the least fatigue damage in comparison with partially and fully

prestressed beams (fatigue damage is evaluated with respect to relative increase in deflection, curvature and crack width with increasing number of cycles).

The three fully prestressed beams, PD1, PD2 and PD3 failed during cycling. The failure resulted from fatigue fracturing of the strands at the location of a crack in the constant moment region of the beam. One wire of the strand was broken at approximately 1 million cycle for beam PD1 and at around 2.0 and 1.8 million cycles for beams PD2 and PD3 respectively. One indication of a wire being broken is a clearly heard bang from inside the beam. The failure of one wire was generally accompanied by a sudden jump in the residual deflection of the load-delection hysteresis loop, substantial reduction in stiffness, increase in crack width and high increase in the area enclosed within the hysteresis loop. The failure of additional wires in the strands reduced the net tensile area of the prestressed steel and therefore increased its stress range. This in effect accelerated the fatigue damage of the beam and reduced its fatigue life.

The observed stress ranges in the prestressing strands in the three fully prestressed beams during the early cycles were 10.0 ksi (69 Mpa), 16.0 ksi (110 Mpa) and 19.0 ksi (131 Mpa) for PD1, PD2 and PD3 (bottom strand) respectively. The stress ranges observed at last reading before failure of the strain gages (See tables 1D-3D) were 16 ksi (110 Mpa), 19.3 ksi (133 Mpa) and 27.1 ksi (187 Mpa) respectively. Beam PD1

failed at 1.212 million cycles after failure of its only prestressed strand. The maximum deflection, crack width and curvature at P_{max} measured in the last reading before failure (1.1 million cycles) were 0.43", 0.35mm and 3x10-4 in-1 respectively. Beam PD2 failed at 2.2 million cycles after several wires in the strands were broken. The maximum deflection and crack width in the last reading (2.17 million cycles) were 0.9" and 1.27 mm respectively. Beam PD3 failed at 1.94 million cycles after the bottom strand totally failed; this was accompanied by a very large increase in crack width. The beam was considered failed for all practical purposes. The maximum measured deflection and curvature at 1.94 million cycles were 0.98" and 10.1x10-4 in-1 respectively.

The fictitious nominal tensile stresses in the bottom concrete tension fiber was calculated assuming uncracked section for all beam specimens in the fatigue series. Results are summarized and compared with the observed stress ranges in the tension reinforcement in table 3.3. The large values of the calculated nominal tensile stresses indicate that little corrolation exists in general between the fictitious nominal tensile stress and the fatigue life of the beam specimens in this test. A nominal tensile stress of up to $32.8\sqrt{f'_c}$ (PP1D3), did not result in fatigue failure. Also, on the other hand a nominal tensile stress as high as $24.1\sqrt{f'_c}$ in the fully prestressed beams (PD3), compared to the $6\sqrt{f'_c}$ limit recommended by the ACI

committee, led to a fatigue failure of the beam at a reasonable number of cycles (1.94 million). Moreover, the stress ranges in the prestressing strands observed in the 3rd cycle were compared with the S-N curve shown earlier (Fig. 1.2). Results are shown in figure 3.7. This figure and also table 3.3, suggest that the stress range in the tension reinforcement is a far more indicative parameter for evaluating the fatigue life of the beam specimens than the fictitious nominal tensile stress.

3.5 Behavior of Fatigue Test Specimens

3.5.1 Deflection

The load-deflection curves for some beams are shown in figures 3.8b,3.9,3.10b-3.12b along with some relevant data pertaining to the beams tested. Load-deflection curves for the remaining beam specimens are shown in figures A1-A7 (Appendix A). These curves show the progressive variation of the load-deflection hysteresis loop measured between Pmin and Pmax with increasing number of cycles. It can be seen that the load-deflection for partially prestressed and fully reinforced beams remained stable throughout most of the test cycles. The continuous narrowing of the hysteresis loop of these beams with subsequent cycles is one indication of their stable behavior under cyclic fatigue loading.

The residual deflection of beams PD1, PD2 and PD3 increased progressively with approximately constant load-

Table 3.3 Calculated Concrete Nominal Tensile Stresses And Observed Stress Ranges In The Reinforcement

Specimen	Stresses under short term loading				Observed for 3rd cycle		Observed at last reading*		
	Nominal tensile stress at $P=P_{min}$		Nominal tensile stress at $P=P_{max}$		Δf_{ps}	Δf_s	Δf_{ps}	Δf_s	N
	Psi	$x\sqrt{f'_c}$	Psi	$x\sqrt{f'_c}$	(ksi)	(ksi)	(ksi)	(ksi)	
PD1	195.0	2.6	664.5	8.9	10.0+	--	16.0+	--	1.21×10^6
PD2	340.9	4.5	1176.0	15.6	16.0+	--	19.3+	--	2.20×10^6
PD3	675.3	8.9	1828.0	24.1	19.0+	--	27.1+	--	1.94×10^6
PP2D1	424.6	5.2	882.1	10.9	5.8	18.1	7.0	15.1	5×10^6
PP2D2	612.4	8.4	1334.2	18.3	9.2	18.6	10.2	18.5	5×10^6
PP2D3	1116.0	14.2	2205.4	28.0	12.8	22.5	14.5	23.5	5×10^6
PP1D1	1233.4	15.9	2074.8	26.7	8.8	17.2	9.8	17.3	5×10^6
PP1D2	1258.2	16.5	2103.6	27.6	7.9	14.3	8.4	14.8	5×10^6
PP1D3	1514.0	19.5	2543.1	32.8	6.9	12.4	7.6	12.9	5×10^6
RD1	1175.8	15.3	1817.1	23.6	--	15.6	--	14.8	3×10^6
RD2	1798.2	23.5	2671.3	34.6	--	11.3	--	12.0	5×10^6
RD3	2255.5	30.3	3383.3	45.4	--	10.4	--	11.1	5×10^6

+ Failed by fracturing of the prestressing strands, all other beams did not fail.

* See Tables 1D-12D for more detailes.

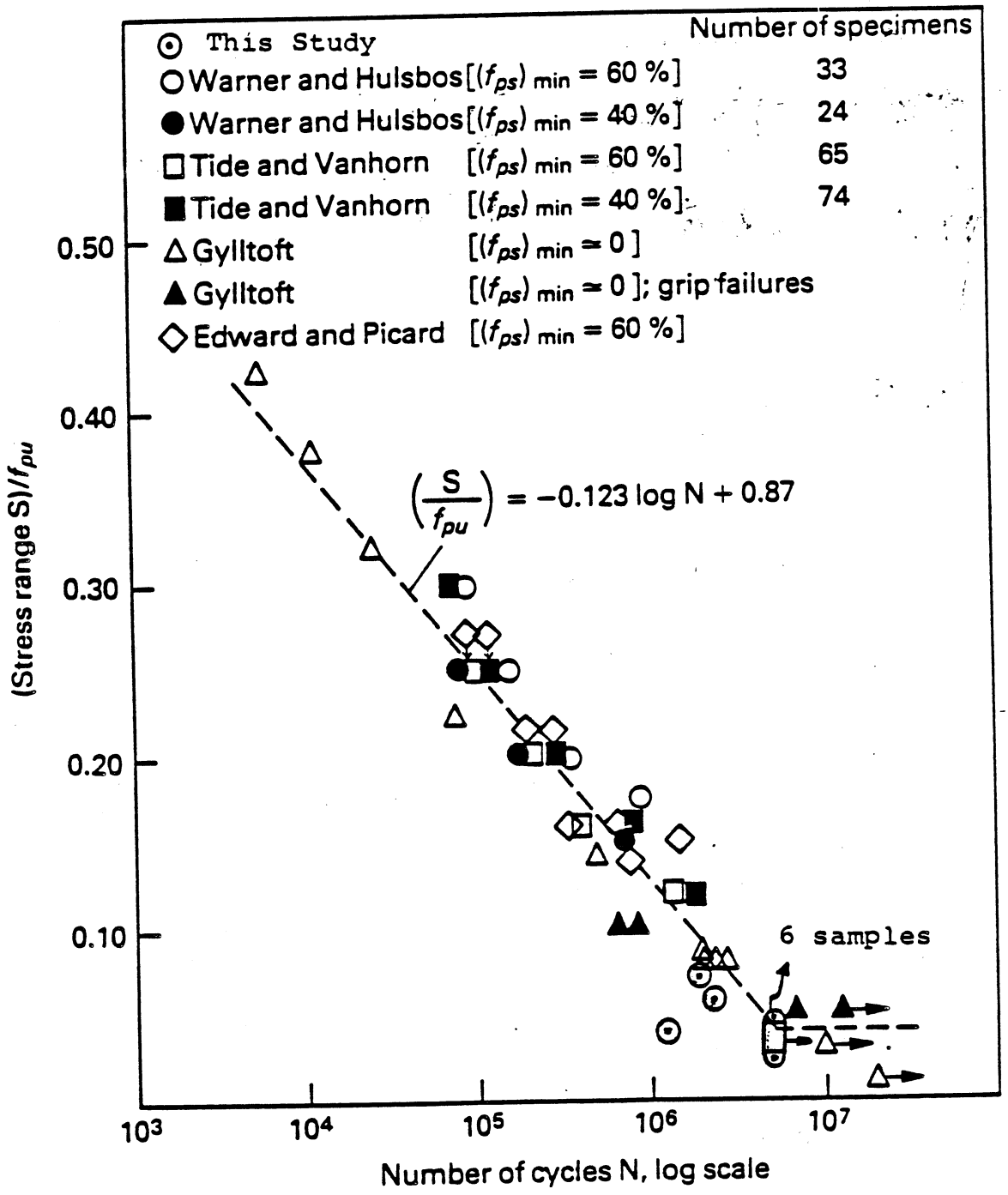

Fig. 3.7 Comparison Of Observed Fatigue Life With Existing Data (Ref. 60)

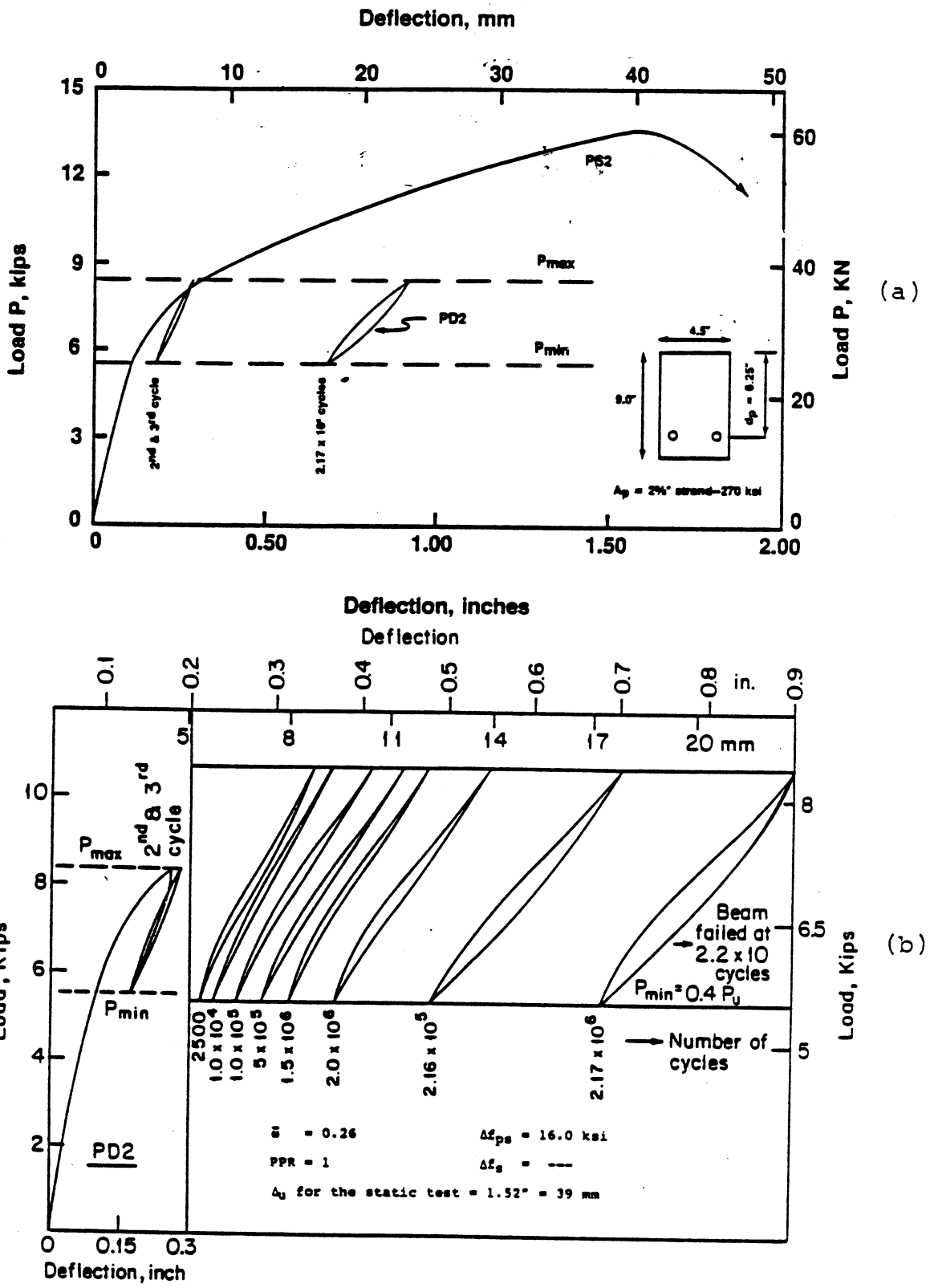

Fig. 3.8 Load-Deflection Curves For Beams: (a) PS2 (Static) (b) PD2 (Cyclic)

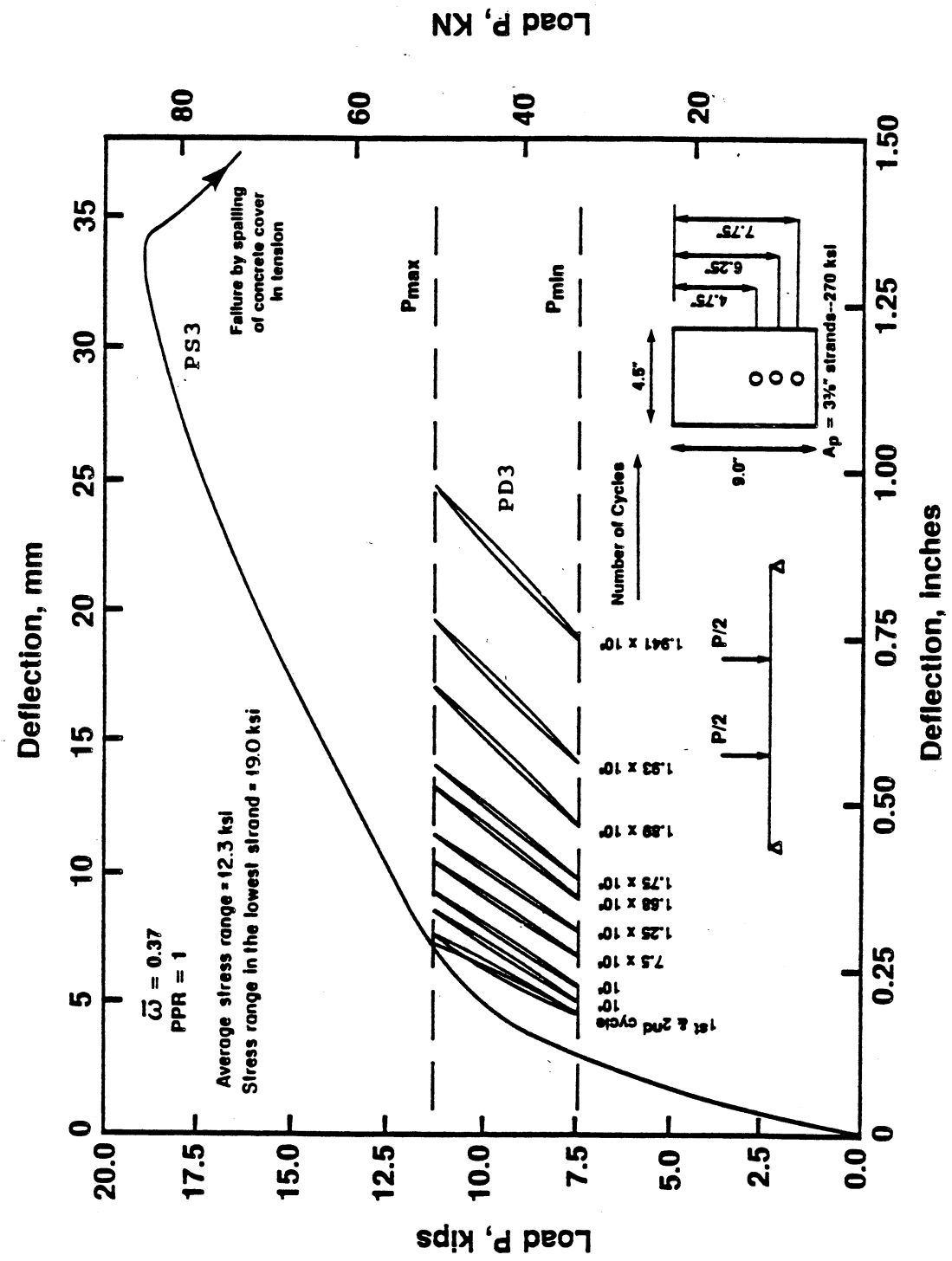

Fig. 3.9 Load-Deflection Curves For Beams PS3 (Static) And PD3 (Cyclic)

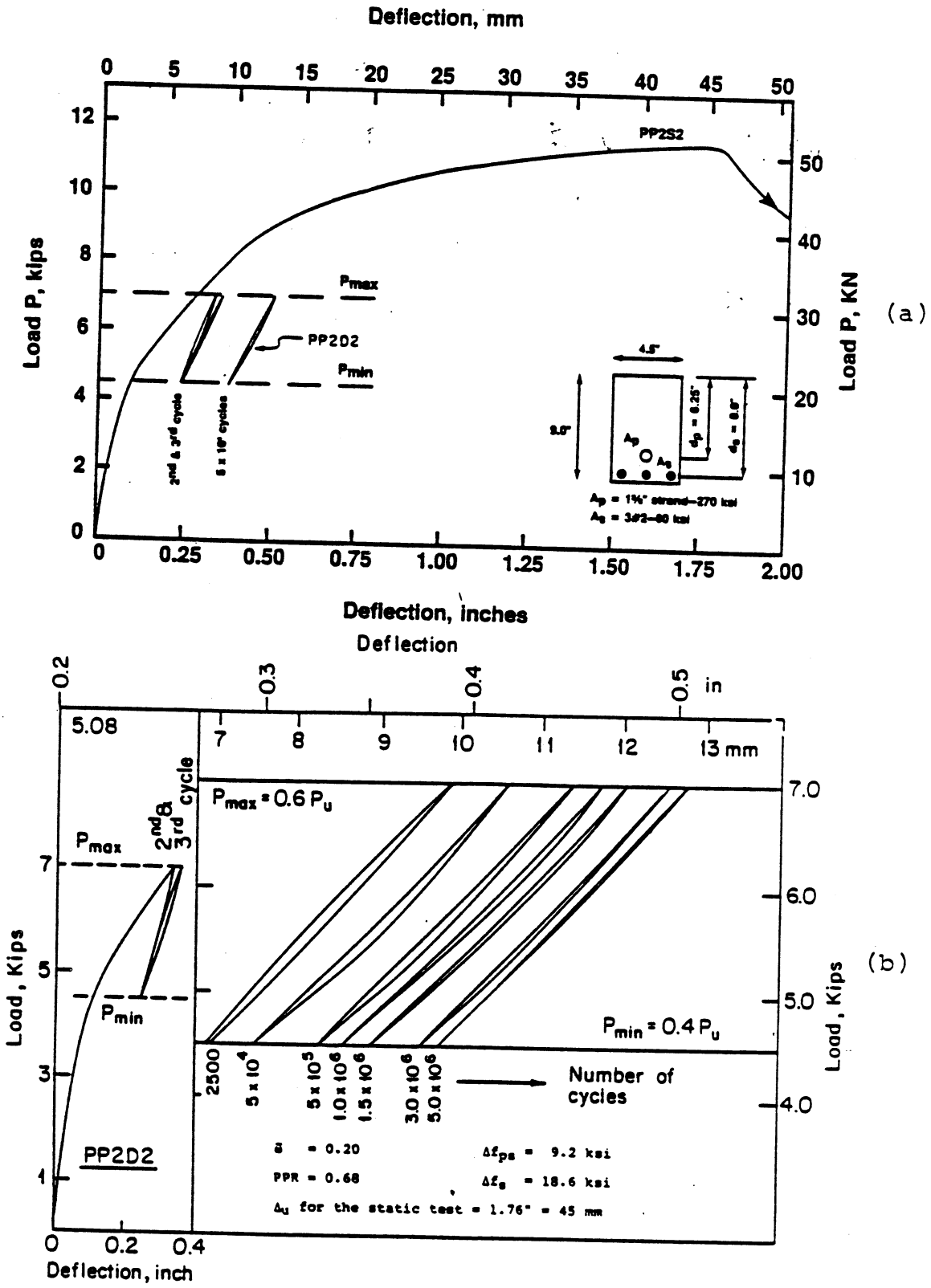

(a)

(b)

Fig.3.10 Load-Deflection Curves For Beams: (a) PP2S2(Static) (b) PP2D2 (Cyclic)

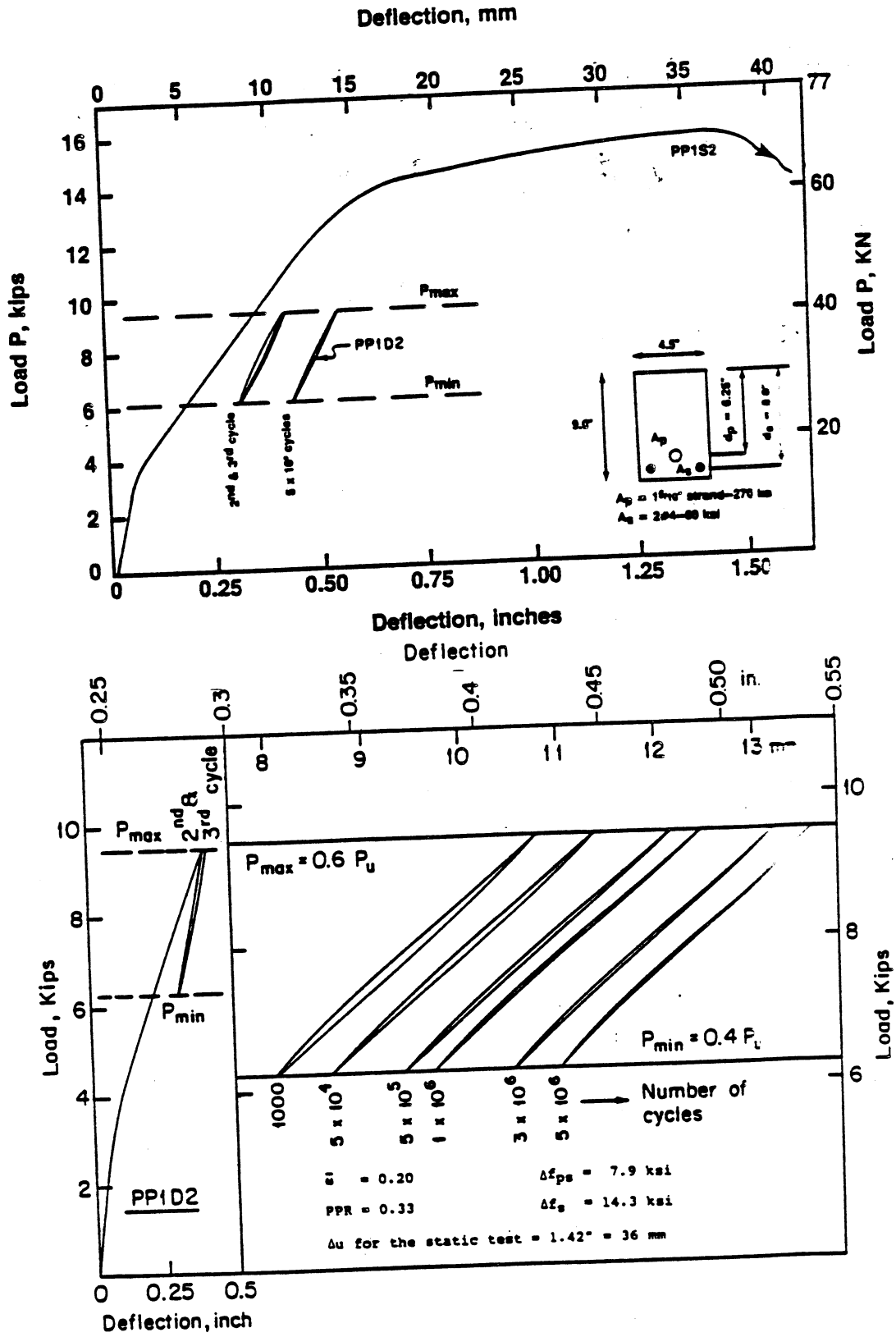

Fig. 3.11 Load-Deflection Curves For Beams: (a) PP1S2(Static)
(b) PP1D2 (Cyclic)

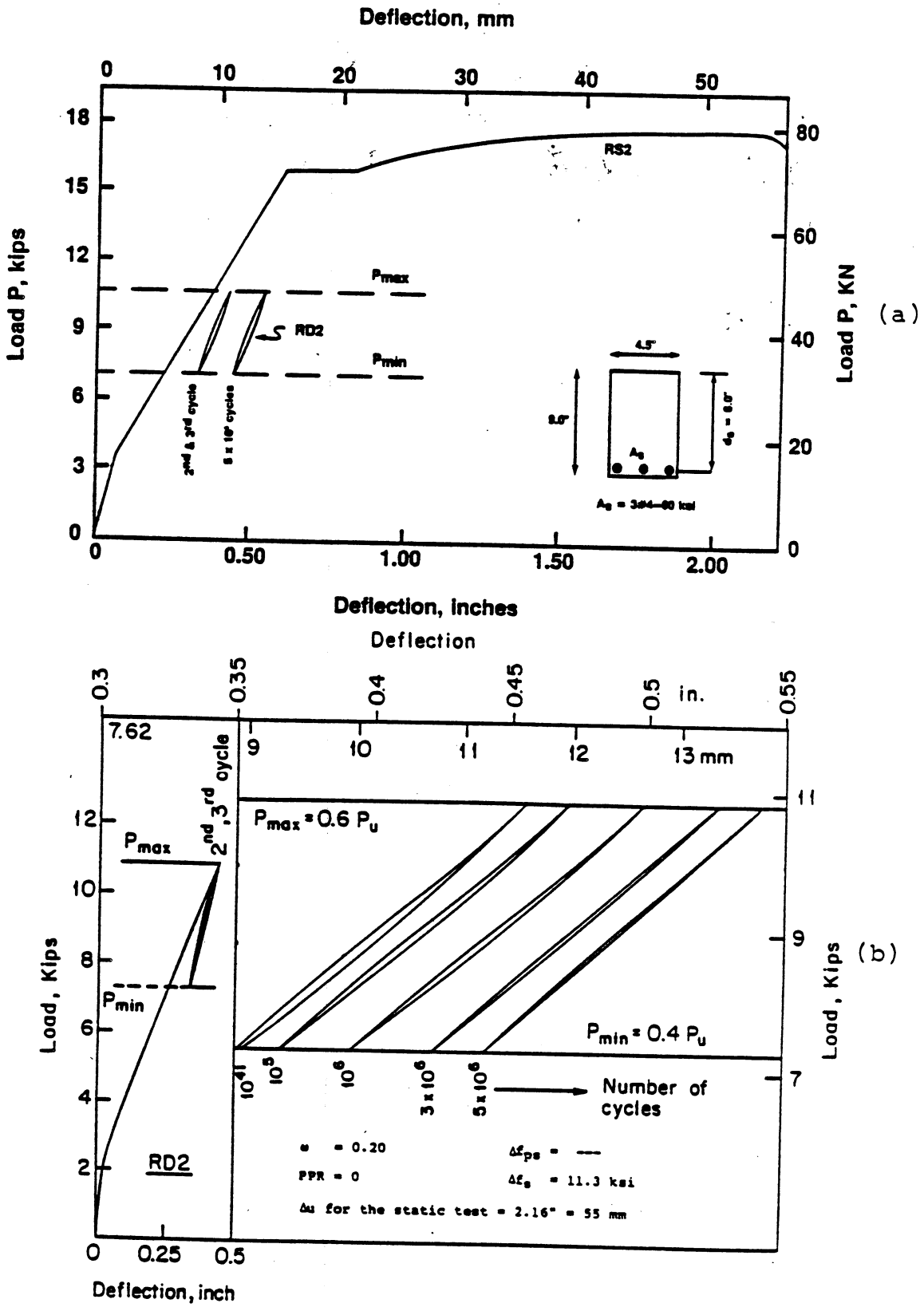

Fig. 3.12 Load-Deflection Curves For Beams: (a) RS2 (Static) (b) RD2 (Cyclic)

deflection slope for most of their fatigue life. However, prior to failure, the residual deflection is observed to increase dramatically, accompanied by a tremendous increase in the area enclosed within the load-deflection loop and a substantial reduction in stiffness. This behavior is a clear indication of the degree of distress and softening suffered by these beams due to fatigue.

The variation of maximum deflection for the various beams versus number of cycles N, measured at P_{max} is shown in figures 3.13-3.15. It can be seen that the curves show three different portions when plotted on a semi-log scale: In the first few hundred cycles there is relatively sharp increase in deflection followed by a second portion with a steady state increase up to 80-90% of the total number of cycles (log scale) and/or total life of the beam. In the third portion, generally all beams showed a sharp increase in deflection with increasing number of cycles. However, the increase in deflection is more pronounced in the fully prestressed beams in comparison with the partially prestressed or the fully reinforced ones indicating that these beams were about to fail. A similar behavior was observed by Bennet and Dave (29).

Generally it can be observed from these figures (3.13-3.15) that the rate of deflection variation with number of cycles (drawn on semi-log scale) tends to increase with an increase in the level of partial prestressing ratio

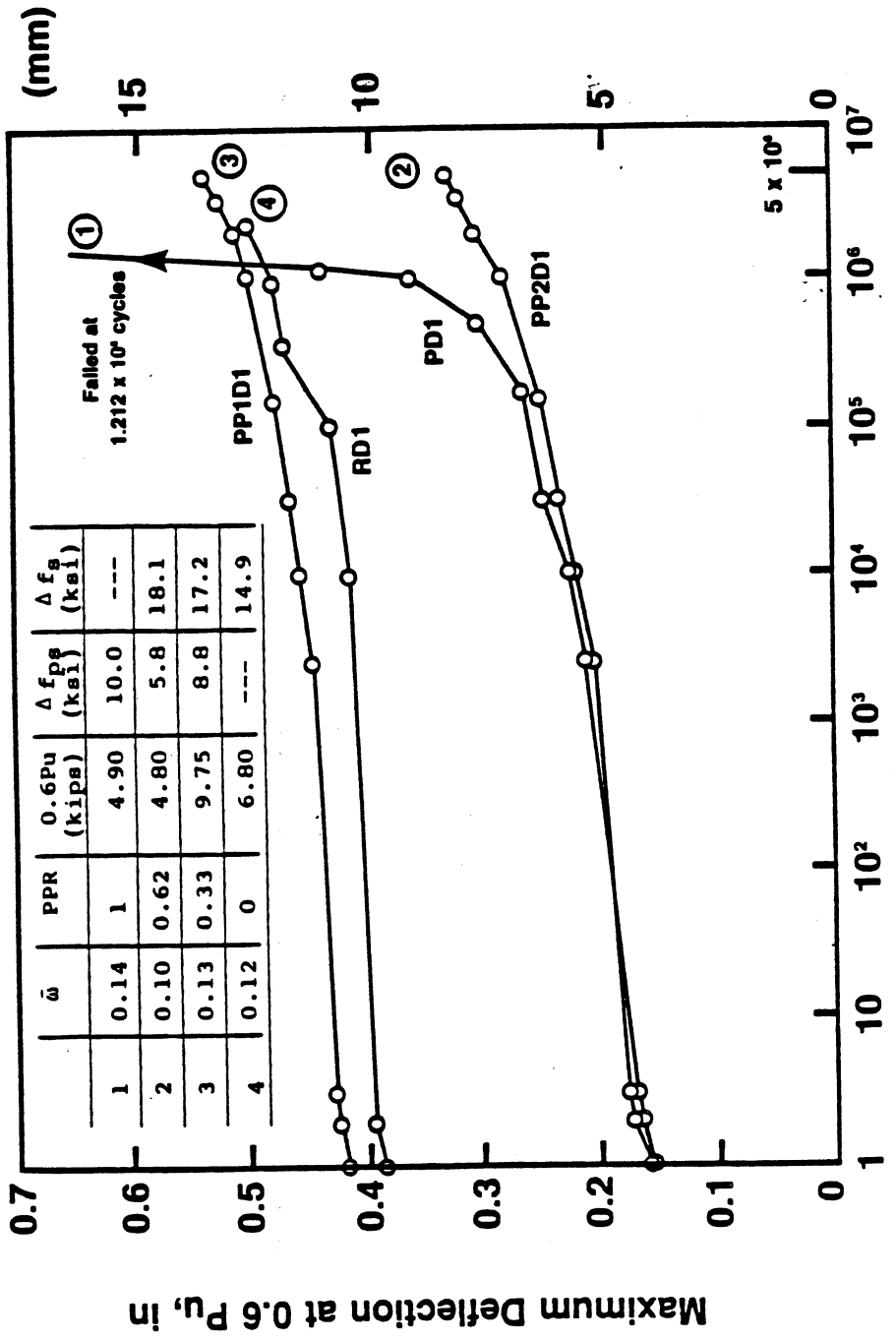

	ω̄	PPR	0.6Pu (kips)	Δ f_{ps} (ksi)	Δ f_s (ksi)
1	0.14	1	4.90	10.0	---
2	0.10	0.62	4.80	5.8	18.1
3	0.13	0.33	9.75	8.8	17.2
4	0.12	0	6.80	---	14.9

Fig. 3.13 Observed Deflection Versus Number Of Cycles ($\bar{\omega} = 1/3\ \omega_{max}$)

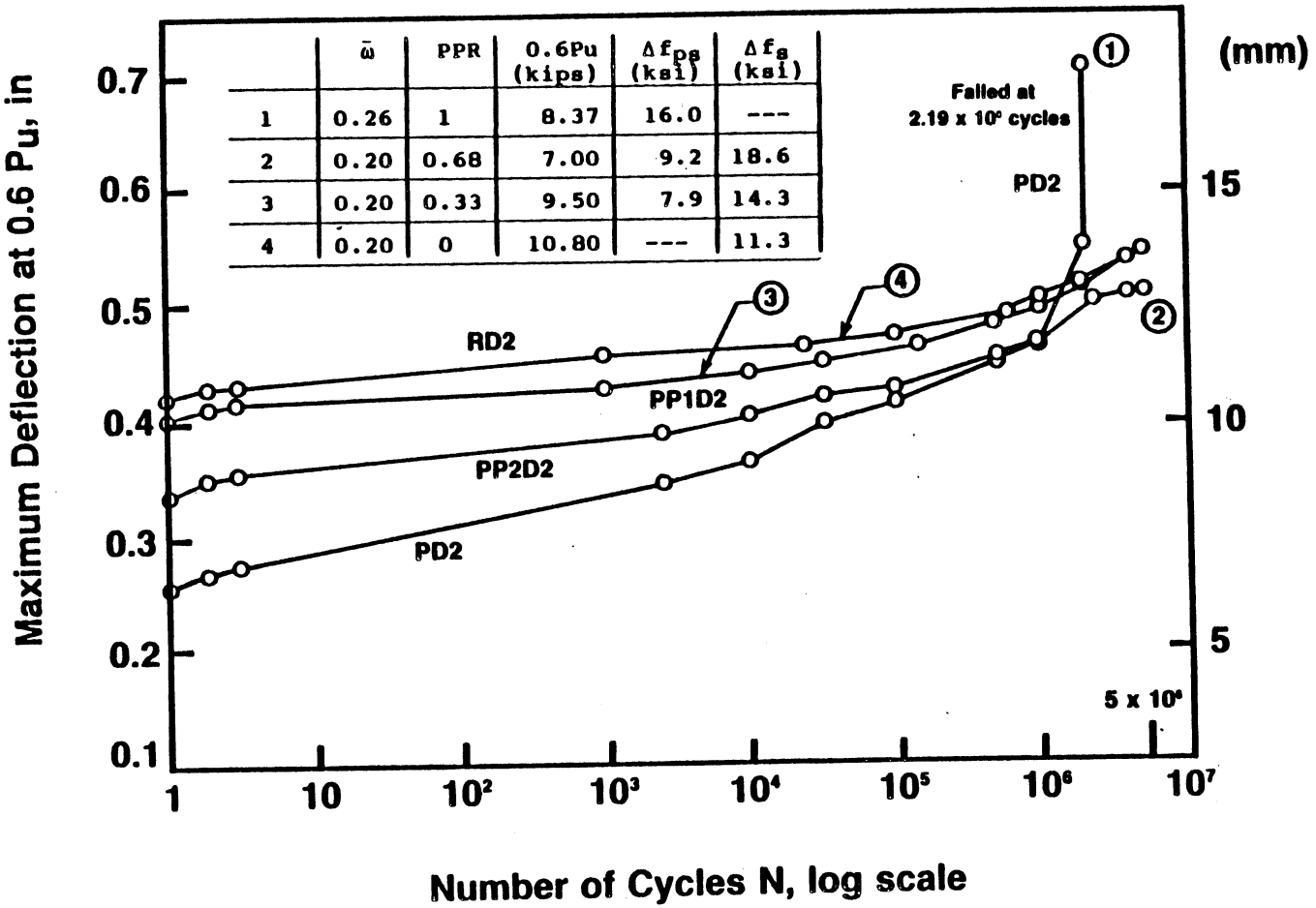

	$\bar{\omega}$	PPR	0.6Pu (kips)	Δf_{ps} (ksi)	Δf_s (ksi)
1	0.26	1	8.37	16.0	---
2	0.20	0.68	7.00	9.2	18.6
3	0.20	0.33	9.50	7.9	14.3
4	0.20	0	10.80	---	11.3

Fig. 3.14 Observed Deflection Versus Number Of Cycles ($\bar{\omega} = 2/3\ \omega_{max}$)

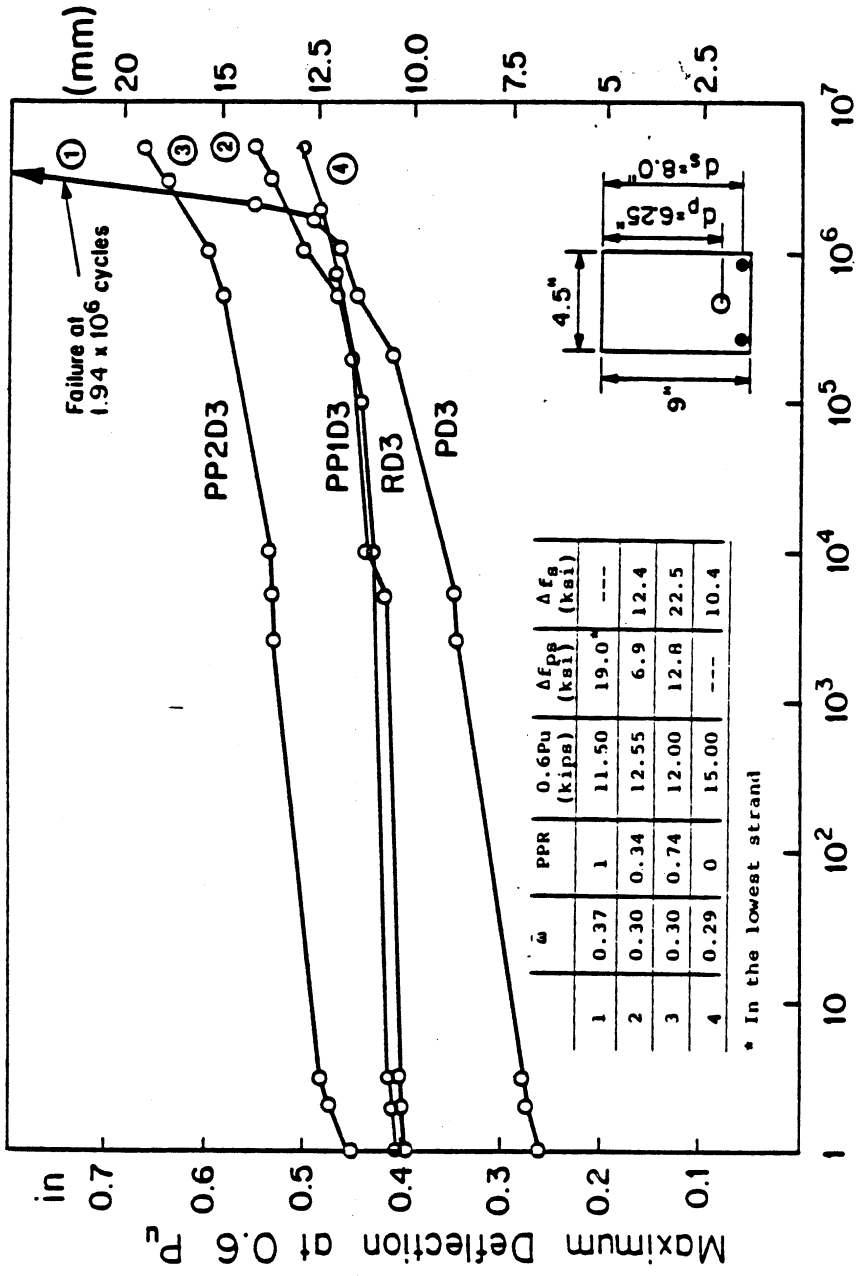

	$\bar{\omega}$	PPR	0.6Pu (kips)	Δf_{pe} (ksi)	Δf_s (ksi)
1	0.37	1	11.50	19.0*	---
2	0.30	0.34	12.55	6.9	12.4
3	0.30	0.74	12.00	12.8	22.5
4	0.29	0	15.00	---	10.4

Fig. 3.15 Observed Deflection Versus Number of Cycles ($\bar{\omega} = \omega_{max}$)

for approximately equal reinforcing index (this obsevation is clearer in figs. 3.14 and 3.15). Moreover, within the load range adopted in this study, the reinforcing index seems to have little influence on the beam deflection response with increasing number of cycles for most specimens (compare 3.13-3.15). However, for fully prestressed beams, the rate of deflection increase with increasing number of cycles was larger, the larger the reinforcing index. This observation for the fully prestressed beams is not general because the fatigue life of the fully prestressed beam with $\bar{\omega}$ close to 0.3 (PD3) was governed by the fatigue life of the strand closest to the bottom tension fiber.

3.5.2 Cracks and crack width

At the beginning of fatigue tests, crack spacing was measured for most of the beam specimens. Cracks that may have developed due to cyclic fatigue were checked occasionally; no such cracks developed for all the test beams. A summary of the average crack spacing and number of observed cracks are shown in table 3.4.

All beams were cracked during the first static cycle to P_{max}. In particular, beams PD1, PD2 and PD3 cracked at loads corresponding respectively to 53%, 51% and 49% of the ultimate load capacity of their sister (control) beam tested under static loading. The crack width at P_{max} in the first cycle was 0.15, 0.25 and 0.16 mm for PD1, PD2 and PD3 respectively measured at 1" from the bottom tension fiber.

The variation of crack width with increasing number of cycles (drawn on a semi-log scale) is shown in figures 3.16-3.18. Similar to the trend observed in deflection, crack width showed in general 3 different portions of

Table 3.4 Measured Crack Spacing And Number Of Cracks

Beam Designation	Average crack spacing (in)	Number of cracks
PD1	8.2	6
PD3	4.8	11
PP2D1	4.3	11
PP2D2	3.1	20
PP2D3	3.6	19
PP1D1	3.3	22
PP1D2	4.2	18
RD3	3.4	22

behavior (as described for deflection), specially for fully prestressed beams. However, this behavior was less pronounced for an increase in the level of reinforcing index specially for partially prestressed and fully reinforced specimens. Also, similar to the deflection trend, the rate of crack width tended to increase with increase in the partial prestressing ratio. This trend is more substantial for PPR equal 1 and PPR equal about 0.72. Fully reinforced beams showed little increase in the crack width with loading cycles.

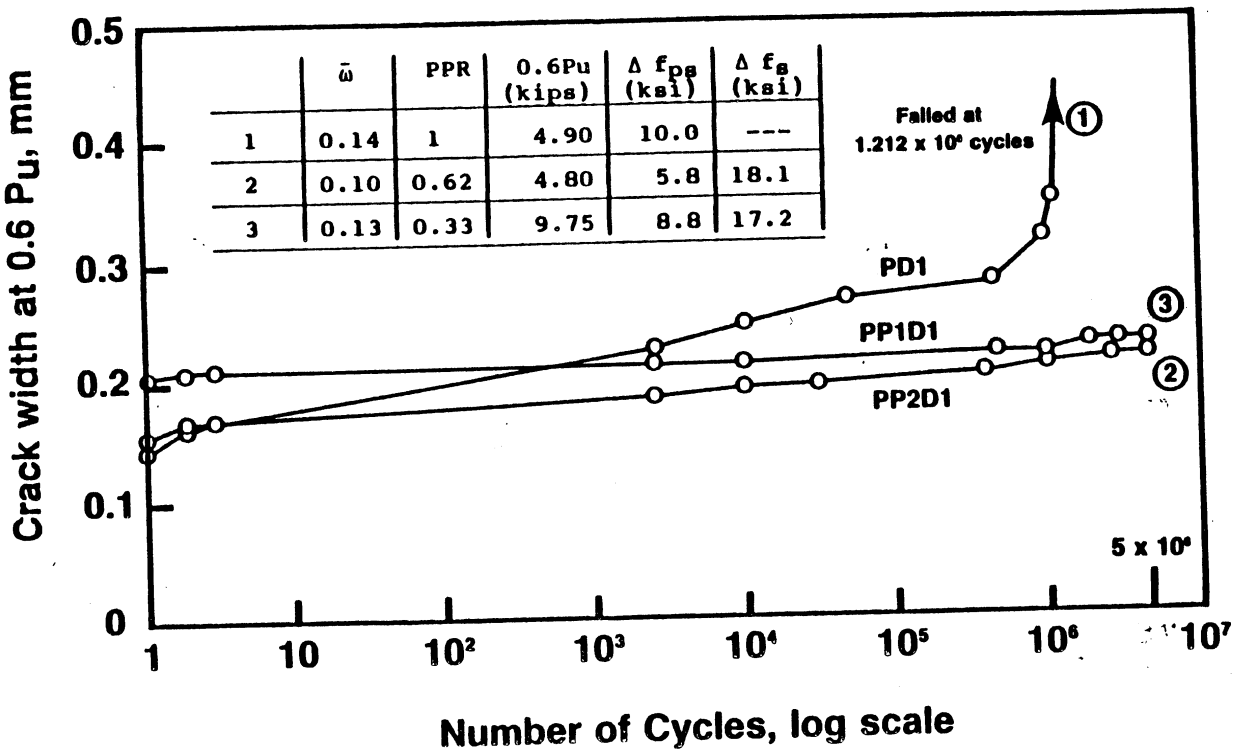

	$\bar{\omega}$	PPR	0.6Pu (kips)	Δf_{ps} (ksi)	Δf_s (ksi)
1	0.14	1	4.90	10.0	---
2	0.10	0.62	4.80	5.8	18.1
3	0.13	0.33	9.75	8.8	17.2

Fig. 3.16 Observed Crack Width Versus Number Of Cycles ($\bar{\omega}_{..} = 1/3\ \phi_{max}$)

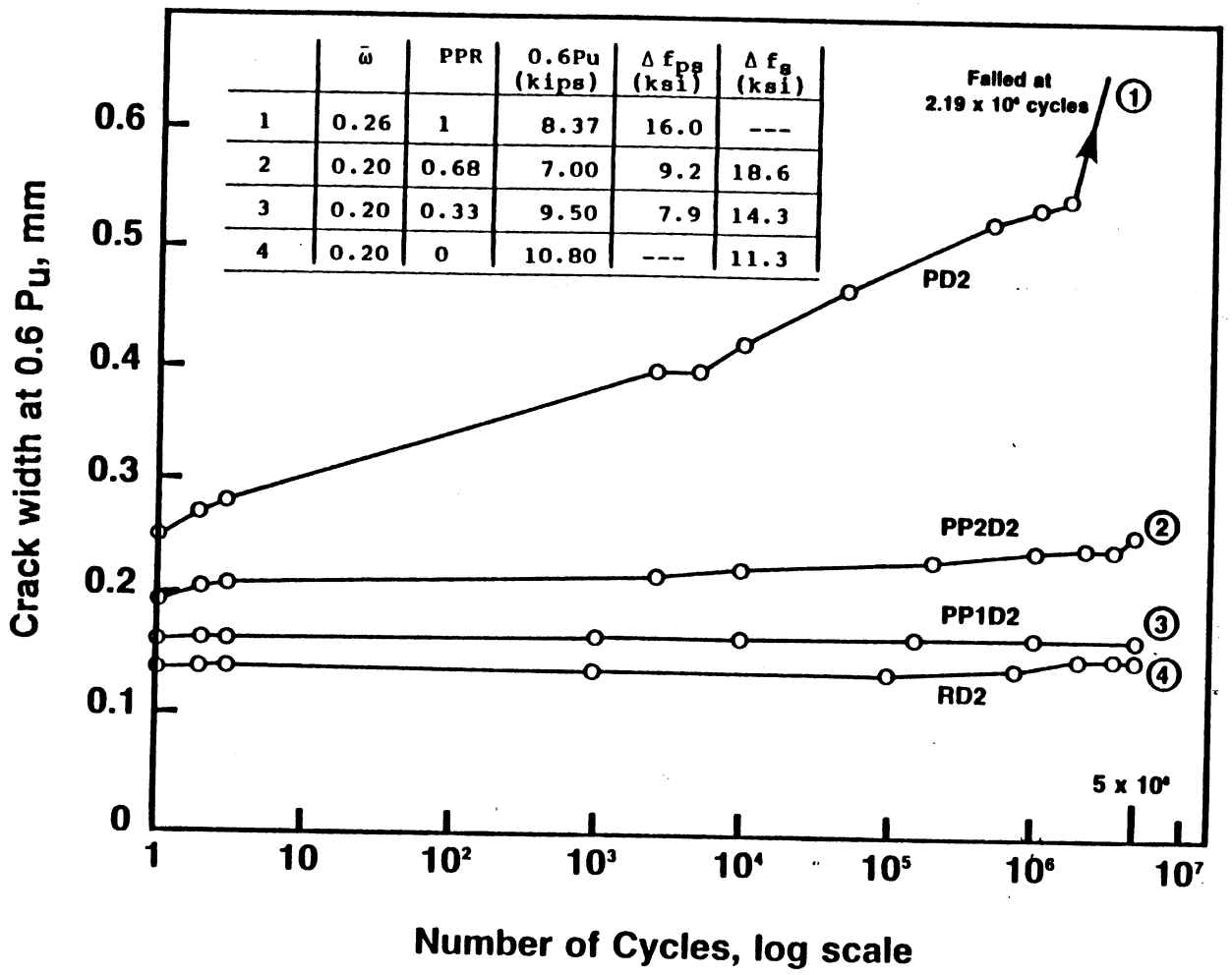

	$\bar{\omega}$	PPR	0.6Pu (kips)	Δf_{ps} (ksi)	Δf_s (ksi)
1	0.26	1	8.37	16.0	---
2	0.20	0.68	7.00	9.2	18.6
3	0.20	0.33	9.50	7.9	14.3
4	0.20	0	10.80	---	11.3

Fig. 3.17 Observed Crack Width Versus Number Of Cycles ($\bar{\omega} = 2/3\ \omega_{max}$)

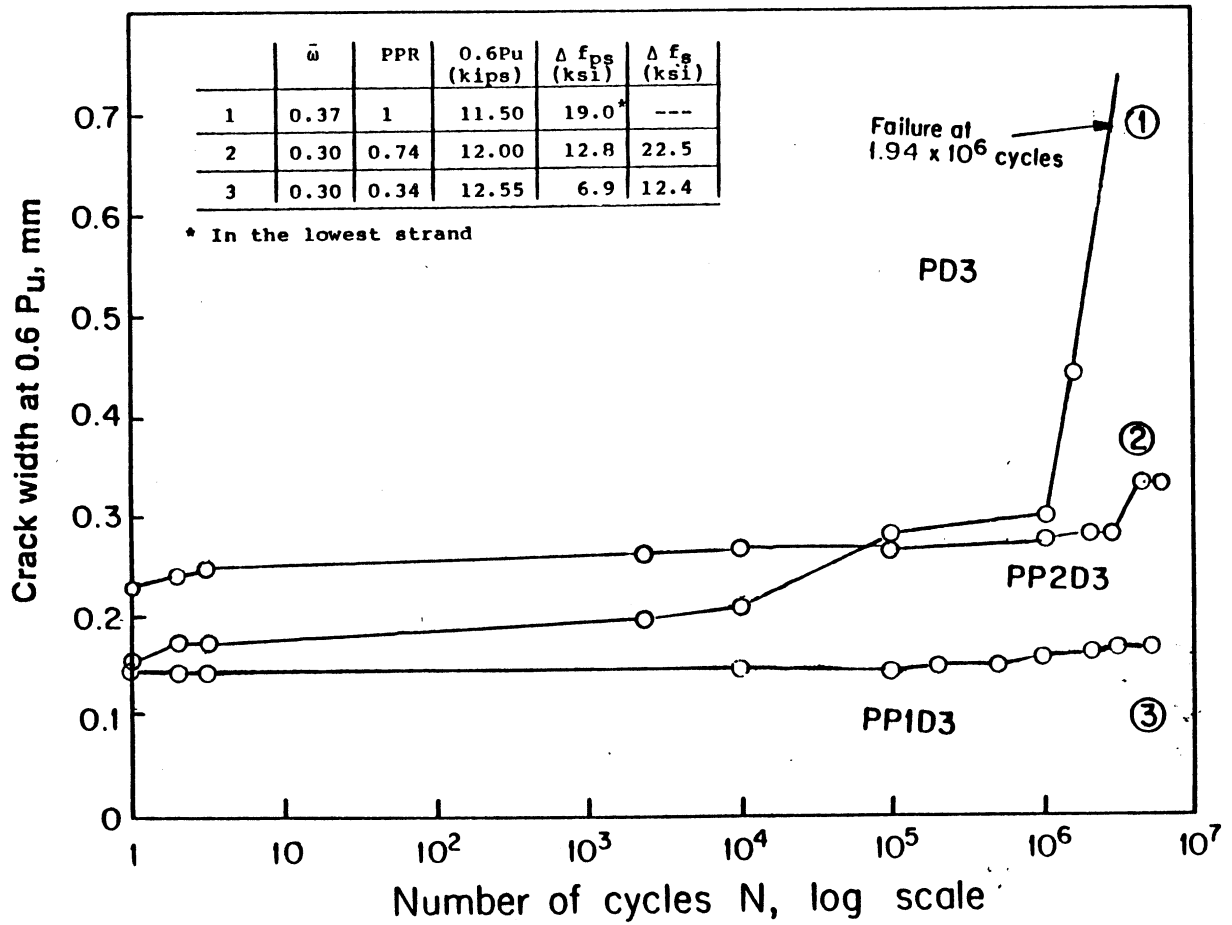

Fig. 3.18 Observed Crack Width Versus Number Of Cycles ($\bar{\omega} = \omega_{max}$)

For most of the beam specimens, the crack depth remained practically constant during the entire test. In the case of fully prestressed beams, cracks in the constant moment region, propagated upward with increasing number of cycles at relatively small rate. However, after one or several wire failures, these cracks were observed to propagate well into the compression zone of the beam branching out in two or three different directions.

Among all test specimens, only beam RD3 developed inclined shear cracks at its end supports during the first cycle to P_{max}. The crack propagated to about 2" (51 mm) from the top compression fiber and showed no sign of width increase througout the entire test (See figure 2.14-Test setup).

3.5.3 Average curvature

The average curvature was measured for 7 beams in the dynamic test over 10" gage length. Variation of curvature versus number of cycles drawn on a semi-log scale is shown in figure 3.19. It can be seen that a very similar trend exist between curvature and deflection variation with increasing number of cycles. Also similar observation can be made i.e 1) three stages of behavior comprising every curve, 2) increase in the slope of the aveage curvature versus logN with increasing PPR and 3) the relatively insignificant effect of the reinforcing index.

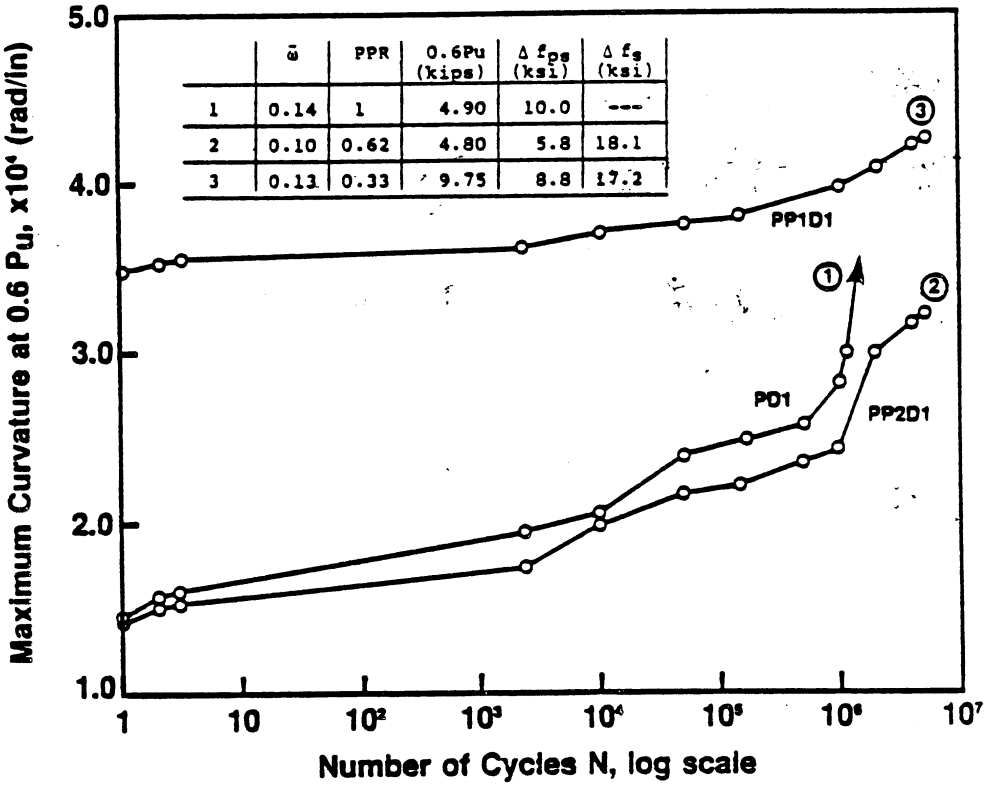

	ω̄	PPR	0.6Pu (kips)	Δ fps (ksi)	Δ fs (ksi)
1	0.14	1	4.90	10.0	---
2	0.10	0.62	4.80	5.8	18.1
3	0.13	0.33	9.75	8.8	17.2

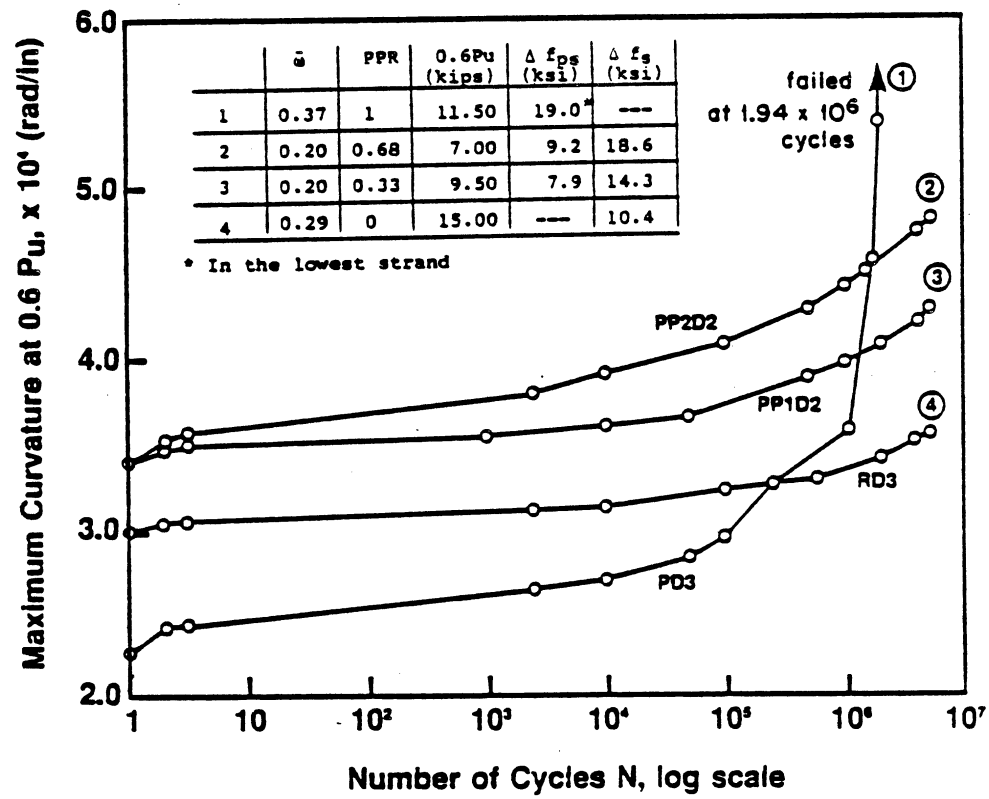

	ω̄	PPR	0.6Pu (kips)	Δ fps (ksi)	Δ fs (ksi)
1	0.37	1	11.50	19.0*	---
2	0.20	0.68	7.00	9.2	18.6
3	0.20	0.33	9.50	7.9	14.3
4	0.29	0	15.00	---	10.4

* In the lowest strand

Fig. 3.19 Variation Of Curvature Versus Number Of Cycles For Various Beam Specimens

3.6 Reinforcement Stresses

The measured strains (or stresses) in the tension reinforcement for the different test beams showed a continuous increase in strain measured at P_{max} and P_{min} and generally a continuous increase in the mean stress level and the stress range with increasing number of cycles. The increase in the stress range of prestressed strands during cyclic loading could be either due to reduction in the effective prestress resulting from slippage, (a similar phenomena was observed by Rabbat et al (23)), or could be due to stress redistribution resulting from the cyclic creep of concrete with increasing number of cycles. However, slip measurement during the test (Fig. 2.10) showed no sign of strand slippage. Moreover, strand slippage leads theoretically to a reduction in the stresses measured at P_{min} and P_{max}. Therefore the increase observed in this study was attributed to cyclic creep only.

Although most of the beams cracked well before P_{min}, specially those with low PPR, the strains in the prestressing strands and reinforcing bars measured during the first cycle at P_{min} were smaller than those measured during the 2^{nd} and 3^{rd} cycles. This phenomena resulted in stress ranges in the reinforcement higher in the first cycle than in subsequent cycles. These subsequent stress ranges were smaller than computed.

Measured and calculated stresses in the tension reinforcement at P_{max} and P_{min} for both static and cyclic beams are shown in tables 3.5, 3.6 and 3.7. In calculating these stresses, a general equation based on equilibrium and compatability (elastic analysis) predicted by Siriaksorn and Naaman (26) was used. These tables show that for most beam specimens, the measured and calculated stresses are quite comparable for the static beams and the first static cycle in the dynamic beams as well as at the maximum load level P_{max} in the 3^{rd} cycle. In the fully and partially prestressed beams where the crack had to close under P_{min}, the observed stress in the reinforcement was consistantly higher than predicted during 3^{rd} cycle at P_{min}. This was attributed to the roughness of the crack which did not close to zero or near zero level. Also, it can be observed from table 3.6 that the difference between the observed and calculated stresses at P_{min} is smaller for beams that cracked at smaller load level (PPR close to 0.3 and PPR equal to 0). The difference reaches an insignificant level in the fully reinforced beams.

3.7 Ultimate Load After Cycling

At the end of the fatigue test provided the beam did not fail before 5 million cycles, the test specimens were unloaded to zero load and then a static load test was conducted up to destruction. This test gives an indication of the performance of the test beams as to their ultimate

Table 3.5 Stresses in the prestressing and reinforcing steel at P_{min} and P_{max}. Cycle # 1

Beam	Load = 0.4 P_u*						Load = 0.6 P_u*					
	Δf_{ps} (ksi)			f_s (ksi)			Δf_{ps} (ksi)			f_s (ksi)		
	Calc.	Test	δ+	Calc.	Test	δ+	Calc.	Test	δ+	Calc.	Test	δ+
PD1	2.4	2.3	0.1	--	--	--	22.9	18.8	4.1	--	--	--
PD2	3.8	3.8	0.0	--	--	--	28.2	25.9	2.3	--	--	--
PD3	5.1	4.7	0.4	--	--	--	21.7	20.3	1.4	--	--	--
PP2D1	7.8	4.4	3.4	10.0	7.2	2.8	25.9	17.8	8.1	36.2	38.6	2.4
PP2D2	9.6	9.4	0.2	11.8	9.6	2.2	29.4	27.4	2.0	38.9	35.0	3.9
PP2D3	14.0	15.3	1.3	17.1	15.0	2.1	34.0	35.3	1.3	47.0	45.1	1.9
PP1D1	18.7	15.8	2.9	26.5	24.7	1.8	33.5	31.4	2.1	48.6	49.8	1.2
PP1D2	16.2	15.7	0.5	23.7	25.2	1.5	28.7	28.1	0.6	42.8	43.6	0.8
PP1D3	14.3	13.5	0.8	20.2	17.9	2.3	24.9	24.6	0.3	36.0	36.8	0.8
RD1	--	--	--	33.2	28.6	4.6	--	--	--	51.2	46.7	4.5
RD2	--	--	--	31.0	25.8	5.2	--	--	--	46.1	41.9	4.2
RD3	--	--	--	28.3	24.9	3.4	--	--	--	42.4	38.6	3.8
		Mean = 1.1 ksi S.D = 0.4 ksi			Mean = 2.9 ksi S.D = 0.5 ksi			Mean = 2.5 ksi S.D = 0.8 ksi			Mean = 2.6 ksi S.D = 0.5 ksi	

* Load values are given in tables 1D-12D

+ δ = | Test-Calc. |

Table 3.6 Stresses in the prestressing and reinforcing steel at P_{min} and P_{max}. Cycle # 3

Beam	Load = 0.4 P_u*						Load = 0.6 P_u*					
	Δf_{ps} (ksi)			f_s (ksi)			Δf_{ps} (ksi)			f_s (ksi)		
	Calc.	Test	δ +	Calc.	Test	δ +	Calc.	Test	δ +	Calc.	Test	δ +
PD1	2.8	11.1	8.3	--	--	--	22.9	21.1	1.5	--	--	--
PD2	4.5	12.0	7.5	--	--	--	28.2	28.0	0.2	--	--	--
PD3	5.2	9.4	4.2	--	--	--	21.7	21.7	0.0	--	--	--
PP2D1	7.8	13.2	5.4	10.0	22.6	12.6	25.9	19.0	6.9	36.2	40.7	4.5
PP2D2	9.6	19.5	9.9	11.8	17.9	6.1	29.4	28.7	0.7	38.9	36.5	2.4
PP2D3	14.0	23.6	9.6	17.1	23.9	6.8	34.0	36.4	2.4	47.0	46.4	0.6
PP1D1	18.7	23.5	4.8	26.5	33.5	7.0	33.5	32.3	1.2	48.6	50.7	2.1
PP1D2	16.2	21.1	4.9	23.7	29.4	5.7	28.7	29.1	0.4	42.8	43.8	1.0
PP1D3	14.3	17.8	3.5	20.2	24.9	4.7	24.9	24.7	0.2	36.0	37.3	1.3
RD1	--	--	--	33.2	32.5	0.7	--	--	--	51.2	47.5	3.7
RD2	--	--	--	31.0	31.7	0.7	--	--	--	46.1	43.0	3.1
RD3	--	--	--	28.3	29.0	0.7	--	--	--	42.4	39.4	3.0
		Mean = 6.5 ksi S.D = 0.9 ksi			Mean = 5.0 ksi S.D = 1.4 ksi			Mean = 1.5 ksi S.D = 0.8 ksi			Mean = 2.4 ksi S.D = 0.5 ksi	

* Load values are given in tables 1D-12D

+ $\delta = |\text{Test-Calc.}|$

Table 3.7 Stresses in the prestressing and reinforcing steel at two load levels, P_{min} and P_{max}. (static beams)

Beam	Load = 0.4 P_u*						Load = 0.6 P_u*					
	Δf_{ps} (ksi)			f_s (ksi)			Δf_{ps} (ksi)			f_s (ksi)		
	Calc.	Test	δ+	Calc.	Test	δ+	Calc.	Test	δ+	Calc.	Test	δ+
PS1	2.4	2.2	0.2	--	--	--	25.0	23.8	1.2	--	--	--
PS2	4.0	4.2	0.2	--	--	--	32.2	31.8	0.4	--	--	--
PS3	5.1	4.6	0.5	--	--	--	26.8	26.8	0.0	--	--	--
PP2S1	7.7	5.3	2.4	10.1	11.0	0.9	25.7	19.1	6.6	36.4	45.3	8.9
PP2S2	8.2	7.8	0.4	9.4	8.2	1.2	28.7	25.9	2.8	37.0	35.0	2.0
PP2S3	13.4	13.0	0.4	16.2	16.8	0.6	33.3	32.5	0.8	45.8	44.6	1.2
PP1S1	18.7	12.9	5.8	26.5	23.7	2.8	33.5	24.1	9.4	48.6	47.4	1.2
PP1S2	15.2	13.4	1.8	21.8	20.0	1.8	27.4	25.9	1.5	40.5	36.5	4.0
PP1S3	14.4	14.6	0.2	20.4	16.7	3.8	25.0	25.8	0.8	36.8	33.5	3.3
RS1	--	--	--	33.2	21.7	11.5x	--	--	--	51.2	36.2	15.0x
RS2	--	--	--	30.9	25.5	5.4	--	--	--	45.9	40.5	5.4
RS3	--	--	--	28.1	21.1	7.0	--	--	--	42.2	34.6	7.6
	Mean = 1.3 ksi S.D = 0.7 ksi			Mean = 2.9 ksi S.D = 0.9 ksi			Mean = 2.6 ksi S.D = 1.1 ksi			Mean = 4.2 ksi S.D = 1.1 ksi		

* Load values are given in tables 1D-12D

\+ $\delta = |\text{Test-Calc.}|$

x - Disregarded

load capacity and ductility after being subjected to 5 million cycles. A summary of the ultimate load and maximum deflection for the various beams in this test is shown in table 3.8. Additional results (deflection, crack width and curvature) are summarized (except for beam RD1) in tables B1-B8 of Appendix B. Load-deflection curves of these beams compared with their sister static beams are shown in figures A8-A15 of Appendix A.

It can be observed from the data that the static strength of the fatigue beams (after 5 million cycles) is not much different from that of their control static specimens. However, their ultimate deformation was generally smaller (except for PP1D2 and PP2D3).

Beam Designation	Deflection at P=0 (in)	Deflection at P=Pu (in)	Pu (kips)
PP2D1	0.13	3.10	8.06
PP2D2	0.17	1.63	11.25
PP2D3	0.21	1.59	19.57
PP1D1	0.15	3.26	15.60
PP1D2	0.20	1.80	15.50
PP1D3	---	1.00	21.80
RD1	---	3.19	11.29
RD2	0.18	1.76	17.20
RD3	0.16	0.85	24.70

Table 3.8 Deflection And Load Characteristics Of Beams Loaded To Failure After 5 Million Cycles

CHAPTER IV

OBSERVATIONS AND CONCLUSIONS

4.1 Observations

The following important observations were made in this study:

1. The rate of increase of deflection, crack width and curvature was significant in the early stages of load cycles. A second phase followed in which they remain essentially the same or increase at a small rate. Significant reduction in stiffness and rapid increase in deflection and crack width were observed in the last phase before failure. This sudden change of behavior is a result of fracturing of some individual wires in the strand which increases the stress range in the remaining tensile reinforcement. This increase in the stress range leads to a rapid fracturing of other wires and hence a rapid increase in deflections an crack widths. Failure of the beams occur shortly thereafter.
2. Failure of the strands in the three fully prestressed beams occurred in the constant moment region of the beam at the location of a crack as expected. Generally failure starts by fracturing of an external wire. The stresses and hence the stress ranges in the tension reinforcement are higher at the crack location than at any uncracked region in the beam. Therefore stress conditions at the crack control the fatigue life of the

tension reinforcement. The local debonding on either side of the crack during the cyclic process results in fretting and abrasion of the strand due to successive closing and opening of the crack under fluctuating load. This phenomenon adds to the probability of fatigue fracture in at least one of the strand's external wires in contact with the surrounding concrete.

3. All prestressed and partially prestressed beams in this investigation showed no sign of bond failure. Therefore strand slippage did not contribute to the fatigue life of the specimens.
4. Fatigue failure in the beams resulted from fatigue fracturing of the strands. The stress ranges versus total number of cycles were compared with recently published data. The result suggest that the fatigue life of the beams could be predicted reasonably well from the fatigue life of strand samples tested freely in air.
5. The stress ranges observed in the early stages of cycles in the strands which failed by fatigue were $0.04f_{pu}$, $0.07f_{pu}$ and $0.06f_{pu}$. Calculated fictitious nominal tensile stress in the corresponding fully prestressed beams were respectively $8.9\sqrt{f'_c}$, $15.6\sqrt{f'_c}$ and $24.1\sqrt{f'_c}$. Moreover fictitious nominal tensile stresses of up to $32.8\sqrt{f'_c}$ were obtained in PPC beams without failure. These results suggest that limiting the

fictitious tensile stress for the design of PC and PPC beams is not a rational design criterion.

6. Stresses in the tension reinforcement measured at P_{min} and P_{max} increased with the number of loading cycles. The stress increase was more pronounced for fully prestressed beams than for either partially prestressed or fully reinforced specimens. This phenomenon increased substantially the stress range under load and led to a reduction in fatigue life.

4.2 Conclusions

The following conclusions could be drawn from this study:

1. For approximatly equal reinforcing index $\bar{\omega}$, the rate of growth of crack width, deflection, and/or curvature under fatigue loading tends to be higher for beams with higher partial prestressing ratios. Large areas of non prestressed tension reinforcement (beams with low PPR) enhance the overall bond characteristics of the tension reinforcement and results in lesser stiffness deterioration with repeated loadings.
2. For approximately equal partial prestressing ratios and for equal load ranges expressed in percent of ultimate load, the reinforcing index appears to have little influence on the rate of increase of crack width, deflection and/or curvature with the number of loading cycles.

3. Stresses observed in the early cycling stages were comparable to stresses computed from linear elastic cracked section analysis.
4. Beams that survived 5 million cycles showed practically no reduction in ultimate load capacity when tested to failure after cycling. However a reduction in ductility was generally observed.

In summary, it appears from this investigation that a reliable evaluation of the fatigue characteristics of prestressed and partially prestressed beams requires the development of a general model based on cracked section analysis to calculate under cyclic loading, stresses and stress ranges induced in the component materials. This model should take into account the progressive time and cyclic dependent changes that accompany the structure throughout its design life time such as creep and shrinkage in the concrete, relaxation and prestress loss in the prestressing steel.

LIST OF REFERENCES

1. ACI Committee 215, "Consideration For Design of Concrete Structures Subjected to Fatigue Loading," ACI Journal, Vol. 71, No.3, March 1974, pp. 97-121.

2. ACI Standard 318-83, "Building Code Requirements For Reinforced Concrete," American Concrete Institute, Detroit, Michigan.

3. The American Association of State Highway and Transportation Officials, (AASHTO), "Standard Specifications For Highway Bridges," 12th Edition, 1977.

4. Murdock, J.W., and Kesler, C.E., "Effect of Stress on Fatigue Strength of Concrete Beams," ACI Journal, Proceedings, Vol.55, No.2, August 1958, pp. 221-231.

5. Hilsdorf, H.K., and Kesler, C.E., "Fatigue Strength of Concrete Under Varying Flexural Stresses," ACI Journal, Proceedings, Vol. 63, No. 10, October 1966, pp. 1059-1075.

6. Mccall, J.T., "Probability of Fatigue Failure of Plain Concrete," ACI Journal, Proceedings, Vol. 55, No. 2, August 1958, pp. 233-244.

7. Norby, G.M., "Fatigue of Concrete - A Review of Research," ACI Journal, Proceedings, Vol. 55, No. 2, August 1958, pp. 191-219.

8. Bennet, E.W., and Raju, N.K., "Cumulative Damage of Plain Concrete in Compression," Proceedings, International Conference of Structures, Solid Mechanics and Engineering Design in Civil Engineering Materials, University of Southampton, April 1969.

9. Shah, S.P, and Chandra, S., "Fracture of Concrete Subjected to Cyclic and Sustained Loading," ACI Journal, Proceedings Vol. 67, No. 10, October 1970, pp. 816-824.

10. Helgason, T., Hanson, J.M., Somes, N.F., Corley, W.G., and Hognestad, E., " Fatigue Strength of High-Yield Reinforcing Bars," Report for NCHRP Projects 4-7 and 4-7/1, Portland Cement Association (PCA), Research and Development Bulletin RD045.01E, Skokie, Illionois, March 1975, 372 pp.

11. ACI Committee 343, Report on "Analysis and Design of Reinforced Concrete Bridge Structures," ACI 343R-77, Detroit, Michigan, 1977, 118 pp.

12. Lane, R.E., and Ekberg, C.E., Jr., "Repeated Load Tests on 7-Wire Prestressing Strands," Progress Report No. 223.21, Fritz Engineering Laboratory, Lehigh University, Bethlehem, Pe., 1959.

13. Tide, H.R., and Van Horn,D.A., "A Statistical Study of the Static and Fatigue Properties of High Strength Prestressing Strands," Report No. 309.2, Fritz Engineering Laboratory, Lehigh University, June 1966, 86 pp.

14. Warner, R.F., and Hulsbos, C.L., "Fatigue Properties of Prestressing Strands," PCI Journal, Vol. 11, No. 1, February 1966, pp. 32-52.

15. Edwards, A.D., and Picard, A., "Fatigue Characteristics of Prestressing Strands," Proceedings, ICE (London), Vol. 53, September 1972, pp. 323-336.

16. Naaman, A.E., "A Proposal to Extend Some Code Provisions on Reinforcement to Partial Prestressing," PCI Journal, Vol. 26, No. 2, March-April 1981, pp. 74-91.

17. Naaman, E.A., "Research Needs in Partial Prestressing," PCI Journal, Vol. 27, No. 4, July-August 1982, pp. 106-107.

18. Naaman, A.E., "Partially Prestressed Concrete Design, American View Point," International Symposium-Nonlinearity and Continuity in Prestressed Concrete, University of Waterloo, Waterloo, Ontario, Canada, July 4-6, 1983.

19. Irwin, C.A.K., "Static and Repetitive Loading Tests on Full Scale Prestressed Concrete Bridge Beams," Transport and Road Research Laboratory, TRRL, Department of Transport, Report 802, England 1977.

20. Hilmes, J.B., and Ekberg, C.E., "Statistical Analysis of the Fatigue Characteristics of Under-Reinforced Prestressed Concrete Flexural Members," Iowa Engineering Experimental Station, Ames, 1965 (Iowa State University of Science and Technology).

21. Fisher, J.W., and Viest, I.M., "Fatigue Tests of Bridge Materials of the AASHTO Road Test," Special Report No. 66, Highway Research Board, 1961, pp. 132-147.

22. Hanson, J.M., Hulsbos, C.L., and Van Horn, D.A., "Fatigue Tests of Prestressed Concrete I-Beams," Proceedings, ASCE, Vol. 96, No. ST11, November 1970, pp. 2443-2463.

LIST OF REFERENCES

1. ACI Committee 215, "Consideration For Design of Concrete Structures Subjected to Fatigue Loading," ACI Journal, Vol. 71, No.3, March 1974, pp. 97-121.

2. ACI Standard 318-83, "Building Code Requirements For Reinforced Concrete," American Concrete Institute, Detroit, Michigan.

3. The American Association of State Highway and Transportation Officials, (AASHTO), "Standard Specifications For Highway Bridges," 12th Edition, 1977.

4. Murdock, J.W., and Kesler, C.E., "Effect of Stress on Fatigue Strength of Concrete Beams," ACI Journal, Proceedings, Vol.55, No.2, August 1958, pp. 221-231.

5. Hilsdorf, H.K., and Kesler, C.E., "Fatigue Strength of Concrete Under Varying Flexural Stresses," ACI Journal, Proceedings, Vol. 63, No. 10, October 1966, pp. 1059-1075.

6. Mccall, J.T., "Probability of Fatigue Failure of Plain Concrete," ACI Journal, Proceedings, Vol. 55, No. 2, August 1958, pp. 233-244.

7. Norby, G.M., "Fatigue of Concrete - A Review of Research," ACI Journal, Proceedings, Vol. 55, No. 2, August 1958, pp. 191-219.

8. Bennet, E.W., and Raju, N.K., "Cumulative Damage of Plain Concrete in Compression," Proceedings, International Conference of Structures, Solid Mechanics and Engineering Design in Civil Engineering Materials, University of Southampton, April 1969.

9. Shah, S.P, and Chandra, S., "Fracture of Concrete Subjected to Cyclic and Sustained Loading," ACI Journal, Proceedings Vol. 67, No. 10, October 1970, pp. 816-824.

10. Helgason, T., Hanson, J.M., Somes, N.F., Corley, W.G., and Hognestad, E., " Fatigue Strength of High-Yield Reinforcing Bars," Report for NCHRP Projects 4-7 and 4-7/1, Portland Cement Association (PCA), Research and Development Bulletin RD045.01E, Skokie, Illionois, March 1975, 372 pp.

11. ACI Committee 343, Report on "Analysis and Design of Reinforced Concrete Bridge Structures," ACI 343R-77, Detroit, Michigan, 1977, 118 pp.

12. Lane, R.E., and Ekberg, C.E., Jr., "Repeated Load Tests on 7-Wire Prestressing Strands," Progress Report No. 223.21, Fritz Engineering Laboratory, Lehigh University, Bethlehem, Pe., 1959.

13. Tide, H.R., and Van Horn,D.A., "A Statistical-Study of the Static and Fatigue Properties of High Strength Prestressing Strands," Report No. 309.2, Fritz Engineering Laboratory, Lehigh University, June 1966, 86 pp.

14. Warner, R.F., and Hulsbos, C.L., "Fatigue Properties of Prestressing Strands," PCI Journal, Vol. 11, No. 1, February 1966, pp. 32-52.

15. Edwards, A.D., and Picard, A., "Fatigue Characteristics of Prestressing Strands," Proceedings, ICE (London), Vol. 53, September 1972, pp. 323-336.

16. Naaman, A.E., "A Proposal to Extend Some Code Provisions on Reinforcement to Partial Prestressing," PCI Journal, Vol. 26, No. 2, March-April 1981, pp. 74-91.

17. Naaman, E.A., "Research Needs in Partial Prestressing," PCI Journal, Vol. 27, No. 4, July-August 1982, pp. 106-107.

18. Naaman, A.E., "Partially Prestressed Concrete Design, American View Point," International Symposium-Nonlinearity and Continuity in Prestressed Concrete, University of Waterloo, Waterloo, Ontario, Canada, July 4-6, 1983.

19. Irwin, C.A.K., "Static and Repetitive Loading Tests on Full Scale Prestressed Concrete Bridge Beams," Transport and Road Research Laboratory, TRRL, Department of Transport, Report 802, England 1977.

20. Hilmes, J.B., and Ekberg, C.E., "Statistical Analysis of the Fatigue Characteristics of Under-Reinforced Prestressed Concrete Flexural Members," Iowa Engineering Experimental Station, Ames, 1965 (Iowa State University of Science and Technology).

21. Fisher, J.W., and Viest, I.M., "Fatigue Tests of Bridge Materials of the AASHTO Road Test," Special Report No. 66, Highway Research Board, 1961, pp. 132-147.

22. Hanson, J.M., Hulsbos, C.L., and Van Horn, D.A., "Fatigue Tests of Prestressed Concrete I-Beams," Proceedings, ASCE, Vol. 96, No. ST11, November 1970, pp. 2443-2463.

23. Rabbat, B.G., Kaar, P.H., Russell, H.G., and Bruce, R.N., Jr., "Fatigue Tests of Full-Size Prestressed Girders," Technical Report No. 113, Portland Cement Association, Research and Development Laboratories, June 1978.

24. Ozel, A.M., and Ardaman, E., "Fatigue Tests of Pretensioned Prestressed Beams," ACI Journal, Proceedings, Vol. 53, No. 4, October 1956, pp. 413-424.

25. Abeles, P.W., Brown, E.I., and Hu, C.H., "Fatigue Resistance of Under-Reinforced Prestressed Beams Subjected to Different Stress Ranges; Miner's Hypothesis," ACI Journal, SP-41, Paper 11, 1974, pp. 237-277.

26. Naaman, A.E., and Siriaksorn, A., "Serviceability Based Design of Partially Prestressed Beams. Part 1: Analytic Formulation," PCI Journal, Vol. 24, No. 2, March-April 1979, pp. 64-89.

27. Siriaksorn, A., and Naaman, A.E., "Serviceability Based Design of Partially Prestressed Beams. Part 2: Computarized Design and Evaluation of Major Parameters," PCI Journal, Vol. 24, No. 3, May-June 1979, pp. 40-60.

28. Naaman, A.E., "Fatigue in Partially Prestressed Beams," ACI Publication SP 75-2, 1982, pp.25-46.

29. Bennet, E.W., and Dave, N.J., "Test Performance and Design of Concrete Beams With Limited Prestress," The Structural Engineer (London), Vol. 47, No. 12, December 1969, pp. 487-496.

30. Dave, N.H., and Garwood, J.J., "The Limit State Behavior of "Class-3" Post-Tensioned Beams Under Short-Term, Sustained and Fatigue Loadings," In Behavior in Service of Concrete Structures, Colloquium Interassociation I.A.B.S.E., F.I.P, C.E.B., R.I.L.E.M., I.A.S.S., Liege, June 1975, pp. 319-330.

31. Fauchart, J., and Trinh, J., "Comportement Sous Charges Repetees de Poutrelles en Beton Arme Preconstraint," Annales de L'Institut Technique du Batiment et des Travaux Publics, Paris, Septembre-Octobre 1973, pp. 87-132.

32. Fauchart, J., Kavyrchine, M., and Trinh, J., "Complement to Ref. 29," Annales I.T.B.T.P., March 1975, pp. 23-32.

33. Corley, W.G., Hanson, J.M., and Halgason, T., "Design

of Reinforced Concrete For Fatigue," ASCE Journal, Vol. 104, No. ST6, June 1978, pp. 921-932.

34. Foo, M.H., and Warner, R.F., "Fatigue Test on Partially Prestressed Concrete Beams," In Partial Prestressing From Theory To Practice, NATO Advanced Research Workshop, Paris, France, June 18-22, 1984.

35. Hawkins, N.M., "Fatigue Design Considerations For Reinforcement in Concrete Bridge Decks," ACI Journal, Vol. 73, No. 2, February 1976, pp. 104-115.

36. Chang, T.S., and Kesler, C.E., "Fatigue Behavior of Reinforced Concrete Beams," ACI Journal, Vol. 55, No. 2, August 1958, pp. 245-259.

37. Ekberg, C.E., Walther, R.E., and Slutter, R.G., "Fatigue Resistance of Prestressed Beams in Bending," ASCE Journal, Structural Division, Vol.83, No. ST4, Proc. 1304.

38. Gylltoft, K., "Fatigue Tests of Concrete Sleepers," Division of Structural Engineering, University of Lulea, Research Report No. TULEA 1978:13.

39. FIP Commission on Prestressing Steel and Systems "Report on Prestressing Steels: Types and Properties," FIP, Wexham Spring, England, August 1976, 18 pp.

40. Venuti, W.J., "A Statistical Approach to the Analysis of Fatigue Failure of Prestressed Concrete Beams," ACI Journal, Proceedings Vol. 62, No. 11, November 1965, pp. 1375-1394.

41. Mansur, M.A., "Partially Prestressed Concrete Beams Under Repeated Loading," International Symposium - Nonlinearity and Continuity in Prestressed Concrete, University of Waterloo, Waterloo, Ontario, Canada, July 4-6, 1983.

42. Balaguru, P.N., Naaman, A.E., and Shah, S.P., "Analysis of Prestressed Concrete Beams For Fatigue Loading," PCI Journal, May-June 1981, pp. 70-94.

43. Balaguru, P.N., Naaman, A.E., and Shah, S.P., "Serviceability of Ferrocement Subjected to Flexural Fatigue," The International Journal of Cement Composites, Vol. 1, No. 1, May 1979, pp. 3-9.

44. Balaguru, P.N., Namman, A.E., and Shah, S.P., "Ferrocement in Bending, Part II: Fatigue Analysis," Report No. 77-1, Department of Materials Engineering, University of Illinois at Chicago, Chicago, October 1977.

45. Warner, R.F., and Hulsbos, C.L., "Probable Fatigue Life of Prestressed Concrete Beams," PCI Journal, Vol. 11, No. 2, April 1966, pp. 16-39.

46. Magura, D.D., Sozen, M.A., and Siess, C.P., "A Study of Stress Relaxation in Prestressing Reinforcement," PCI Journal, Vol. 9, No. 2, April 1964, pp. 13-57.

47. Gylltoft, K., "Bond Properties of Strands in Fatigue Loading," Division of Structural Engineering, University of Lulea, Research Report No. TULEA 1979:22.

48. Watcharaumnuay, S., and Naaman, A.E., "Deflection of Partially Prestressed Concrete Beams Under Sustained and Cyclic Fatigue Loading," Report In Progress.

49. ACI Committee 224, "Control of Cracking in Concrete Structures," ACI Journal, No. 69, December 1972, pp. 717-753.

50. Nawy, E.G., and Huang, P.T., "Crack and Deflection Control of Pretensioned Prestressed Beams," PCI Journal, Vol. 22, No. 3, May-June 1977, pp. 30-47.

51. Bennet, E.W., and Chandrasekhar, C.S., "Calculation of the Width of Cracks in 'Class 3' Prestressed Beams," Proceedings, Institution of Civil Engineers (London), Vol. 49, July 1971, pp. 333-346.

52. Nilson, A.H., "Flexural Stresses after Cracking in Partially Prestressed Beams," PCI Journal, Vol. 21, No. 4, July-August 1976, pp. 72-81.

53. Gergely, P., and Lutz, L.A., "Maximum Crack Width in Reinforced Flexural Members," In Causes, Mechanisms and Control of Cracking in Concrete, SP-20, ACI, Detroit, 1968, pp. 87-117.

54. Park, R., and Thompson, K.J., "Cyclic Load Tests on Prestressed and Partially Prestressed Beam-Column Joints," PCI Journal, Vol. 22, No. 5, September-October 1977, pp. 84-111.

55. Park, R., and Thompson, K.J., "Ductility of Prestressed and Partially Prestressed Concrete Sections," PCI Journal, Vol. 25, No. 2, March-April 1980, pp. 45-69.

56. Cohn, M.Z., and Bartlett, M., "Nonlinear Flexural Response of Partially Prestressed Concrete Sections," Solid Mechanics Division, University of Waterloo, Waterloo, Ontario, Canada, Paper No. 168, October 1981.

57. Pfrang, E.O., Siess, C.P., and Sozen, M.A., "Load

Moment-Curvature Characteristics of Reinforced Concrete Cross Sections," ACI Journal, Proceedings, Vol. 61, No. 7, July 1964, pp. 763-778.

58. Mattock, A.H, "Rotational Capacity of Hinging Region in Reinforced Concrete Beams," Proceedings Int'l. Symposium on Flexural Mechanics of Reinforced Concrete, ASCE, 1965, pp. 143-181.

59. Warwaruk, J., Sozen, M.A., and Siess, C.P., "Strength and Behavior in Flexure of Prestressed Concrete Beams" University of Illinois Engineering Experiment Station, Bulletin No. 464, Urbana, Illinois, August 1962.

60. Naaman, A.E., "Prestressed Concrete Analysis and Design" Macgraw Hill Company, 1982.

61. Park, R., and Paulay, T., "Reinforced Concrete Structures," John Wiley and Sons, Inc., 1975.

APPENDIX A

Load-Deflection Curves

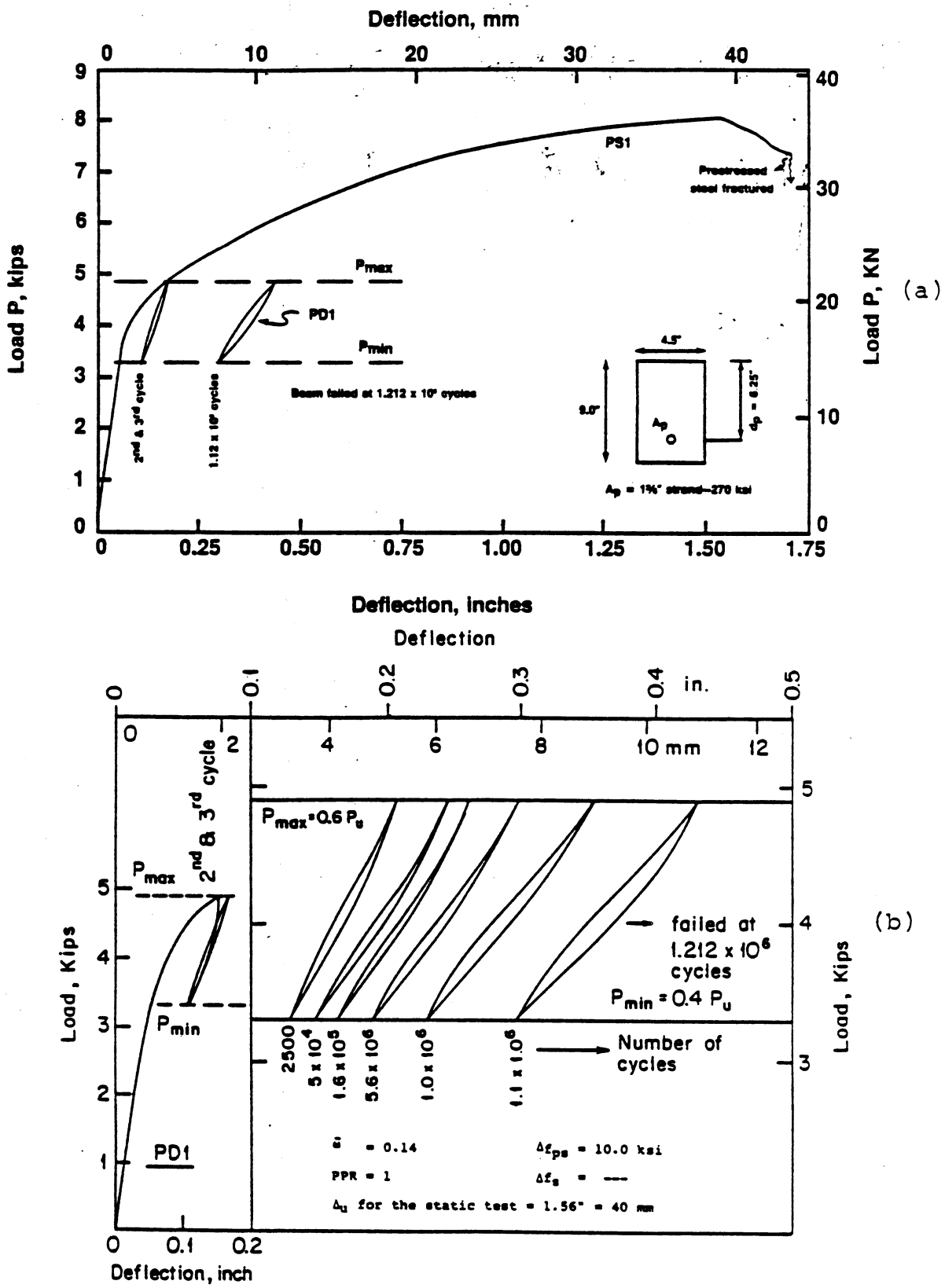

Fig. A1 Load-Deflection Curves For Beams: (a) PS1 (Static) (b) PD1 (Cyclic)

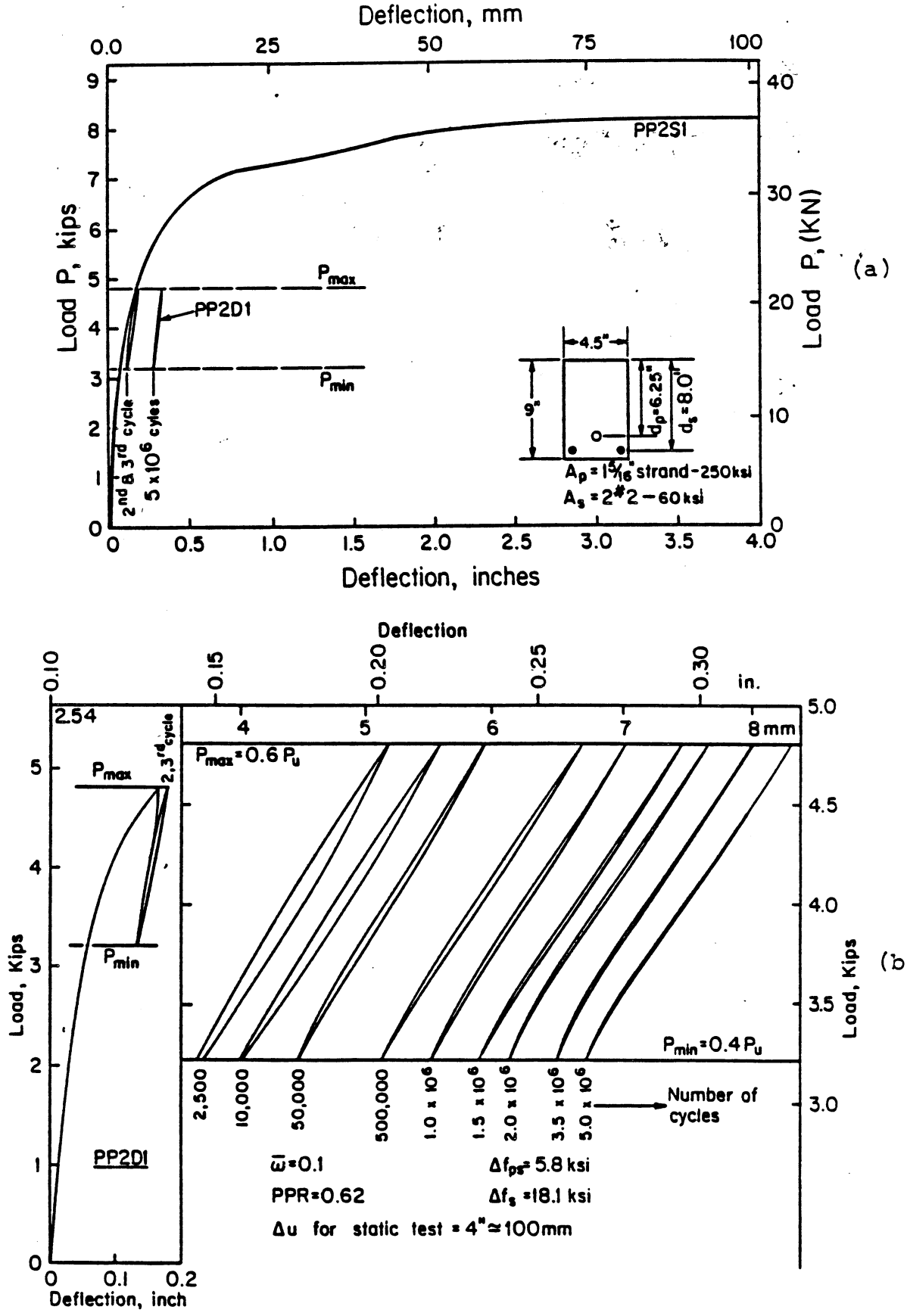

Fig. A2 Load-Deflection Curves For Beams: (a) PP2S1(Static) (b) PP2D1 (Cyclic)

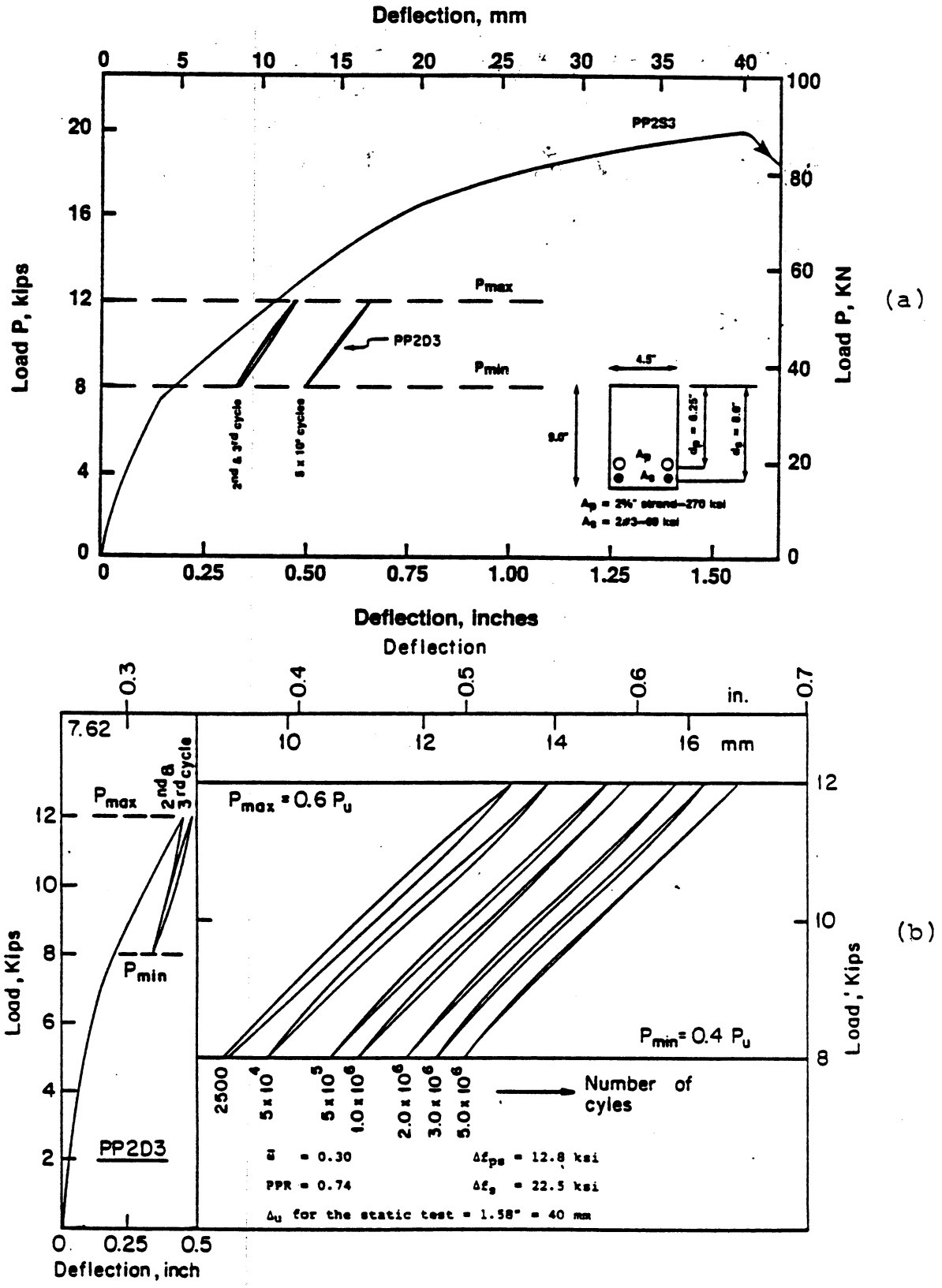

(a)

(b)

Fig. A3 Load-Deflection Curves For Beams: (a) PP2S3(Static) (b) PP2D3 (Cyclic)

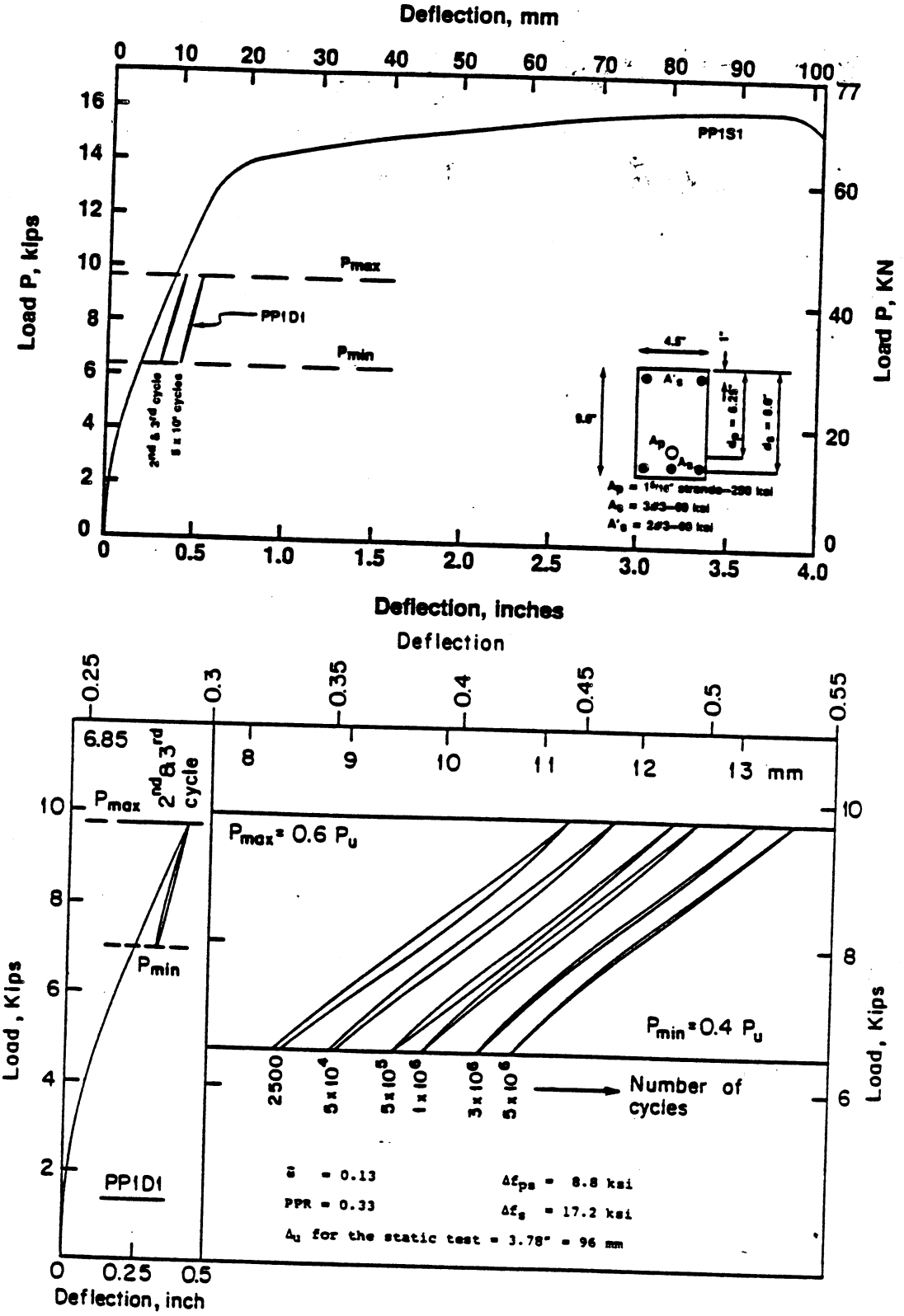

(a)

(b)

Fig. A4 Load-Deflection Curves For Beams: (a) PP1S1(Static) (b) PP1D1 (Cyclic)

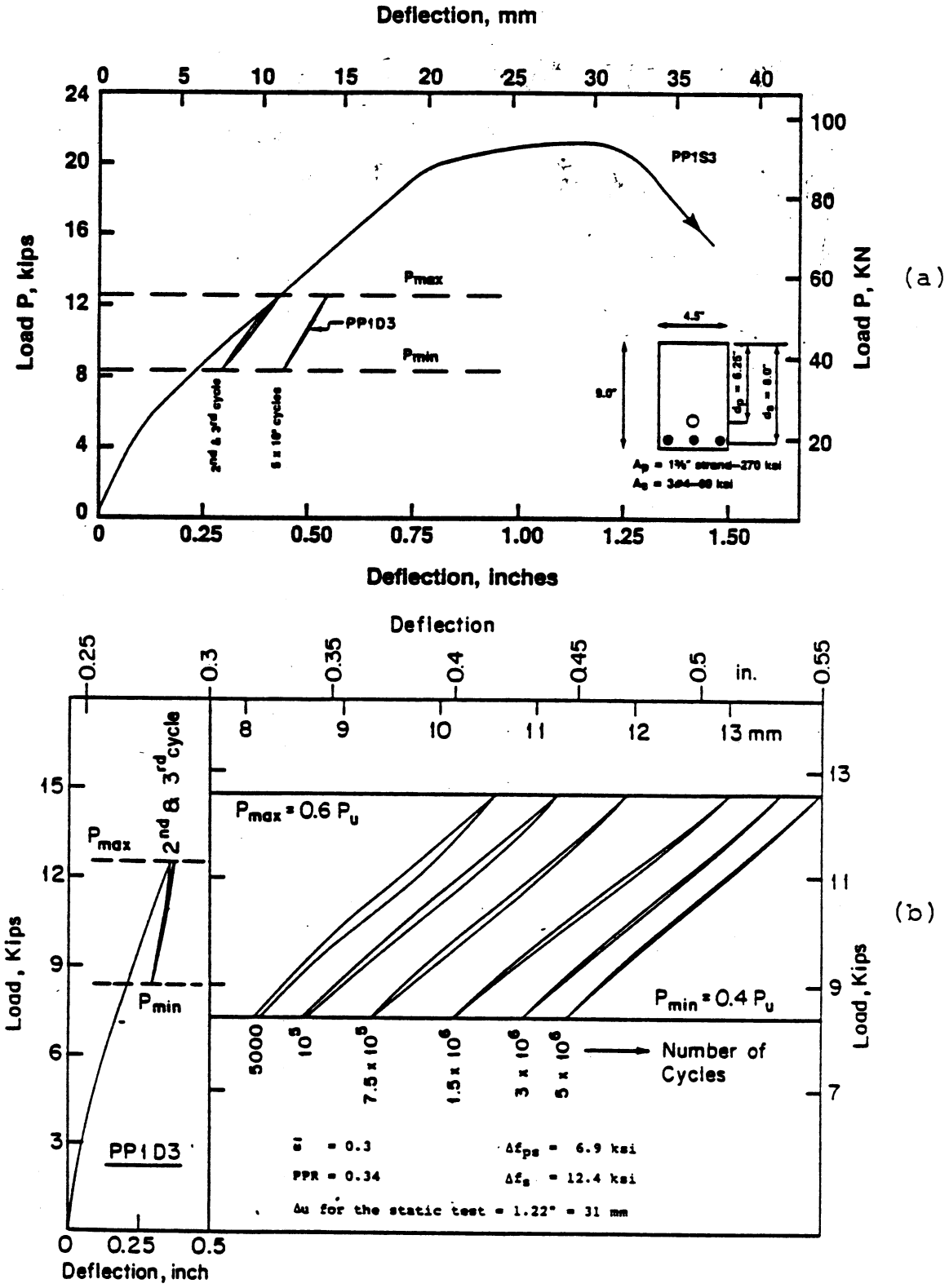

Fig. A5 Load-Deflection Curves For Beams: (a) PP1S3(Static) (b) PP1D3 (Cyclic)

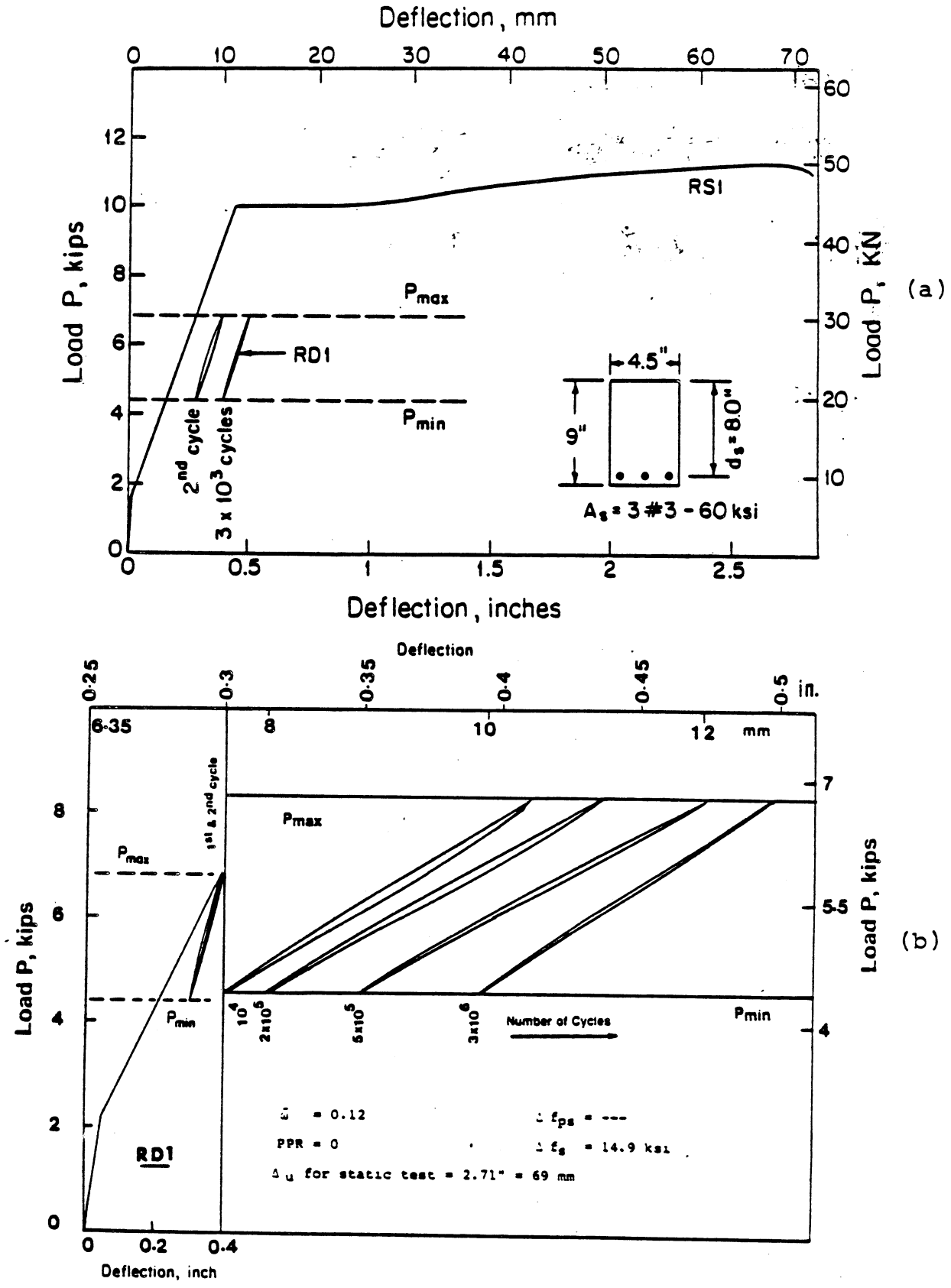

Fig. A6 Load-Deflection Curves For Beams: (a) RS1 (Static) (b) RD1 (Cyclic)

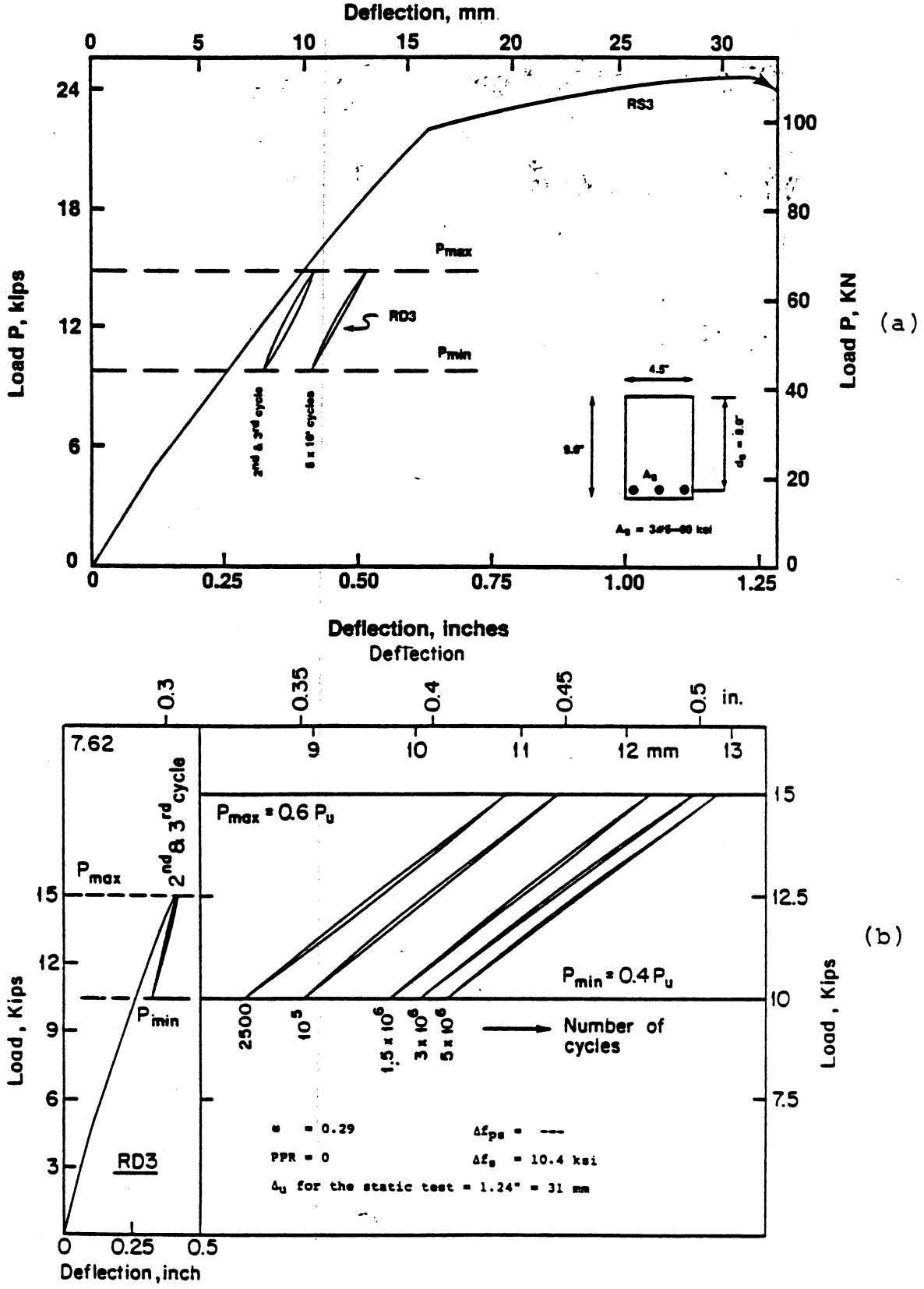

Fig. A7 Load-Deflection Curves For Beams: (a) RS3 (Static) (b) RD3 (Cyclic)

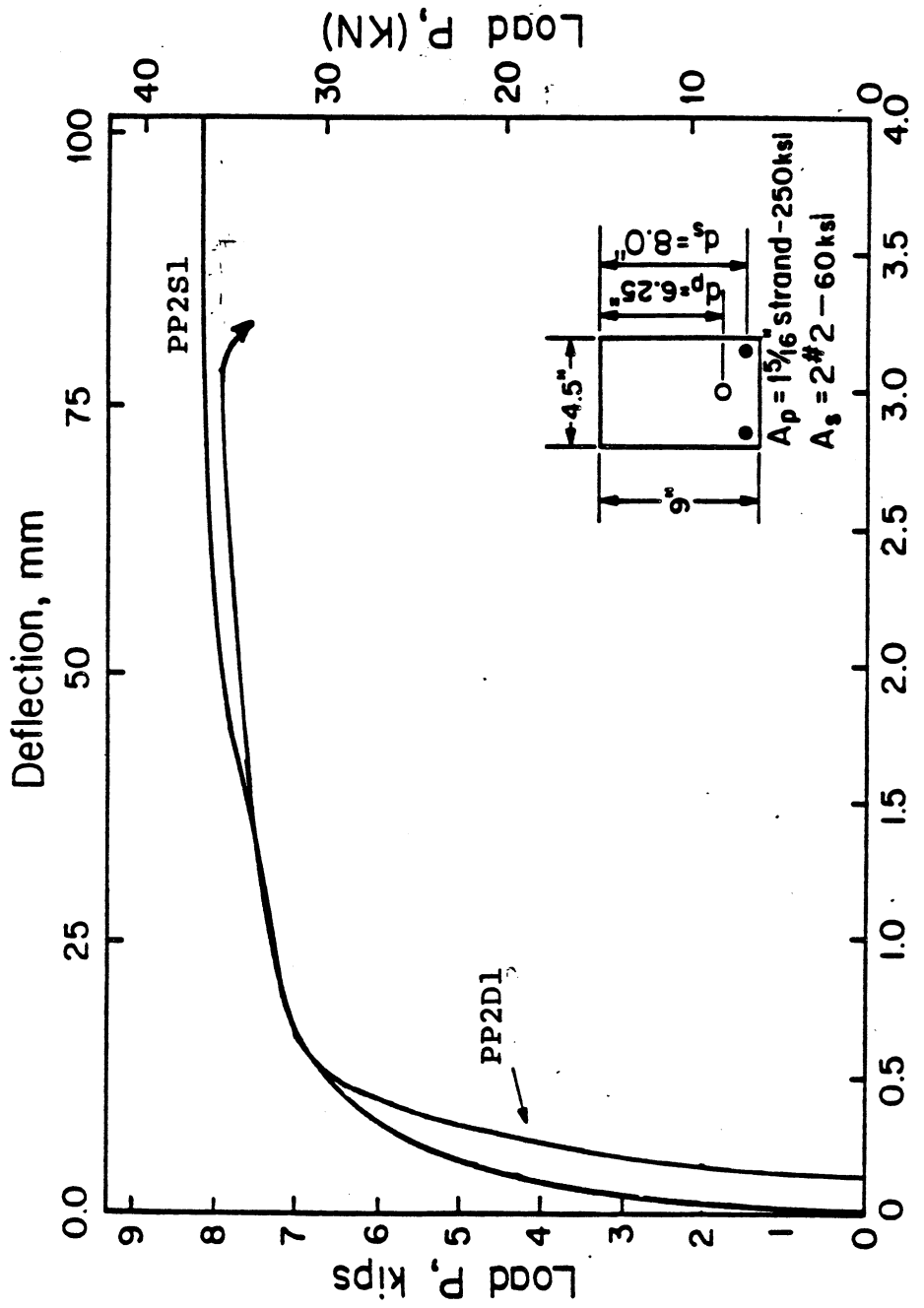

Fig. A8 Load-Deflection Curve of Beam PP2D1 After 5 Million Cycles in Comparison With its Control Static Beam (PP2S1).

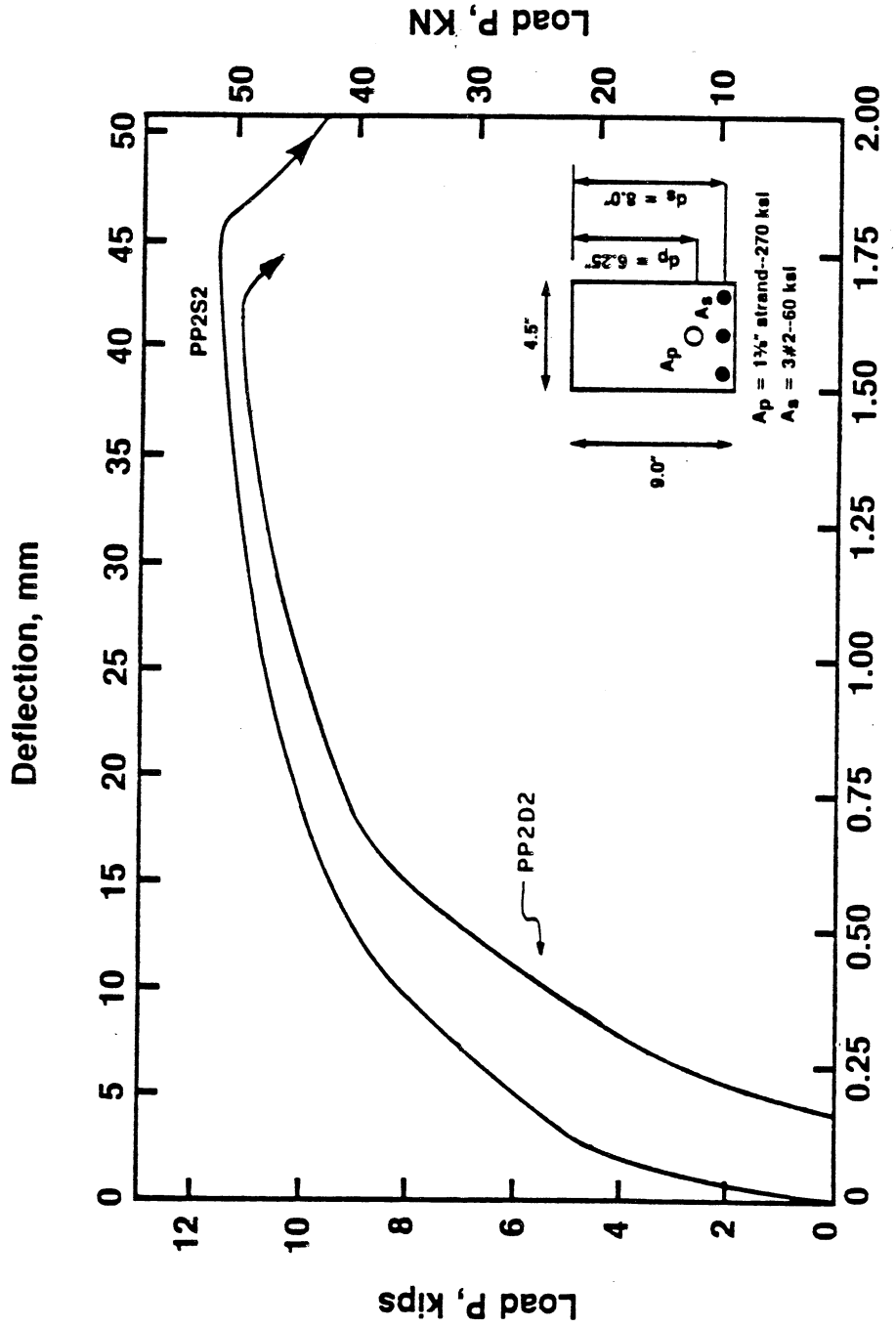

Fig. A9 Load-Deflection Curve of Beam PP2D2 After 5 Million Cycles in Comparison With its Control Static Beam (PP2S2).

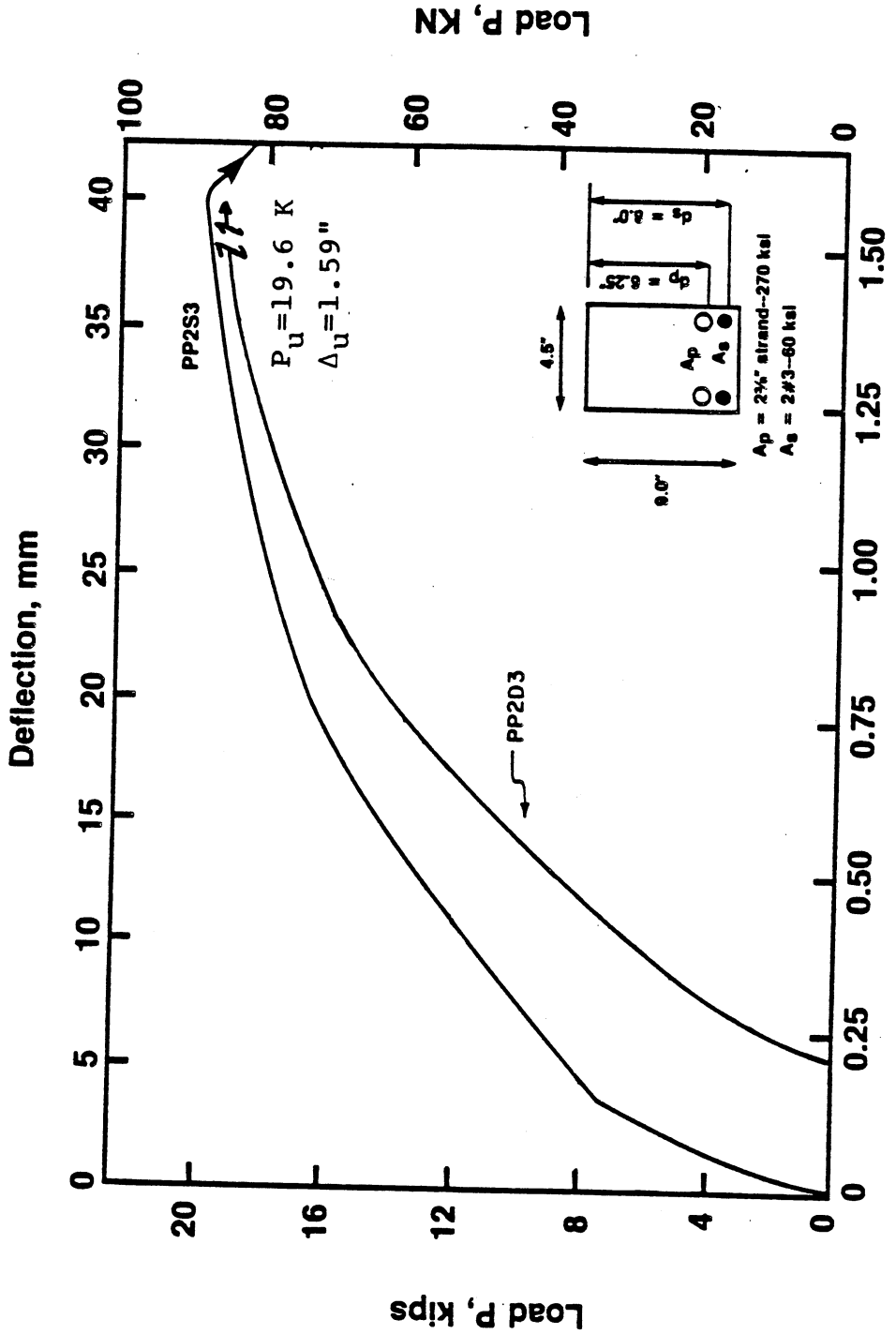

Fig. A10 Load-Deflection Curve of Beam PP2D3 After 5 Million Cycles in Comparison With its Control Static Beam (PP2S3).

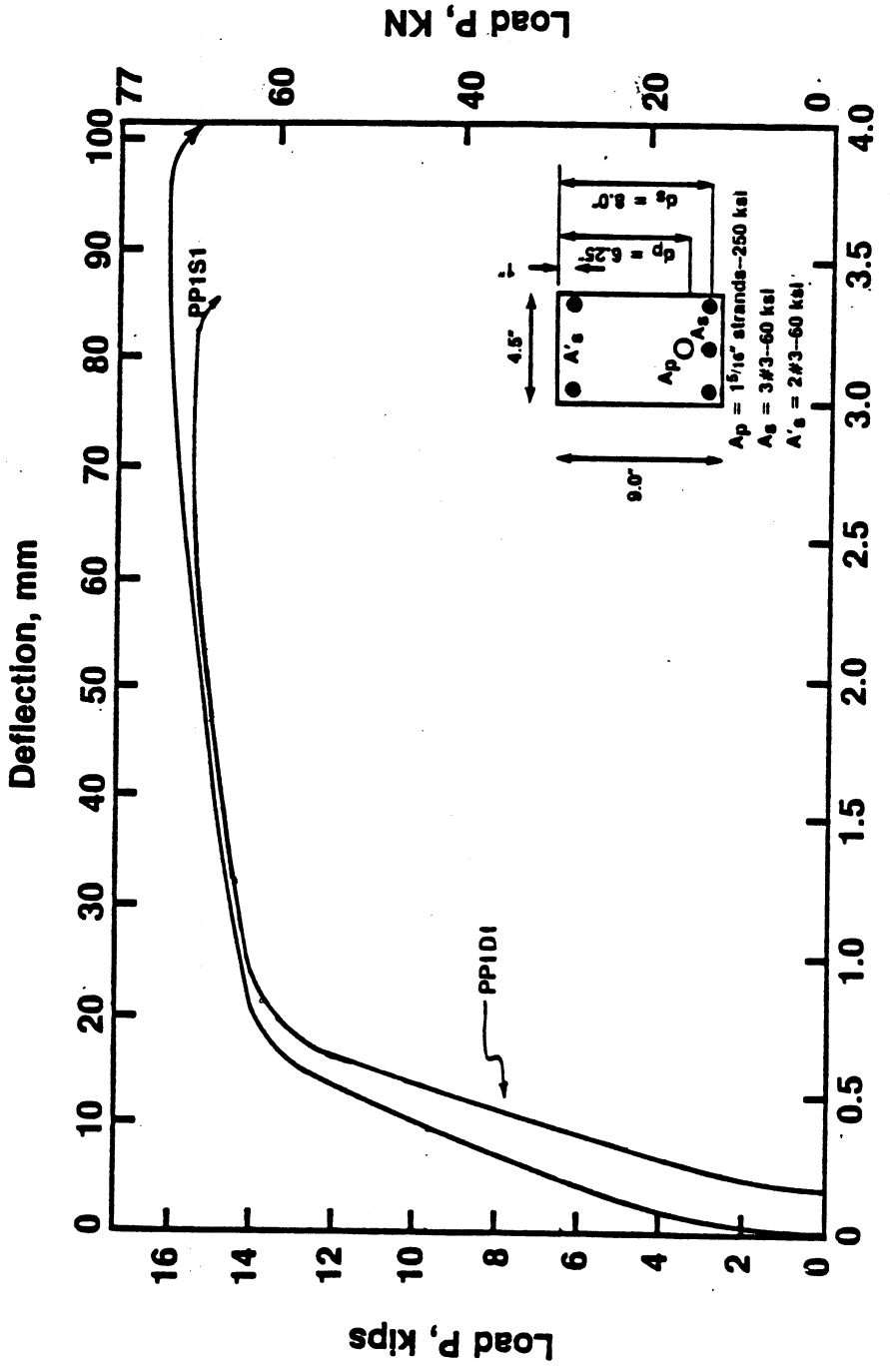

Fig. All Load-Deflection Curve of Beam PP1D1 After 5 Million Cycles in Comparison With its Control Static Beam (PP1S1).

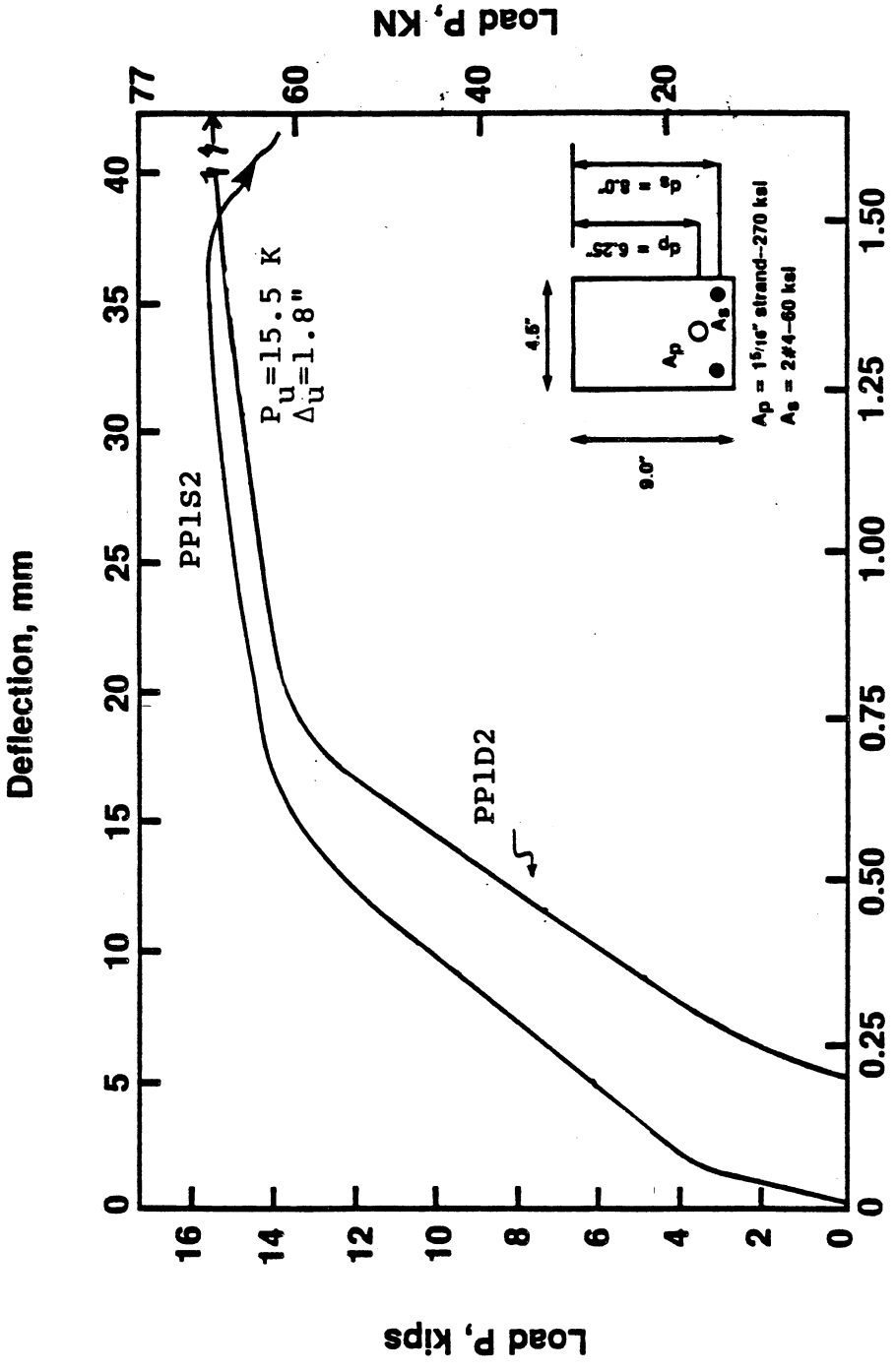

Fig. A12 Load-Deflection Curve of Beam PP1D2 After 5 Million Cycles in Comparison With its Control Static Beam (PP1S2).

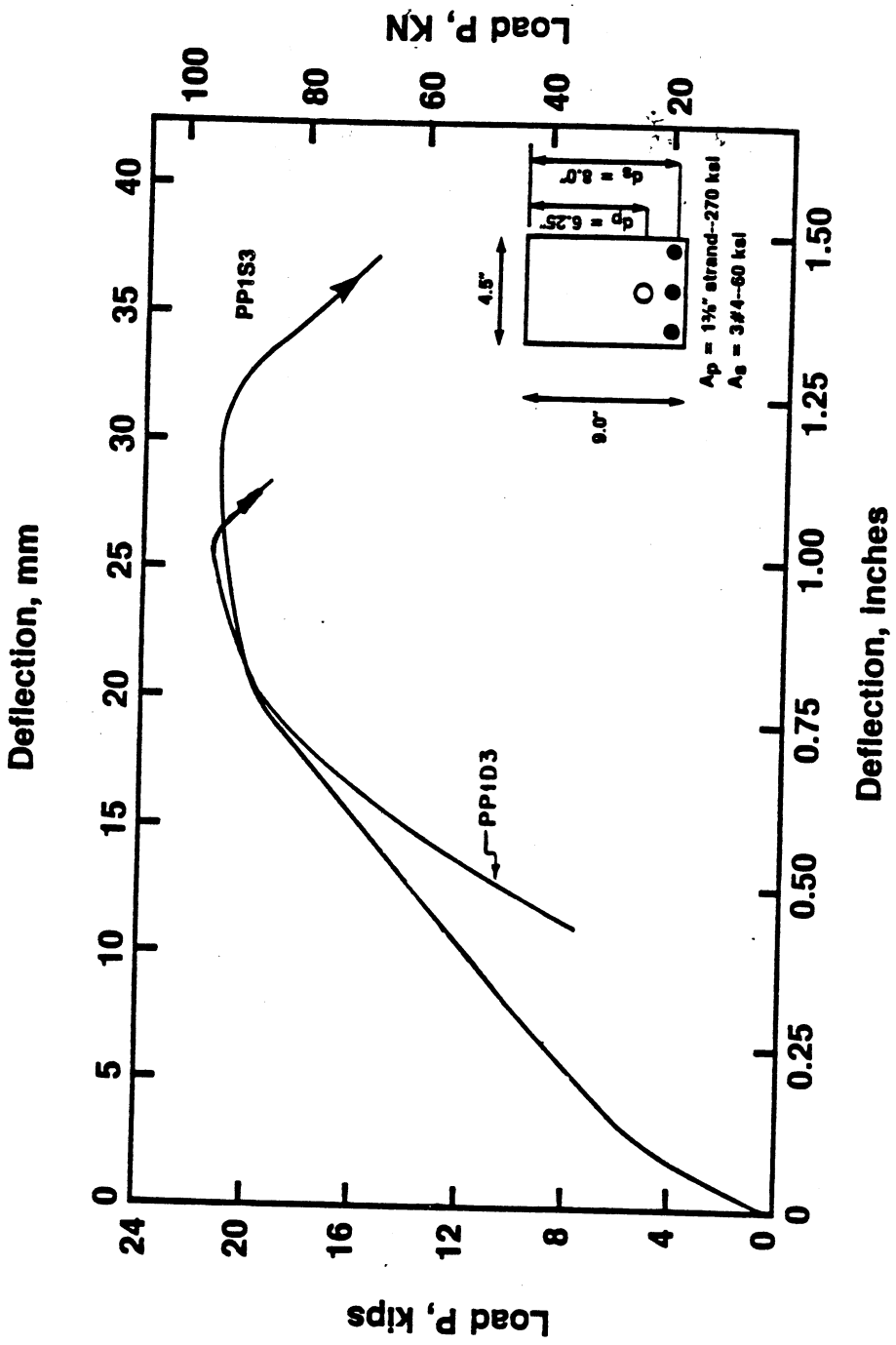

Fig. A13 Load-Deflection Curve of Beam PP1D3 After 5 Million Cycles in Comparison With its Control Static Beam (PP1S3).

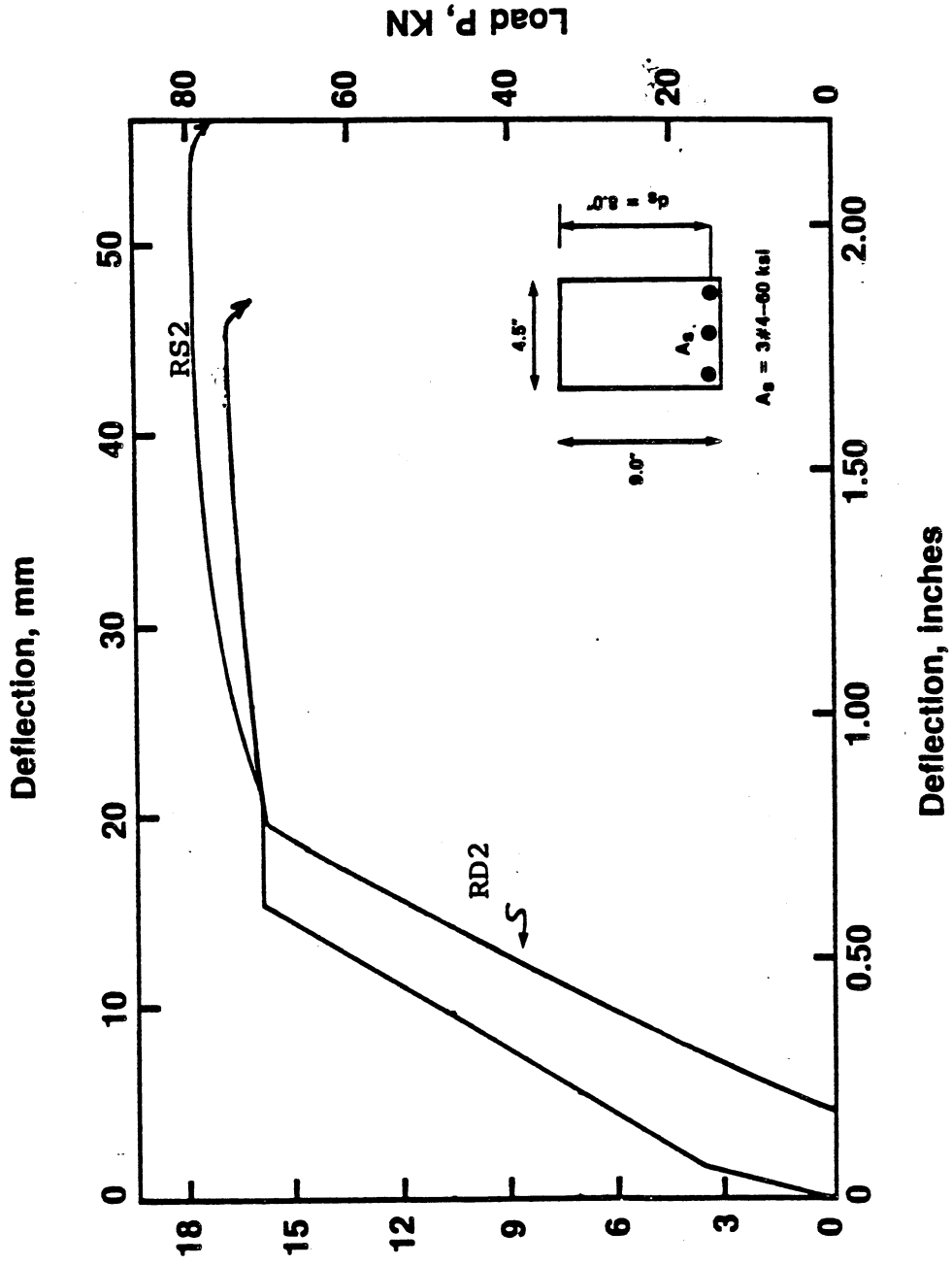

Fig. A14 Load-Deflection Curve of Beam RD2 After 5 Million Cycles in Comparison With its Control Static Beam (RS2).

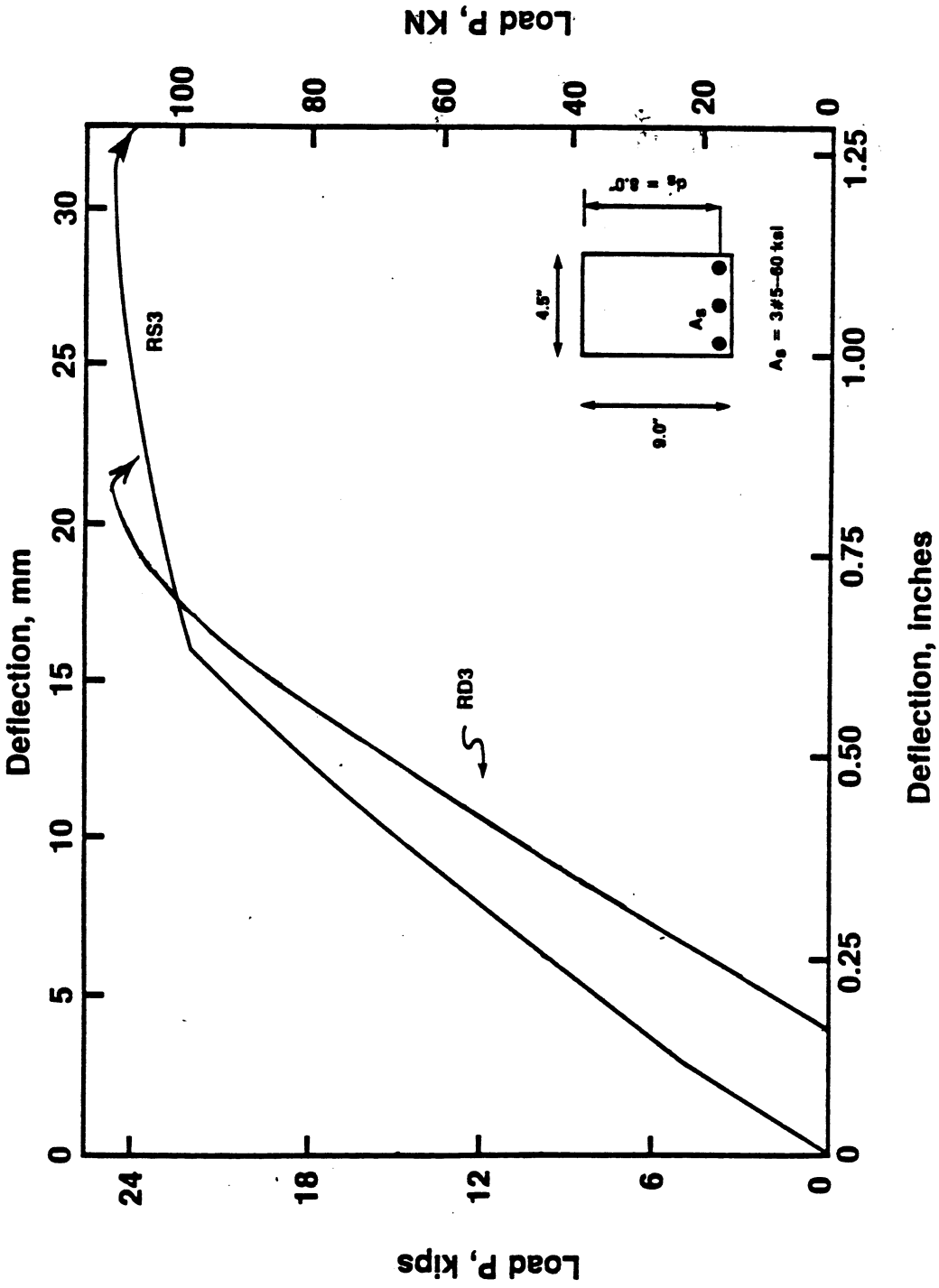

Fig. A15 Load-Deflection Curve of Beam RD3 After 5 Million Cycles in Comparison With its Control Static Beam (RS3).

APPENDIX B

Data Tables

Table B1 Ultimate Load Cycle For Beam PP2D1

Load P (Kip)	Moment at midspan (Kip-in)	Deflection (inch)	Crack width (mm)	Curvature ($in^{-1} x 10^4$)
0.00	0.00	0.13	0.08	1.29
1.00	18.00	0.14	0.08	1.42
2.00	36.00	1.80	0.10	1.74
3.00	54.00	0.23	0.14	2.26
4.00	72.00	0.29	0.18	2.81
5.00	90.00	0.33	0.22	3.27
6.00	108.00	0.40	0.31	4.10
7.10	127.80	0.63	0.704	6.53
7.80	140.40	1.26	2.08	12.50
8.06	145.08	3.10	--	24.10

Table B2 Ultimate Load Cycle For Beam PP2D2

Load P (Kip)	Moment at midspan (Kip-in)	Deflection (inch)	Crack width (mm)	Curvature ($in^{-1} x 10^4$)
0.00	0.00	0.17	0.08	1.58
1.25	22.50	0.19	0.08	1.76
2.50	45.00	0.24	0.10	2.20
3.75	67.50	0.30	0.14	2.89
5.00	90.00	0.38	0.19	3.61
7.50	135.00	0.52	0.26	4.94
9.17	165.06	0.72	0.58	7.67
9.80	176.40	0.88	0.73	9.35
10.50	189.00	1.11	0.92	11.51
11.25	202.50	1.63	1.32	16.20

Table B3 Ultimate Load Cycle For Beam PP2D3

Load P (Kip)	Moment at midspan (Kip-in)	Deflection (inch)	Crack width (mm)	Curvature ($in^{-1}x10^4$)
0.00	0.00	0.21	0.13	--
2.50	45.00	0.26	0.14	--
3.75	67.50	0.30	0.15	--
5.00	90.00	0.34	0.17	--
7.50	135.00	0.45	0.23	--
11.25	202.50	0.62	0.32	--
15.00	270.00	0.80	0.43	--
17.50	315.00	1.08	0.69	--
18.50	333.00	1.26	0.80	--
19.57	352.26	1.59	--	--

Table B4 Ultimate Load Cycle For Beam PP1D1

Load P (Kip)	Moment at midspan (Kip-in)	Deflection (inch)	Crack width (mm)	Curvature ($in^{-1}x10^4$)
0.00	0.00	0.15	0.06	1.19
2.50	45.00	0.21	0.08	1.62
3.75	67.50	0.26	0.10	2.02
5.00	90.00	0.32	0.13	2.50
7.50	135.00	0.43	0.18	3.42
10.00	180.00	0.53	0.23	4.28
11.25	202.50	0.59	0.25	4.73
14.25	256.50	1.00	0.73	9.32
15.13	272.34	1.85	1.04	19.30
15.60	280.80	3.26	--	25.70

Table B5 Ultimate Load Cycle For Beam PP1D2

Load P (Kip)	Moment at midspan (Kip-in)	Deflection (inch)	Crack width (mm)	Curvature ($in^{-1} x 10^4$)
0.00	0.00	0.18	0.04	1.52
1.25	22.50	0.22	0.04	1.62
3.75	67.50	0.30	0.07	2.30
6.25	112.00	0.41	0.12	3.17
8.75	157.50	0.51	0.15	4.00
11.25	202.50	0.60	0.19	4.80
13.13	236.34	0.69	0.22	5.49
14.43	259.74	0.87	0.59	8.00
15.00	270.00	1.22	0.73	11.94
15.50	279.00	1.80	--	18.26

Table B6 Ultimate Load Cycle For Beam PP1D3

Load P* (Kip)	Moment at midspan (Kip-in)	Deflection (inch)	Crack width (mm)	Curvature ($in^{-1}x10^4$)
8.37	150.66	0.45	0.13	--
11.01	198.18	0.52	0.14	--
12.55	225.90	0.55	0.17	--
14.32	257.76	0.61	0.18	--
15.42	277.56	0.64	0.20	--
17.62	317.16	0.71	0.22	--
18.72	336.96	0.76	0.23	--
19.82	356.76	0.91	0.44	--
21.80	392.40	1.01	0.53	--

* This beam was loaded to failure starting at P_{min}

Table B7 Ultimate Load Cycle For Beam RD2

Load P (Kip)	Moment at midspan (Kip-in)	Deflection (inch)	Crack width (mm)	Curvature ($in^{-1}x10^4$)
0.00	0.00	0.18	0.04	--
2.20	39.60	0.23	0.05	--
4.41	79.38	0.31	0.08	--
7.71	138.78	0.43	0.12	--
9.91	178.38	0.51	0.14	--
12.11	217.98	0.58	0.17	--
13.77	247.86	0.64	0.19	--
16.08	289.44	0.77	0.35	--
16.47	296.46	0.95	0.56	--
17.20	309.60	1.76	--	

Table B8 Ultimate Load Cycle For Beam RD3

Load P (Kip)	Moment at midspan (Kip-in)	Deflection (inch)	Crack width (mm)	Curvature ($in^{-1} x 10^4$)
0.00	0.00	0.16	0.02	--
2.50	45.00	0.21	0.02	--
5.00	90.00	0.27	0.04	--
7.50	135.00	0.33	0.07	--
10.00	180.00	0.39	0.09	--
12.50	225.00	0.45	0.11	--
17.50	315.00	0.56	0.14	--
21.25	382.50	0.67	0.17	--
22.50	405.00	0.71	0.18	--
24.70	444.60	0.85	0.35	--

TABLE 1S

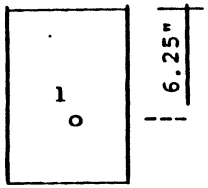

Beam Designation: PS1
Type of Loading: Static
Reinforcing steel = --
Prestressing steel = 1 3/8"-270 Ksi

f'_c at time of loading = 5570 Psi
Effective prestress, f_{pe} = 169.0 Ksi

Stress in the Tension Reinforcement(c):

$f_s = E_s \epsilon_s \ldots (E_s = 29 \times 10^3$ Ksi) (a)
$f_{ps} = E_p \epsilon_p \ldots (E_p = 28.6 \times 10^3$ Ksi) (b)

Note: 1,2,3, etc. are the locations of strain gages.

Load P (kips)	Moment at Mid-span (k-in)	Stress in Reinforcing Bar f_s(ksi)			Increase in stress in the prestressed Strand Δf_{ps} (ksi)				Deflection (in)	Crack width (mm) (L.V.D.T. reading)	Curvature $x10^{-4}$ (rad/in)
		--	--	Average	1	--	--	Average			
0.25	4.50	--	--	--	0.26	--	--	0.26	0.002	0.000	0.02
0.75	13.50	--	--	--	0.46	--	--	0.46	0.004	0.000	0.07
1.50	27.00	--	--	--	0.94	--	--	0.94	0.021	0.001	0.15
2.00	36.00	--	--	--	1.23	--	--	1.23	0.029	0.001	0.21
2.50	45.00	--	--	--	1.56	--	--	1.56	0.037	0.003	0.27
3.00	54.00	--	--	--	1.90	--	--	1.90	0.046	0.003	0.33
3.50	63.00	--	--	--	2.33	--	--	2.33	0.055	0.006	0.40
3.75	67.50	--	--	--	2.72	--	--	2.72	0.06	0.012	0.46
4.00[d]	72.00	--	--	--	5.03	--	--	5.03	0.073	0.038	0.62
4.50	81.00	--	--	--	13.00	--	--	13.10	0.119	0.103	1.03

a) ϵ_s = Reading of one strain gage on each reinforcing bar, as numbered, at mid-span. Adjusted to account for initial prestrain.
b) ϵ_p = Average reading of two or three strain gages on each strand at mid span.
c) In the non linear range, the stress is obtained directly from the actual stress strain curves of the tension reinforcement.
d) Onset of cracking.

TABLE 1S (CONTINUED)

Load P (kips)	Moment at Mid-span (k-in)	Stress in Reinforcing Bar f_s(ksi)			Increase in stress in the prestressed Strand Δf_{ps} (ksi)				Deflection (in)	Crack width (mm) (L.V.D.T. reading)	Curvature x10^{-4} (rad/in)
		--	--	Average	1	--	--	Average			
4.75	85.50	--	--	--	17.46	--	--	17.46	0.145	0.144	1.29
5.00	90.00	--	--	--	28.00	--	--	28.00	0.184	0.256	1.97
5.50	99.00	--	--	--	42.80	--	--	42.80	0.292	0.464	3.19
6.00	108.00	--	--	--	54.50	--	--	54.50	0.405	0.683	4.46
6.50	117.00	--	--	--	66.30	--	--	66.30	0.556	0.885	5.65
7.00	126.00	--	--	--	73.40	--	--	73.40	0.706	1.084	6.85
7.40	133.20	--	--	--	82.80	--	--	82.80	0.843	1.280	8.03
7.92	142.56	--	--	--	90.40	--	--	90.40	1.258	1.920	11.37
8.18	147.24	--	--	--	99.60	--	--	99.60	1.560	2.360	13.58

f- Strain gage failed.
y- Yielding of Reinforcing steel.

N.A depth at ultimate = 0.75"

TABLE 2S

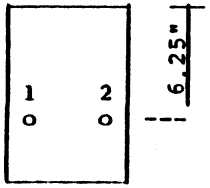

Beam Designation: PS2
Type of Loading: Static
Reinforcing steel = --
Prestressing steel = 2 3/8"-270 Ksi

f'_c at time of loading = 5300 Psi
Effective prestress, f_{pe} = 137.0 Ksi

Stress in the Tension Reinforcement(c):

$f_s = E_s \varepsilon_s$...(E_s=29x10^3 Ksi) (a)
$f_{ps} = E_p \varepsilon_p$...($E_p$=28.6x10^3 Ksi) (b)

Note: 1,2,3, etc. are the locations of strain gages.

Load P (kips)	Moment at Mid-span (k-in)	Stress in Reinforcing Bar f_s(ksi)			Increase in stress in the prestressed Strand Δf_{ps} (ksi)				Deflection (in)	Crack width (mm) (L.V.D.T. reading)	Curvature x10^{-4} (rad/in)
		--	--	Average	1	2	--	Average			
0.55	9.90	--	--	--	0.24	0.13	--	0.18	0.007	0.000	0.04
1.10	19.80	--	--	--	0.58	0.43	--	0.51	0.016	0.000	0.06
2.20	39.60	--	--	--	1.24	0.93	--	1.08	0.036	0.000	0.15
3.30	59.40	--	--	--	2.02	1.67	--	1.85	0.057	0.000	0.37
4.40	79.20	--	--	--	2.95	2.57	--	2.76	0.080	0.008	0.57
5.50	99.00	--	--	--	4.50	3.98	--	4.24	0.108	0.024	0.80
6.06	109.08	--	--	--	7.36	6.68	--	7.02	0.127	0.053	1.03
6.61(d)	118.98	--	--	--	11.53	10.83	--	11.18	0.160	0.091	1.33
7.16	128.88	--	--	--	15.59	15.24	--	15.42	0.192	0.135	1.69
7.71	138.78	--	--	--	22.49	22.99	--	22.74	0.240	0.222	2.27

a) ε_{ls} = Reading of one strain gage on each reinforcing bar, as numbered, at mid-span. Adjusted to account for initial prestrain.
b) ε_p = Average reading of two or three strain gages on each strand at mid span.
c) In the non linear range, the stress is obtained directly from the actual stress strain curves of the tension reinforcement.
d) Onset of cracking.

TABLE 2S (CONTINUED)

Load P (kips)	Moment at Mid-span (k-in)	Stress in Reinforcing Bar f_s(ksi)			Increase in stress in the prestressed Strand Δf_{ps} (ksi)				Deflection (in)	Crack width (mm) (L.V.D.T. reading)	Curvature x10^{-4} (rad/in)
		--	--	Average	1	2	--	Average			
8.81	158.58	--	--	--	38.07	39.77	--	38.92	0.383	0.465	3.89
9.36	168.48	--	--	--	45.93	48.28	--	47.10	0.477	0.592	4.77
10.46	188.28	--	--	--	60.60	63.50	--	62.10	0.674	0.909	6.55
11.01	198.18	--	--	--	68.20	70.60	--	69.40	0.784	1.069	7.67
11.67	210.06	--	--	--	77.60	83.50	--	80.60	0.928	1.275	8.91
12.66	227.88	--	--	--	94.10	98.80	--	96.40	1.041	1.637	11.24
13.22	237.96	--	--	--	103.50	108.20	--	105.90	1.194	--	13.32
13.92	250.56	--	--	--	111.70	116.40	--	114.10	1.520	--	15.30

f- Strain gage failed.
y- Yielding of Reinforcing steel.

N.A depth at ultimate = --

TABLE 3S

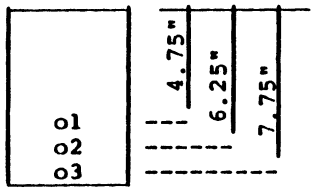

Beam Designation: PS3
Type of Loading: Static
Reinforcing steel = --
Prestressing steel = 3 3/8"-270 Ksi

f'_c at time of loading = 5730 Psi
Effective prestress, f_{pe} = 136.0 Ksi

Stress in the Tension Reinforcement[c]:
$f_s = E_s \varepsilon_s \ldots (E_s = 29 \times 10^3$ Ksi) (a)
$f_{ps} = E_p \varepsilon_p \ldots (E_p = 28.6 \times 10^3$ Ksi) (b)

Note: 1,2,3, etc. are the locations of strain gages.

Load P (kips)	Moment at Mid-span (k-in)	Stress in Reinforcing Bar f_s(ksi)			Increase in stress in the prestressed Strand Δf_{ps} (ksi)				Deflection (in)	Crack width (mm) (L.V.D.T. reading)	Curvature x10^{-4} (rad/in)
		--	--	Average	1	2	3	Average			
0.63	11.34	--	--	--	0.09	0.27	0.51	0.29	0.007	0.001	0.02
2.50	45.00	--	--	--	0.09	1.30	2.43	1.27	0.034	0.002	0.20
3.75	67.50	--	--	--	0.17	2.12	3.85	2.05	0.054	0.003	0.34
5.00	90.00	--	--	--	0.31	2.87	5.26	2.81	0.073	0.005	0.49
6.25	112.50	--	--	--	0.37	3.69	6.75	3.60	0.094	0.006	0.04
7.50	135.00	--	--	--	0.51	4.69	8.62	4.61	0.117	0.009	0.82
8.13	146.34	--	--	--	0.69	5.73	10.50	5.64	0.131	0.018	0.94
8.75[d]	157.50	--	--	--	1.20	8.22	14.24	7.89	0.150	0.044	1.14
9.38	168.84	--	--	--	2.40	11.78	18.20	10.79	0.178	0.073	1.36
10.00	180.00	--	--	--	4.75	17.13	23.18	15.02	0.213	0.114	1.66

a) ε_s = Reading of one strain gage on each reinforcing bar, as numbered, at mid-span. Adjusted to account for initial prestrain.
b) ε_p = Average reading of two or three strain gages on each strand at mid span.
c) In the non linear range, the stress is obtained directly from the actual stress strain curves of the tension reinforcement.
d) Onset of cracking.

TABLE 3S (CONTINUED)

Load P (Kips)	Moment at Mid-span (k-in)	Stress in Reinforcing Bar f_s(ksi)			Increase in stress in the prestressed Strand Δf_{ps} (ksi)				Deflection (in)	Crack width(mm) (L.V.D.T reading)	Curvature $x10^{-4}$ (rad/in)
		--	--	Average	1	2	3	Average			
10.63	191.34	---	---	---	8.35	21.96	28.87	19.73	0.253	0.166	2.03
11.25	202.50	---	---	---	11.55	26.97	34.76	23.43	0.300	0.222	2.44
12.50	225.00	---	---	---	21.91	37.51	49.06	36.16	0.404	0.362	3.43
13.75	247.50	---	---	---	32.32	47.76	64.00	48.03	0.522	0.506	4.41
15.00	270.00	---	---	---	42.30	56.94	80.50	59.90	0.665	0.665	5.50
15.88	285.84	---	---	---	48.93	65.18	88.70	67.60	0.771	0.780	6.31
16.25	292.50	---	---	---	51.77	71.10	91.10	71.30	0.820	0.830	6.66
16.75	301.50	---	---	---	54.60	75.80	96.40	75.60	0.892	0.901	7.17
18.18	327.24	---	---	---	65.80	88.70	108.70	87.70	1.120	1.116	8.70
19.00	342.00	---	---	---	71.10	96.90	114.60	94.20	1.372	---	10.40

f- Strain gage failed.
y- Yielding of reinforcing steel.

N.A depth at ultimate = 2.0"

TABLE 4S

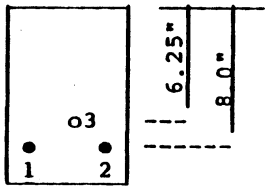

Beam Designation: PP2S1
Type of Loading: Static
Reinforcing steel = 2#2-60 Ksi
Prestressing steel = 1 5/16"-250 Ksi

f'_c at time of loading = 6576 Psi
Effective prestress, f_{pe} = 165.0 Ksi

Stress in the Tension Reinforcement[c]:
$f_s = E_s \epsilon_s \ldots (E_s = 29 \times 10^3$ Ksi) (a)
$f_{ps} = E_p \epsilon_p \ldots (E_p = 28.0 \times 10^3$ Ksi) (b)

Note: 1,2,3, etc. are the locations of strain gages.

Load P (kips)	Moment at Mid-span (k-in)	Stress in Reinforcing Bar f_s(ksi)			Increase in stress in the prestressed Strand Δf_{ps} (ksi)				Deflection (in)	Crack width (mm) (L.V.D.T. reading)	Curvature $\times 10^{-4}$ (rad/in)
		1	2	Average	3	--	--	Average			
0.50	9.00	-5.51	-5.51	-5.51	0.18	---	---	0.18	0.005	0.000	0.03
1.00	18.00	-4.84	-4.67	-4.76	0.49	---	---	0.49	0.012	0.001	0.09
1.75	31.50	-3.19	-2.52	-2.87	1.12	---	---	1.12	0.024	0.005	0.19
2.25	40.50	-1.67	-0.66	-1.17	1.57	---	---	1.57	0.033	0.009	0.27
2.50	45.00	-0.72	0.41	-0.16	1.86	---	---	1.86	0.038	0.012	0.31
3.00	54.00	3.48	5.46	4.47	3.07	---	---	3.07	0.049	0.027	0.44
3.25[d]	58.50	11.28	14.01	12.65	5.83	---	---	5.83	0.060	0.053	0.61
3.50	63.00	17.08	19.69	18.39	8.04	---	---	8.04	0.069	0.074	0.76
4.00	72.00	27.81	31.70	29.76	12.75	---	---	12.75	0.100	0.117	1.05
4.50	81.00	37.94	41.62	39.78	17.05	---	---	17.05	0.142	0.157	1.33

a) ϵ_s = Reading of one strain gage on each reinforcing bar, as numbered, at mid-span. Adjusted to account for initial prestrain.
b) ϵ_p = Average reading of two or three strain gages on each strand at mid span.
c) In the non linear range, the stress is obtained directly from the actual stress strain curves of the tension reinforcement.
d) Onset of cracking.

TABLE 4S (CONTINUED)

Load P (kips)	Moment at Mid-span (k-in)	Stress in Reinforcing Bar f_s(ksi)			Increase in stress in the prestressed Strand Δf_{ps} (ksi)				Deflection (in)	Crack width(mm) (L.V.D.T. reading)	Curvature x10^{-4} (rad/in)
		1	2	Average	3	--	--	Average			
5.00	90.00	47.71	51.42	49.57	20.96	---	---	20.96	0.187	0.195	1.59
5.50	99.00	58.76	62.73	60.75	25.59	---	---	25.59	0.239	0.242	1.90
6.25Y	112.50	68.00	68.00	68.00	35.00	---	---	35.00	0.354	0.351	3.34
6.50	117.00	78.00	f	78.00	55.70	---	---	55.70	0.433	0.661	5.07
7.00	126.00	f	--	--	72.90	---	---	72.90	0.696	1.046	7.24
7.90	142.20	--	--	--	92.90	---	---	92.90	1.817	1.800	24.92
8.20	147.60	--	--	--	94.00	---	---	94.00	2.700	---	30.73
8.40	151.20	--	--	--	94.50	---	---	94.50	4.000	---	35.24

f- Strain gage failed
y- Yielding of reinforcing steel.

N.A depth at ultimate = 0.75"

TABLE 5S

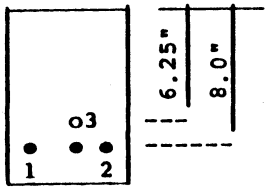

Beam Designation: PP2S2
Type of Loading: Static
Reinforcing steel = 3#2-60 Ksi
Prestressing steel = 1 3/8"-270 Ksi

f'_c at time of loading = 5290 Psi
Effective prestress, f_{pe} = 167.0 Ksi

Stress in the Tension Reinforcement[c]:
$f_s = E_s\varepsilon_s \ldots (E_s = 29 \times 10^3$ Ksi) (a)
$f_{ps} = E_p\varepsilon_p \ldots (E_p = 28.6 \times 10^3$ Ksi) (b)

Note: 1,2,3, etc. are the locations of strain gages.

Load P (kips)	Moment at Mid-span (k-in)	Stress in Reinforcing Bar f_s(ksi)			Increase in stress in the prestressed Strand Δf_{ps} (ksi)				Deflection (in)	Crack width (mm) (L.V.D.T. reading)	Curvature $\times 10^{-4}$ (rad/in)
		1	2	Average	3	--	--	Average			
0.63	11.34	-9.87	-9.87	-9.87	0.30	---	---	0.30	0.007	0.000	0.04
1.25	22.50	-8.74	-8.65	-8.70	0.72	---	---	0.72	0.018	0.000	0.12
1.88	33.84	-7.52	-7.41	-7.47	1.16	---	---	1.16	0.029	0.002	0.21
3.13	56.34	-4.33	-4.19	-4.26	2.27	---	---	2.27	0.053	0.011	0.41
3.75	67.50	0.08	1.03	0.56	3.92	---	---	3.92	0.069	0.029	0.57
4.38[d]	78.84	5.47	7.39	6.43	6.88	---	---	6.88	0.090	0.054	0.80
5.00	90.00	10.98	13.53	12.26	11.50	---	---	11.50	0.122	0.083	1.12
6.25	112.50	24.03	26.87	25.45	20.46	---	---	20.46	0.219	0.150	2.09
7.50	135.00	38.97	40.85	39.91	28.97	---	---	28.97	0.324	0.221	2.98
8.75	157.50	55.90	57.60	56.75	41.92	---	---	41.92	0.453	0.350	4.12

a) ε_s = Reading of one strain gage on each reinforcing bar, as numbered, at mid-span. Adjusted to account for initial prestrain.
b) ε_p = Average reading of two or three strain gages on each strand at mid span.
c) In the non linear range, the stress is obtained directly from the actual stress strain curves of the tension reinforcement.
d) Onset of cracking.

TABLE 5S (CONTINUED)

Load P (kips)	Moment at Mid-span (k-in)	Stress in Reinforcing Bar f_s(ksi)			Increase in stress in the prestressed Strand Δf_{ps} (ksi)				Deflection (in)	Crack width(mm) (L.V.D.T. reading)	Curvature $x10^{-4}$ (rad/in)
		1	2	Average	3	--	--	Average			
9.38Y	168.84	f	68.00	68.00	58.38	---	---	58.38	0.568	0.590	5.75
10.08	181.44	---	f	---	72.50	---	---	72.50	0.758	0.778	7.48
10.83	194.94	---	---	---	83.70	---	---	83.70	1.006	0.996	9.74
11.23	202.14	---	---	---	86.60	---	---	86.60	1.162	1.153	11.26
11.58	208.44	---	---	---	91.30	---	---	91.30	1.447	1.424	14.14
11.60	208.80	---	---	---	94.80	---	---	94.80	1.760	1.605	16.18

f- Strain gage failed
y- Yielding of reinforcing steel.

N.A depth at ultimate = 2.50"

TABLE 6S

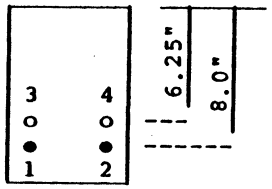

Beam Designation: PP2S3
Type of Loading: Static
Reinforcing steel = 2#3-60 Ksi
Prestressing steel = 2 3/8"-270 Ksi

f'_c at time of loading = 6200 Psi
Effective prestress, f_{pe} = 133.0 Ksi

Stress in the Tension Reinforcement(c):
$f_s = E_s \varepsilon_s \ldots (E_s = 29 \times 10^3$ Ksi) (a)
$f_{ps} = E_p \varepsilon_p \ldots (E_p = 28.6 \times 10^3$ Ksi) (b)

Note: 1,2,3, etc. are the locations of strain gages.

Load P (kips)	Moment at Mid-span (k-in)	Stress in Reinforcing Bar f_s(ksi)			Increase in stress in the prestressed Strand Δf_{ps} (ksi)				Deflection (in)	Crack width (mm) (L.V.D.T. reading)	Curvature $x10^{-4}$ (rad/in)
		1	2	Average	3	4	--	Average			
0.63	11.34	-12.81	-12.89	-12.85	0.00	0.37	---	0.35	0.006	0.000	0.04
1.25	22.50	-11.97	-12.20	-12.09	0.66	0.61	---	0.64	0.015	0.000	0.10
2.50	45.00	-10.14	-10.27	-10.27	1.42	1.33	---	1.38	0.035	0.004	0.27
3.75	67.50	-7.88	-8.08	-7.98	2.20	2.16	---	2.18	0.056	0.009	0.44
5.00	90.00	-4.08	-4.60	-4.34	3.42	3.35	---	3.39	0.079	0.020	0.63
5.63	101.34	-0.13	-0.89	-0.51	4.72	4.73	---	4.73	0.093	0.034	0.77
6.25[d]	112.50	4.10	5.20	4.65	6.88	6.98	---	6.93	0.111	0.052	0.95
7.50	135.00	10.50	11.44	10.97	11.31	11.90	---	11.61	0.156	0.084	1.21
8.75	157.50	19.12	19.76	19.44	17.42	15.72	---	16.57	0.217	0.127	1.62
10.00	180.00	27.35	29.30	28.33	23.27	21.44	---	22.36	0.297	0.162	2.35

a) ε_s = Reading of one strain gage on each reinforcing bar, as numbered, at mid-span. Adjusted to account for initial prestrain.
b) ε_p = Average reading of two or three strain gages on each strand at mid span.
c) In the non linear range, the stress is obtained directly from the actual stress strain curves of the tension reinforcement.
d) Onset of cracking.

TABLE 6S (CONTINUED)

Load P (kips)	Moment at Mid-span (k-in)	Stress in Reinforcing Bar f_s(ksi)			Increase in stress in the prestressed Strand Δf_{ps} (ksi)				Deflection (in)	Crack width(mm) (L.V.D.T. reading)	Curvature $x10^{-4}$ (rad/in)
		1	2	Average	3	4	--	Average			
12.50	225.00	47.28	50.88	49.08	35.98	34.38	---	35.18	0.461	0.222	3.84
13.75	247.50	57.46	62.10	59.78	42.47	41.34	---	41.91	0.545	0.254	4.52
15.00	270.00	68.37	73.57	70.97	49.44	48.19	---	48.82	0.637	0.288	5.08
16.25y	292.50	f	f	---	59.90	53.40	---	56.70	0.735	0.355	5.97
16.88	303.84	---	---	---	68.70	66.40	---	67.50	0.824	0.471	6.80
17.45	314.10	---	---	---	80.50	78.10	---	79.30	0.990	---	8.16
18.60	334.80	---	---	---	97.60	95.20	---	96.40	1.156	---	9.88
19.50	351.00	---	---	---	110.50	110.80	---	110.60	1.401	---	11.84
20.00	360.00	---	---	---	116.40	116.80	---	116.60	1.580	---	13.26

f- Strain gage failed
y- Yielding of reinforcing steel.

N.A depth at ultimate = 3.25"

TABLE 7S

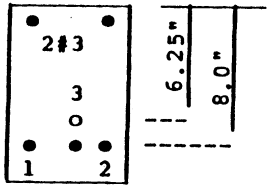

Beam Designation: PP1S1
Type of Loading: Static
Reinforcing steel = 3#3-60 Ksi
Prestressing steel = 1 5/16"-2 50 Ksi

f'_c at time of loading = 6040 Psi
Effective prestress, f_{pe} = 164.0 Ksi

Stress in the Tension Reinforcement(c):
$f_s = E_s \epsilon_s \ldots (E_s = 29 \times 10^3$ Ksi) (a)
$f_{ps} = E_p \epsilon_p \ldots (E_p = 28.0 \times 10^3$ Ksi) (b)

Note: 1,2,3, etc. are the locations of strain gages.

Load P (kips)	Moment at Mid-span (k-in)	Stress in Reinforcing Bar f_s(ksi)			Increase in stress in the prestressed Strand Δf_{ps} (ksi)				Deflection (in)	Crack width (mm) (L.V.D.T. reading)	Curvature x10^{-4} (rad/in)
		1	2	Average	3	--	--	Average			
0.63	11.34	-5.85	-5.70	-5.78	0.20	---	---	0.20	0.007	0.001	0.05
1.88	33.84	-3.67	-3.50	-3.59	0.98	---	---	0.98	0.026	0.005	0.19
3.13	56.34	-0.89	0.10	-0.40	2.14	---	---	2.14	0.055	0.015	0.37
3.75	67.50	1.66	3.81	2.74	3.18	---	---	3.18	0.064	0.028	0.48
4.38[d]	78.84	5.43	9.93	7.68	5.35	---	---	5.35	0.084	0.044	0.70
5.00	90.00	9.29	15.03	12.16	7.55	---	---	7.55	0.110	0.058	0.94
6.25	112.50	19.85	23.44	21.65	12.05	---	---	12.05	0.184	0.088	1.64
7.50	135.00	29.62	33.21	31.42	16.28	---	---	16.28	0.257	0.120	2.25
8.75	157.50	39.68	42.90	41.29	20.65	---	---	20.65	0.333	0.150	2.77
10.00	180.00	49.77	52.35	51.06	24.93	---	---	24.93	0.407	0.180	3.32

a) ϵ_s = Reading of one strain gage on each reinforcing bar, as numbered, at mid-span. Adjusted to account for initial prestrain.
b) ϵ_p = Average reading of two or three strain gages on each strand at mid span.
c) In the non linear range, the stress is obtained directly from the actual stress strain curves of the tension reinforcement.
d) Onset of cracking.

TABLE 7S (CONTINUED)

Load P (kips)	Moment at Mid-span (k-in)	Stress in Reinforcing Bar f_s(ksi)			Increase in stress in the prestressed Strand Δf_{ps} (ksi)				Deflection (in)	Crack width(mm) (L.V.D.T. reading)	Curvature x10^{-4} (rad/in)
		1	2	Average	3	4	--	Average			
11.25	202.50	59.72	61.40	60.56	27.38	---	---	27.38	0.482	0.208	3.87
13.13y	236.34	76.63	77.16	76.90	30.83	---	---	30.83	0.600	0.255	4.78
13.55	243.90	77.00	77.50	77.25	46.34	---	---	46.34	0.661	0.480	6.22
14.18	255.24	80.00	80.00	80.00	60.14	---	---	60.14	0.868	0.661	9.16
14.88	267.84	81.80	f	81.80	77.40	---	---	77.40	1.489	0.861	16.11
15.27	274.86	83.20	---	83.20	82.60	---	---	82.60	2.060	0.955	20.42
15.68	282.24	f	---	---	86.00	---	---	86.00	2.520	1.142	24.40
15.88	285.84	---	---	---	89.10	---	---	89.10	2.880	---	26.31
16.28	293.04	---	---	---	92.40	---	---	92.40	3.780	---	32.84

f- Strain gage failed
y- Yielding of reinforcing steel.

N.A depth at ultimate = 0.75"

TABLE 8S

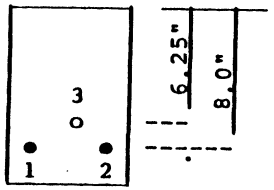

Beam Designation: PP1S2
Type of Loading: Static
Reinforcing steel = 2#4-60 Ksi
Prestressing steel = 1 5/16"-250 Ksi

f'_c at time of loading = 5800 Psi
Effective prestress, f_{pe} = 160.0 Ksi

Stress in the Tension Reinforcement[c]:
$f_s = E_s\epsilon_s \ldots (E_s = 29 \times 10^3$ Ksi) (a)
$f_{ps} = E_p\epsilon_p \ldots (E_p = 28.0 \times 10^3$ Ksi) (b)

Note: 1,2,3, etc. are the locations of strain gages.

Load P (kips)	Moment at Mid-span (k-in)	Stress in Reinforcing Bar f_s(ksi)			Increase in stress in the prestressed Strand Δf_{ps} (ksi)				Deflection (in)	Crack width (mm) (L.V.D.T. reading)	Curvature x10^{-4} (rad/in)
		1	2	Average	3	--	--	Average			
0.63	11.34	-5.90	-5.46	-5.68	0.32	---	---	0.32	0.001	0.000	0.06
1.25	22.50	-4.74	-4.52	-4.63	0.77	---	---	0.77	0.003	0.003	0.14
2.50	45.00	-1.89	-1.63	-1.76	1.96	---	---	1.96	0.021	0.014	0.33
3.75[d]	67.50	5.87	5.45	5.66	5.27	---	---	5.27	0.060	0.043	0.63
5.00	90.00	13.21	12.50	12.85	9.35	---	---	9.35	0.119	0.070	1.21
6.25	112.50	20.55	19.49	20.02	13.41	---	---	13.41	0.187	0.097	1.75
7.50	135.00	27.68	25.22	26.45	17.64	---	---	17.64	0.252	0.121	2.28
8.75	157.50	33.46	32.10	32.78	22.15	---	---	22.15	0.301	0.145	2.81
10.00	180.00	40.63	38.85	39.74	26.88	---	---	26.88	0.366	0.168	3.34
11.25	202.50	47.80	45.18	46.49	28.00	---	---	29.66	0.433	0.190	3.87

a) ϵ_s = Reading of one strain gage on each reinforcing bar, as numbered, at mid-span. Adjusted to account for initial prestrain.
b) ϵ_p = Average reading of two or three strain gages on each strand at mid span.
c) In the non linear range, the stress is obtained directly from the actual stress strain curves of the tension reinforcement.
d) Onset of cracking.

TABLE 8S (CONTINUED)

Load P (kips)	Moment at Mid-span (k-in)	Stress in Reinforcing Bar f_s(ksi)			Increase in stress in the prestressed Strand Δf_{ps} (ksi)				Deflection (in)	Crack width(mm) (L.V.D.T. reading)	Curvature x10^{-4} (rad/in)
		1	2	Average	3	--	--	Average			
12.50	225.00	58.33	56.17	57.25	31.38	---	---	31.38	0.509	0.239	4.59
13.13	236.34	63.63	f	63.63	36.55	---	---	36.55	0.540	0.281	5.03
14.18^{y}	255.24	72.40	---	72.40	50.30	---	---	50.30	0.661	0.486	6.72
14.50	261.00	f	---	---	53.80	---	---	53.80	0.763	0.564	7.36
15.10	271.80	---	---	---	64.10	---	---	64.10	0.991	0.665	9.68
15.40	277.20	---	---	---	67.60	---	---	67.60	1.134	0.725	10.86
15.75	283.50	---	---	---	---	---	---	---	1.422	---	13.25

f- Strain gage failed
y- Yielding of reinforcing steel.

N.A depth at ultimate = 1.75"

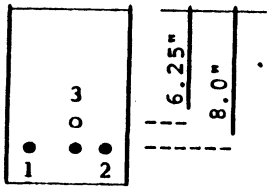

TABLE 9S

Beam Designation: PP1S3
Type of Loading: Static
Reinforcing steel = 3#4-60 Ksi
Prestressing steel = 1 3/8"-270 Ksi

f'_c at time of loading = 5998 Psi
Effective prestress, f_{pe} = 147.0 Ksi

Stress in the Tension Reinforcement(c):
$f_s = E_s \epsilon_s \ldots (E_s = 29 \times 10^3$ Ksi) (a)
$f_{ps} = E_p \epsilon_p \ldots (E_p = 28.6 \times 10^3$ Ksi) (b)

Note: 1,2,3, etc. are the locations of strain gages.

Load P (kips)	Moment at Mid-span (k-in)	Stress in Reinforcing Bar f_s(ksi)			Increase in stress in the prestressed Strand Δf_{ps} (ksi)				Deflection (in)	Crack width (mm) (L.V.D.T. reading)	Curvature $\times 10^{-4}$ (rad/in)
		1	2	Average	3	--	--	Average			
0.55	9.90	-6.68	-6.56	-6.62	0.24	---	---	0.24	0.007	0.000	0.01
1.10	19.80	-6.04	-5.81	-5.93	0.44	---	---	0.44	0.016	0.000	0.07
2.20	39.60	-4.42	-3.90	-4.16	1.17	---	---	1.17	0.034	0.008	0.26
3.30	59.40	-2.01	-1.84	-1.93	2.17	---	---	2.17	0.058	0.018	0.48
4.41	79.38	1.15	1.59	1.37	4.09	---	---	4.09	0.087	0.031	0.76
5.51[d]	99.18	4.92	5.82	5.37	6.52	---	---	6.52	0.121	0.046	1.11
6.61	118.98	9.30	10.02	9.66	9.41	---	---	9.41	0.165	0.061	1.51
7.71	138.78	13.79	14.75	14.27	13.03	---	---	13.03	0.213	0.078	1.94
8.81	158.58	17.62	19.01	18.32	15.79	---	---	15.79	0.260	0.092	2.37
10.46	188.28	23.86	25.86	24.86	20.25	---	---	20.25	0.332	0.113	2.91

a) ϵ_s = Reading of one strain gage on each reinforcing bar, as numbered, at mid-span. Adjusted to account for initial prestrain.
b) ϵ_p = Average reading of two or three strain gages on each strand at mid span.
c) In the non linear range, the stress is obtained directly from the actual stress strain curves of the tension reinforcement.
d) Onset of cracking.

TABLE 9S (CONTINUED)

Load P (kips)	Moment at Mid-span (k-in)	Stress in Reinforcing Bar f_s (ksi)			Increase in stress in the prestressed Strand Δf_{ps} (ksi)				Deflection (in)	Crack width(mm) (L.V.D.T. reading)	Curvature x10^{-4} (rad/in)
		1	2	Average	3	--	--	Average			
12.66	227.88	32.91	35.78	34.35	26.11	---	---	26.11	0.430	0.135	3.71
14.87	267.66	42.21	45.29	43.75	31.75	---	---	31.75	0.535	0.158	4.56
16.52	297.37	49.03	51.49	50.26	35.74	---	---	35.74	0.615	0.173	5.18
17.62	317.16	53.84	55.99	54.92	38.42	---	---	38.42	0.674	0.183	5.64
18.72	336.96	58.51	60.60	59.56	41.17	---	---	41.17	0.732	0.194	6.10
19.82Y	356.76	68.50	67.10	67.80	44.10	---	---	44.10	0.799	0.211	7.76
20.92	376.56	68.50	67.10	67.80	66.40	---	---	66.40	1.030	0.443	9.50
21.34	384.12	68.50	67.10	67.80	74.70	---	---	74.70	1.217	---	10.92

f- Strain gage failed
y- Yielding of reinforcing steel.

N.A depth at ultimate = ----

TABLE 10S

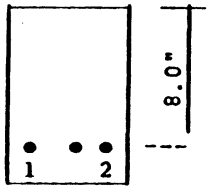

Beam Designation: RS1
Type of Loading: Static
Reinforcing steel = 3#3-60 Ksi
Prestressing steel = ---

f'_c at time of loading = 5940 Psi
Effective prestress, f_{pe} = --- Ksi

Stress in the Tension Reinforcement[c]:
$f_s = E_s \epsilon_s \ldots (E_s = 29 \times 10^3$ Ksi) (a)
$f_{ps} = E_p \epsilon_p \ldots (E_p = 28.6 \times 10^3$ Ksi) (b)

Note: 1,2,3, etc. are the locations of strain gages.

Load P (kips)	Moment at Mid-span (k-in)	Stress in Reinforcing Bar f_s(ksi)			Increase in stress in the prestressed Strand Δf_{ps} (ksi)				Deflection (in)	Crack width (mm) (L.V.D.T. reading)	Curvature $\times 10^{-4}$ (rad/in)
		1	2	Average	--	--	--	Average			
0.95	17.10	2.26	f	2.26	---	---	---	---	0.006	0.005	---
1.57[d]	28.62	5.08	---	5.08	---	---	---	---	0.026	0.013	---
2.26	40.68	8.90	---	8.90	---	---	---	---	0.056	0.032	---
2.67	48.06	11.46	---	11.46	---	---	---	---	0.074	0.035	---
3.19	57.42	14.94	---	14.94	---	---	---	---	0.091	0.044	---
3.56	64.08	16.85	---	16.85	---	---	---	---	0.114	0.051	---
4.45	80.10	21.98	---	21.98	---	---	---	---	0.156	0.067	---
5.33	95.94	27.00	---	27.00	---	---	---	---	0.198	0.083	---
6.00	108.00	31.46	---	31.46	---	---	---	---	0.231	0.102	---
6.61	118.98	35.00	---	35.00	---	---	---	---	0.261	0.114	---

a) ϵ_s = Reading of one strain gage on each reinforcing bar, as numbered, at mid-span. Adjusted to account for initial prestrain.
b) ϵ_p = Average reading of two or three strain gages on each strand at mid span.
c) In the non linear range, the stress is obtained directly from the actual stress strain curves of the tension reinforcement.
d) Onset of cracking.

TABLE 10S (CONTINUED)

Load P (kips)	Moment at Mid-span (k-in)	Stress in Reinforcing Bar f_s(ksi)			Increase in stress in the prestressed Strand Δf_{ps} (ksi)				Deflection (in)	Crack width(mm) (L.V.D.T. reading)	Curvature x10^{-4} (rad/in)
		1	2	Average	--	--	--	Average			
7.05	126.90	37.85	---	37.85	---	---	---	---	0.291	0.127	---
7.93	142.74	43.82	---	43.82	---	---	---	---	0.337	0.145	---
8.46	152.28	47.45	---	47.45	---	---	---	---	0.369	0.152	---
8.81	158.58	49.90	---	49.90	---	---	---	---	0.392	0.165	---
9.91Y	178.40	f	---	---	---	---	---	---	0.584	---	---
10.66	191.88	---	---	---	---	---	---	---	1.605	---	---
10.79	194.22	---	---	---	---	---	---	---	2.135	---	---
11.34	204.12	---	---	---	---	---	---	---	2.707	---	---

f- Strain gage failed
y- Yielding of reinforcing steel.

N.A depth at ultimate = ----

TABLE 11S

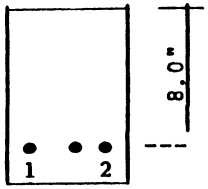

Beam Designation: RS2
Type of Loading: Static
Reinforcing steel = 3#4-60 Ksi
Prestressing steel = ---

f'_c at time of loading = 7000 Psi
Effective prestress, f_{pe} = --- Ksi

Stress in the Tension Reinforcement(c):
$f_s = E_s\varepsilon_s \ldots (E_s = 29 \times 10^3$ Ksi) (a)
$f_{ps} = E_p\varepsilon_p \ldots (E_p = 28.6 \times 10^3$ Ksi) (b)

Note: 1,2,3, etc. are the locations of strain gages.

Load P (kips)	Moment at Mid-span (k-in)	Stress in Reinforcing Bar f_s(ksi)			Increase in stress in the prestressed Strand Δf_{ps} (ksi)				Deflection (in)	Crack width (mm) (L.V.D.T. reading)	Curvature $\times 10^{-4}$ (rad/in)
		1	2	Average	--	--	--	Average			
1.28	23.04	2.97	2.57	2.77	---	---	---	---	0.021	0.006	0.17
2.31	41.58	4.92	4.37	4.65	---	---	---	---	0.039	0.013	0.30
3.63[d]	65.34	10.25	9.12	9.69	---	---	---	---	0.069	0.032	0.60
4.69	84.42	15.01	14.17	14.59	---	---	---	---	0.113	0.051	0.97
5.64	101.42	19.27	18.34	18.81	---	---	---	---	0.156	0.070	1.33
6.70	120.60	23.33	22.81	23.07	---	---	---	---	0.202	0.083	1.70
8.00	144.00	28.55	28.49	28.52	---	---	---	---	0.259	0.102	2.16
10.35	186.30	38.38	38.85	38.62	---	---	---	---	0.362	0.127	2.95
11.76	211.68	44.18	44.70	44.44	---	---	---	---	0.423	0.146	3.42
13.26	238.68	50.04	50.77	50.41	---	---	---	---	0.489	0.165	3.91

a) ε_s = Reading of one strain gage on each reinforcing bar, as numbered, at mid-span. Adjusted to account for initial prestrain.
b) ε_p = Average reading of two or three strain gages on each strand at mid span.
c) In the non linear range, the stress is obtained directly from the actual stress strain curves of the tension reinforcement.
d) Onset of cracking.

TABLE 11S (CONTINUED)

Load P (kips)	Moment at Mid-span (k-in)	Stress in Reinforcing Bar f_s(ksi)			Increase in stress in the prestressed Strand Δf_{ps} (ksi)				Deflection (in)	Crack width(mm) (L.V.D.T. reading)	Curvature x10^{-4} (rad/in)
		1	2	Average	--	--	--	Average			
14.67	264.06	55.78	56.51	56.15	---	---	---	---	0.552	0.184	4.40
15.51	279.18	59.52	60.34	59.93	---	---	---	---	0.594	0.200	4.70
16.17Y	291.06	62.80	63.81	63.30	---	---	---	---	0.620	0.211	4.89
16.39	295.02	62.80	63.81	63.30	---	---	---	---	0.883	0.330	13.64
17.27	310.86	f	f	---	---	---	---	---	1.167	---	18.50
18.00	324.00	---	---	---	---	---	---	---	2.160	---	22.00

f- Strain gage failed
y- Yielding of reinforcing steel.

N.A depth at ultimate = ----

TABLE 12S

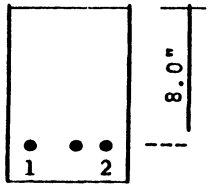

Beam Designation: RS3
Type of Loading: Static
Reinforcing steel = 3#5-60 Ksi
Prestressing steel = ---

f'_c at time of loading = 7000 Psi
Effective prestress, f_{pe} = --- Ksi

Stress in the Tension Reinforcement[c]:
$f_s = E_s \varepsilon_s \ldots (E_s = 29 \times 10^3$ Ksi) (a)
$f_{ps} = E_p \varepsilon_p \ldots (E_p = 28.6 \times 10^3$ Ksi) (b)

Note: 1,2,3, etc. are the locations of strain gages.

Load P (kips)	Moment at Mid-span (k-in)	Stress in Reinforcing Bar f_s(ksi)			Increase in stress in the prestressed Strand Δf_{ps} (ksi)				Deflection (in)	Crack width (mm) (L.V.D.T. reading)	Curvature $\times 10^{-4}$ (rad/in)
		1	2	Average	--	--	--	Average			
1.32	23.76	-0.24	0.49	0.13	---	---	---	---	0.018	0.003	0.12
2.42	43.56	0.17	1.07	0.62	---	---	---	---	0.038	0.009	0.30
3.31	59.58	2.17	3.36	2.77	---	---	---	---	0.058	0.019	0.47
4.18	75.24	4.17	5.88	5.03	---	---	---	---	0.077	0.031	0.65
5.07[d]	91.26	7.07	8.67	7.87	---	---	---	---	0.107	0.044	0.87
5.90	106.20	9.40	11.30	10.35	---	---	---	---	0.126	0.054	1.07
7.53	135.54	15.14	16.09	15.62	---	---	---	---	0.175	0.070	1.42
10.22	183.96	21.00	22.18	21.59	---	---	---	---	0.250	0.095	2.00
11.54	207.72	25.87	24.56	25.22	---	---	---	---	0.290	0.109	2.30
13.22	237.96	28.77	30.65	29.71	---	---	---	---	0.336	0.127	2.68

a) ε_s = Reading of one strain gage on each reinforcing bar, as numbered, at mid-span. Adjusted to account for initial prestrain.
b) ε_p = Average reading of two or three strain gages on each strand at mid span.
c) In the non linear range, the stress is obtained directly from the actual stress strain curves of the tension reinforcement.
d) Onset of cracking.

TABLE 12S (CONTINUED)

Load P (kips)	Moment at Mid-span (k-in)	Stress in Reinforcing Bar f_s(ksi)			Increase in stress in the prestressed Strand Δf_{ps} (ksi)				Deflection (in)	Crack width(mm) (L.V.D.T. reading)	Curvature $x10^{-4}$ (rad/in)
		1	2	Average	--	--	--	Average			
15.95	287.10	35.96	38.48	37.22	---	---	---	---	0.421	0.152	3.35
17.62	317.16	40.42	43.18	41.80	---	---	---	---	0.472	0.165	3.69
19.82	356.76	46.22	49.62	47.92	---	---	---	---	0.546	0.191	4.24
22.03	396.54	52.31	56.40	54.36	---	---	---	---	0.628	0.210	4.86
23.26[y]	418.68	65.00	65.00	65.00	---	---	---	---	0.783	0.343	7.17
24.00	432.00	65.00	65.00	65.00	---	---	---	---	0.958	0.622	13.60
24.67	444.06	65.00	65.00	65.00	---	---	---	---	1.244	---	17.70

f- Strain gage failed
y- Yielding of reinforcing steel.

N.A depth at ultimate = ----

TABLE 1D

Beam Designation: PD1
Type of Loading: Dynamic (cyclic)
f'_c at time of loading = 5570 Psi
Effective prestress, f_{pe} = 173.0 Ksi

Stress range in the prestressing strand = $\Delta f_{ps(max)} - \Delta f_{ps(min)}$

Stress range in the reinforcing bars = $f_{s(max)} - f_{s(min)}$

Note: See Table 1S for more details.

Number of Cycles N	Δf_{ps} at P_{min} & P_{max} (ksi)		f_s at P_{min} & P_{max} (ksi)		Deflection at P_{min} and P_{max} (in)		Crack width at P_{min} & P_{max} (mm)		Curvature at P_{min} and P_{max} x 10^{-4} (rad/in)		Remarks
	min	max	min	max	min	max	W_{min}	W_{max}	min	max	
1	2.30	18.78	--	--	0.053	0.152	0.031	0.144	0.44	1.43	
2	11.16	20.57	--	--	0.109	0.164	0.098	0.163	1.02	1.55	$\bar{\omega}$ = 0.14
3	11.10	21.11	--	--	0.110	0.168	0.100	0.168	1.03	1.59	PPR = 1
2500	11.35	25.38	--	--	0.128	0.207	0.121	0.228	1.17	1.93	P_{min} = 3.3 Kips
10^4	11.35	26.17	--	--	0.140	0.222	0.131	0.245	1.23	2.04	P_{max} = 4.9 Kips
$5x10^4$	12.21	28.16	--	--	0.147	0.245	0.134	0.266	1.49	2.39	
$1.6x10^5$	12.04	28.00	--	--	0.163	0.261	0.144	0.280	1.55	2.48	
$5.0x10^5$	f	f	--	--	0.189	0.299	0.147	0.282	1.66	2.57	
$7.5x10^5$	--	--	--	--	0.199	0.318	0.157	0.308	1.75	2.76	Beam failed at
10^6	--	--	--	--	0.229	0.356	0.165	0.316	1.81	2.82	$1.212x10^6$ cycles
$1.1x10^6$	--	--	--	--	0.297	0.431	0.193	0.348	1.97	3.00	

TABLE 2D

Beam Designation: PD2
Type of Loading: Dynamic (cyclic)
f'_c at time of loading = 5660 Psi
Effective prestress, f_{pe} = 143.0 Ksi

Stress range in the prestressing strand = $\Delta f_{ps(max)} - \Delta f_{ps(min)}$

Stress range in the reinforcing bars = $f_{s(max)} - f_{s(min)}$

Note: See Table 2S for more details.

Number of Cycles N	Δf_{ps} at P_{min} & P_{max} (ksi)		f_s at P_{min} & P_{max} (ksi)		Deflection at P_{min} and P_{max} (in)		Crack width at P_{min} & P_{max} (mm)		Curvature at P_{min} and P_{max} x 10^{-4} (rad/in)		Remarks
	min	max	min	max	min	max	W_{min}	W_{max}	min	max	
1	3.81	25.94	--	--	0.096	0.257	0.023	0.254			
2	11.90	27.32	--	--	0.174	0.270	0.134	0.273			$\bar{\omega}$ = 0.26
3	12.00	27.97	--	--	0.176	0.277	0.144	0.283			PPR = 1
2500	12.70	29.77	--	--	0.211	0.344	0.200	0.397			P_{min} = 5.5 Kips
5000	12.70	30.00	--	--	0.211	0.345	0.196	0.397			P_{max} = 8.37 Kips
10^4	13.00	31.19	--	--	0.227	0.364	0.215	0.420			
$5x10^4$	15.67	34.27	--	--	0.244	0.395	0.240	0.466			
$7.5x10^4$	17.80	35.41	--	--	0.246	0.403	0.243	0.472			
10^5	17.27	36.60	--	--	0.254	0.410	0.246	0.491			
$2.5x10^5$	f	f	--	--	0.269	0.432	0.265	0.516			
$5x10^5$	--	--	--	--	0.282	0.446	0.277	0.528			

TABLE 2D (CONTINUED)

Number of Cycles N	Δf_{ps} at P_{min} & P_{max} (ksi)		fs at P_{min} & P_{max} (ksi)		Deflection at P_{min} and P_{max} (in)		Crack width at P_{min} & P_{max} (mm)		Curvature at P_{min} and P_{max} x 10^{-4} (rad/in)		Remarks
	min	max	min	max	min	max	W_{min}	W_{max}	min	max	
7.5×10^5	f	f	--	--	0.293	0.457	0.288	0.541			
10^6	--	--	--	--	0.302	0.463	0.295	0.542			Beam failed at
1.5×10^6	--	--	--	--	0.314	0.474	0.299	0.546			2.2×10^6 cycles
2.16×10^6	--	--	--	--	0.481	0.700	0.575	0.929			
2.17×10^6	--	--	--	--	0.677	0.900	0.983	1.269			

TABLE 3D

Beam Designation: PD3
Type of Loading: Dynamic (cyclic)
f'_c at time of loading = 5730 Psi
Effective prestress, f_{pe} = 146.0 Ksi

Stress range in the prestressing strand = $\Delta f_{ps(max)} - \Delta f_{ps(min)}$

Stress range in the reinforcing bars = $f_{s(max)} - f_{s(min)}$

Note: See Table 3S for more details.

Number of Cycles N	Δf_{ps} at P_{min} & P_{max} (ksi)		f_s at P_{min} & P_{max} (ksi)		Deflection at P_{min} and P_{max} (in)		Crack width at P_{min} & P_{max} (mm)		Curvature at P_{min} and P_{max} x 10^{-4} (rad/in)		Remarks
	min	max	min	max	min	max	W_{min}	W_{max}	min	max	
1	4.70	20.26	--	--	0.118	0.280	0.026	0.158	0.92	2.26	
2	9.37	21.93	--	--	0.182	0.300	0.071	0.178	1.47	2.42	$\bar{\omega}$ = 0.37
3	9.38	21.66	--	--	0.186	0.301	0.073	0.178	1.50	2.42	PPR = 1
2500	10.00	23.68	--	--	0.198	0.329	0.084	0.205	1.73	2.63	P_{min} = 7.5 Kips
10^4	10.20	24.02	--	--	0.202	0.337	0.088	0.214	1.76	2.68	P_{max} = 11.5 Kips
$5x10^4$	10.90	25.24	--	--	0.218	0.356	0.095	0.227	1.85	2.81	
10^5	11.84	26.72	--	--	0.224	0.365	0.100	0.241	1.92	2.93	
$2.5x10^5$	10.36	30.44	--	--	0.243	0.401	0.105	0.278	2.04	3.25	
$7.5x10^5$	f	f	--	--	0.269	0.412	0.134	0.285	2.29	3.34	
$1.1x10^6$	--	--	--	--	0.290	0.435	0.153	0.305	2.50	3.57	
$1.25x10^6$	--	--	--	--	0.308	0.456	0.170	0.325	2.66	3.74	

TABLE 3D (CONTINUED)

Number of Cycles N	Δf_{ps} at P_{min} & P_{max} (ksi)		fs at P_{min} & P_{max} (ksi)		Deflection at P_{min} and P_{max} (in)		Crack width at P_{min} & P_{max} (mm)		Curvature at P_{min} and P_{max} x 10^{-4} (rad/in)		Remarks
	min	max	min	max	min	max	W_{min}	W_{max}	min	max	
$1.38x10^6$	--	--	--	--	0.319	0.470	0.184	0.338	2.75	3.85	
$1.68x10^6$	--	--	--	--	0.358	0.525	0.224	0.434	3.08	4.55	
$1.75x10^6$	--	--	--	--	0.386	0.556	0.476	0.70	3.61	5.05	Beam failed at $1.94x10^6$ cycle
$1.8x10^6$	--	--	--	--	0.399	0.580	0.504	0.738	3.77	5.38	
$1.89x10^6$	--	--	--	--	0.469	0.669	0.662	0.944	4.59	6.71	
$1.93x10^6$	--	--	--	--	0.557	0.771	0.780	1.121	5.61	7.83	
$1.94x10^6$	--	--	--	--	0.741	0.981	1.080	--	7.54	10.12	

TABLE 4D

Beam Designation: PP2D1
Type of Loading: Dynamic (cyclic)
f'_c at time of loading = 6576 Psi
Effective prestress, f_{pe} = 165.0 Ksi

Stress range in the prestressing strand = $\Delta f_{ps(max)} - \Delta f_{ps(min)}$

Stress range in the reinforcing bars = $f_{s(max)} - f_{s(min)}$

Note: See Table 4S for more details.

Number of Cycles N	Δf_{ps} at P_{min} & P_{max} (ksi)		f_s at P_{min} & P_{max} (ksi)		Deflection at P_{min} and P_{max} (in)		Crack width at P_{min} & P_{max} (mm)		Curvature at P_{min} and P_{max} x 10^{-4} (rad/in)		Remarks
	min	max	min	max	min	max	W_{min}	W_{max}	min	max	
1	4.44	17.79	7.20	38.63	0.055	0.159	0.058	0.158	0.27	1.42	
2	12.90	18.72	22.14	40.35	0.125	0.173	0.122	0.167	1.08	1.50	$\bar{\omega}$ = 0.1
3	13.20	18.98	22.62	40.73	0.128	0.176	0.125	0.171	1.11	1.53	PPR = 0.62
2500	14.46	21.36	22.70	42.18	0.145	0.203	0.134	0.186	1.28	1.77	P_{min} = 3.2 Kips
10^4	15.40	22.85	22.75	40.70	0.158	0.219	0.136	0.191	1.45	1.98	P_{max} = 4.8 Kips
$5x10^4$	16.46	24.43	23.89	40.99	0.175	0.233	0.139	0.195	1.57	2.15	
$1.5x10^5$	14.35	22.25	21.59	38.09	0.184	0.247	0.138	0.194	1.63	2.21	
$3.5x10^5$	16.83	24.85	24.86	41.20	0.196	0.257	0.146	0.204	1.73	2.31	
$5x10^5$	17.56	25.55	25.85	42.34	0.202	0.263	0.148	0.205	1.78	2.34	
$7.5x10^5$	17.50	25.43	26.20	42.34	0.212	0.272	0.150	0.207	1.82	3.88	
10^6	17.92	25.91	26.74	42.98	0.217	0.278	0.153	0.211	1.87	2.44	

TABLE 4D (CONTINUED)

Number of Cycles N	Δf_{ps} at P_{min} & P_{max} (ksi)		fs at P_{min} & P_{max} (ksi)		Deflection at P_{min} and P_{max} (in)		Crack width at P_{min} & P_{max} (mm)		Curvature at P_{min} and P_{max} x 10^{-4} (rad/in)		Remarks
	min	max	min	max	min	max	W_{min}	W_{max}	min	max	
$1.5x10^6$	19.60	27.45	26.45	41.74	0.231	0.295	0.150	0.198	2.25	2.90	Beam was loaded statically to failure at $5x10^6$ cycles
$2x10^6$	19.48	27.67	26.55	42.21	0.241	0.303	0.151	0.206	2.35	2.99	
$2.5x10^6$	21.24	29.15	28.30	43.92	0.246	0.308	0.157	0.212	2.42	3.06	
$2.85x10^6$	22.19	30.17	29.35	45.06	0.250	0.311	0.160	0.214	2.46	3.10	
$3.25x10^6$	22.30	30.24	29.19	45.11	0.251	0.314	0.162	0.215	2.50	3.14	
$3.5x10^6$	22.99	30.92	29.97	45.85	0.256	0.316	0.164	0.217	2.52	3.16	
$4x10^6$	21.48	30.03	29.20	44.79	0.262	0.321	0.161	0.215	2.55	3.19	
$4.5x10^6$	21.20	29.24	28.11	43.90	0.267	0.326	0.158	0.212	2.58	3.21	
$5x10^6$	21.52	28.55	28.00	43.05	0.267	0.327	0.161	0.214	2.61	3.24	

TABLE 5D

Beam Designation: PP2D2
Type of Loading: Dynamic (cyclic)
f'_c at time of loading = 5290 Psi
Effective prestress, f_{pe} = 160.0 Ksi

Stress range in the prestressing strand = $\Delta f_{ps(max)} - \Delta f_{ps(min)}$

Stress range in the reinforcing bars = $f_{s(max)} - f_{s(min)}$

Note: See Table 5S for more details.

Number of Cycles N	Δf_{ps} at P_{min} & P_{max} (ksi)		f_s at P_{min} & P_{max} (ksi)		Deflection at P_{min} and P_{max} (in)		Crack width at P_{min} & P_{max} (mm)		Curvature at P_{min} and P_{max} x 10^{-4} (rad/in)		Remarks
	min	max	min	max	min	max	W_{min}	W_{max}	min	max	
1	9.44	27.35	9.64	35.00	0.109	0.337	0.077	0.199	1.08	3.38	
2	19.02	28.38	17.31	36.07	0.244	0.351	0.148	0.207	2.45	3.51	$\bar{\omega}$ = 0.2
3	19.53	28.70	17.89	36.48	0.249	0.356	0.150	0.209	2.50	3.57	PPR = 0.68
2500	20.87	30.61	19.20	39.55	0.27	0.389	0.162	0.217	2.68	3.79	P_{min} = 4.5 Kips
5000	21.08	31.03	19.25	40.13	0.273	0.395	0.163	0.220	2.72	3.85	P_{max} = 7.0 Kips
10^4	21.55	31.56	19.72	40.66	0.277	0.400	0.166	0.224	2.76	3.90	
$5x10^4$	22.75	33.10	20.82	41.47	0.296	0.417	0.170	0.228	2.87	4.03	
10^5	23.14	33.36	21.23	41.61	0.304	0.424	0.171	0.229	2.93	4.08	
$2x10^5$	23.44	33.71	21.28	41.50	0.312	0.435	0.171	0.231	3.00	4.16	
$5x10^5$	24.63	35.12	21.89	42.13	0.328	0.449	0.172	0.234	3.09	4.28	
$7.5x10^5$	25.34	35.74	22.33	42.42	0.335	0.456	0.175	0.237	3.17	4.34	

TABLE 5D (CONTINUED)

Number of Cycles N	Δf_{ps} at P_{min} & P_{max} (ksi)		fs at P_{min} & P_{max} (ksi)		Deflection at P_{min} and P_{max} (in)		Crack width at P_{min} & P_{max} (mm)		Curvature at P_{min} and P_{max} x 10^{-4} (rad/in)		Remarks
	min	max	min	max	min	max	W_{min}	W_{max}	min	max	
10^6	25.85	36.13	22.70	42.60	0.339	0.463	0.177	0.239	3.23	4.39	
$1.5x10^6$	26.38	36.81	23.23	42.74	0.351	0.475	0.177	0.244	3.30	4.50	Beam was loaded
$1.75x10^6$	26.48	36.79	23.49	42.54	0.360	0.481	0.177	0.241	3.38	4.55	statically to
$2.25x10^6$	27.35	37.74	24.04	43.32	0.363	0.486	0.179	0.244	3.44	4.61	failure at
$2.75x10^6$	26.68	37.16	23.23	42.37	0.372	0.492	0.178	0.241	3.51	4.65	$5x10^6$ cycles
$3x10^6$	26.79	37.05	23.28	42.25	0.376	0.496	0.179	0.243	3.55	4.68	
$3.5x10^6$	26.78	37.27	23.14	42.00	0.378	0.499	0.179	0.243	3.56	4.69	
$4x10^6$	28.02	38.41	24.39	43.32	0.382	0.502	0.181	0.246	3.61	4.74	
$4.5x10^6$	30.23	39.48	27.03	45.27	0.383	0.503	0.185	0.250	3.65	4.77	
$5x10^6$	31.72	41.87	28.48	46.95	0.385	0.504	0.192	0.256	3.69	4.80	

TABLE 6D

Beam Designation: PP2D3
Type of Loading: Dynamic (cyclic)
f'_c at time of loading = 6200 Psi
Effective prestress, f_{pe} = 131.0 Ksi

Stress range in the prestressing strand = $\Delta f_{ps(max)} - \Delta f_{ps(min)}$

Stress range in the reinforcing bars = $f_{s(max)} - f_{s(min)}$

Note: See Table 6S for more details.

Number of Cycles N	Δf_{ps} at P_{min} & P_{max} (ksi)		f_s at P_{min} & P_{max} (ksi)		Deflection at P_{min} and P_{max} (in)		Crack width at P_{min} & P_{max} (mm)		Curvature at P_{min} and P_{max} x 10^{-4} (rad/in)		Remarks
	min	max	min	max	min	max	W_{min}	W_{max}	min	max	
1	15.32	35.25	15.04	45.12	0.201	0.459	0.108	0.234			$\bar{\omega}$ = 0.30
2	23.36	36.00	23.54	45.81	0.332	0.473	0.164	0.240			PPR = 0.74
3	23.60	36.39	23.86	46.36	0.338	0.481	0.165	0.243			P_{min} = 8.0 Kips
2500	24.52	39.33	24.96	49.06	0.355	0.525	0.169	0.259			P_{max} = 12.0 Kips
5000	24.78	39.61	25.37	49.29	0.362	0.529	0.171	0.259			
10^4	25.07	39.90	25.77	49.67	0.368	0.535	0.174	0.261			
$5x10^4$	25.50	40.32	27.00	50.51	0.381	0.547	0.178	0.265			
10^5	25.94	40.97	27.80	51.38	0.388	0.556	0.179	0.268			
$2.5x10^5$	27.29	42.15	29.57	53.12	0.406	0.568	0.185	0.273			
$5x10^5$	27.33	41.88	30.09	53.18	0.418	0.581	0.188	0.274			
$7.5x10^5$	27.37	41.61	30.61	53.58	0.421	0.584	0.190	0.275			

TABLE 6D (CONTINUED)

Number of Cycles N	Δf_{ps} at P_{min} & P_{max} (ksi)		fs at P_{min} & P_{max} (ksi)		Deflection at P_{min} and P_{max} (in)		Crack width at P_{min} & P_{max} (mm)		Curvature at P_{min} and P_{max} x 10^{-4} (rad/in)		Remarks
	min	max	min	max	min	max	W_{min}	W_{max}	min	max	
10^6	26.07	40.71	32.76	55.55	0.434	0.596	0.186	0.272			
1.25×10^6	25.19	39.75	31.63	55.14	0.446	0.605	0.185	0.271			Beam was loaded
1.5×10^6	25.83	40.12	f	f	0.452	0.613	0.188	0.274			statically to
1.75×10^6	25.71	39.87	--	--	0.457	0.618	0.186	0.272			failure at
2×10^6	25.68	41.43	--	--	0.461	0.623	0.191	0.275			5×10^6 cycles
2.5×10^6	27.74	42.19	--	--	0.471	0.632	0.194	0.278			
2.75×10^6	28.32	42.66	--	--	0.474	0.636	0.196	0.280			
3×10^6	26.15	41.09	--	--	0.480	0.640	0.193	0.277			
3.25×10^6	26.52	41.30	--	--	0.480	0.642	0.240	0.327			
3.75×10^6	27.37	42.24	--	--	0.485	0.649	0.242	0.329			
4.25×10^6	28.26	42.71	--	--	0.491	0.653	0.242	0.328			
4.75×10^6	26.52	41.22	--	--	0.494	0.658	0.242	0.328			
5×10^6	28.54	43.02	--	--	0.497	0.660	0.246	0.332			

TABLE 7D

Beam Designation: PP1D1
Type of Loading: Dynamic (cyclic)
f'_c at time of loading = 6040 Psi
Effective prestress, f_{pe} = 164.0 Ksi

Stress range in the prestressing strand = $\Delta f_{ps(max)} - \Delta f_{ps(min)}$

Stress range in the reinforcing bars = $f_{s(max)} - f_{s(min)}$

Note: See Table 7S for more details.

Number of Cycles N	Δf_{ps} at P_{min} & P_{max} (ksi)		f_s at P_{min} & P_{max} (ksi)		Deflection at P_{min} and P_{max} (in)		Crack width at P_{min} & P_{max} (mm)		Curvature at P_{min} and P_{max} x 10^{-4} (rad/in)		Remarks
	min	max	min	max	min	max	W_{min}	W_{max}	min	max	
1	15.75	31.35	24.71	49.78	0.208	0.416	0.120	0.205	1.84	3.48	
2	23.20	32.12	33.10	50.46	0.310	0.424	0.151	0.207	2.58	3.53	$\bar{\omega}$ = 0.13
3	23.47	32.29	33.50	50.67	0.314	0.427	0.153	0.209	2.61	3.55	PPR = 0.33
2500	24.08	33.34	34.30	51.53	0.327	0.444	0.155	0.211	2.73	3.63	P_{min} = 6.5 Kips
10^4	24.15	33.97	34.54	52.25	0.340	0.453	0.156	0.213	2.76	3.71	P_{max} = 9.75 Kips
$5x10^4$	24.20	34.15	35.04	52.73	0.349	0.463	0.156	0.215	2.85	3.75	
$1.5x10^5$	24.14	34.09	35.31	52.99	0.360	0.473	0.157	0.216	2.92	3.81	
$5x10^5$	23.90	33.78	35.57	53.20	0.373	0.486	0.159	0.218	3.03	3.91	
10^6	23.68	33.63	35.92	53.39	0.385	0.496	0.159	0.219	3.10	3.99	
$1.5x10^6$	25.60	35.50	39.34	56.85	0.392	0.503	0.166	0.225	3.17	4.06	
$2x10^6$	26.04	36.06	39.98	57.57	0.398	0.509	0.169	0.228	3.22	4.11	

TABLE 7D (CONTINUED)

Number of Cycles N	Δf_{ps} at P_{min} & P_{max} (ksi)		fs at P_{min} & P_{max} (ksi)		Deflection at P_{min} and P_{max} (in)		Crack width at P_{min} & P_{max} (mm)		Curvature at P_{min} and P_{max} x 10^{-4} (rad/in)		Remarks
	min	max	min	max	min	max	W_{min}	W_{max}	min	max	
$2.5x10^6$	24.42	34.23	38.41	55.93	0.405	0.514	0.163	0.222	3.25	4.13	
$3x10^6$	24.60	34.34	38.96	56.33	0.408	0.518	0.164	0.223	3.27	4.17	Beam was loaded
$3.5x10^6$	25.00	34.82	38.99	56.36	0.413	0.522	0.165	0.224	3.31	4.19	statically to
$4x10^6$	26.70	36.46	40.90	58.25	0.413	0.523	0.173	0.230	3.36	4.23	failure at
$4.5x10^6$	25.60	35.52	40.00	57.46	0.419	0.527	0.169	0.226	3.37	4.24	$5x10^6$ cycles
$5x10^6$	25.54	35.34	40.15	57.46	0.422	0.533	0.167	0.226	3.38	4.26	

TABLE 8D

Beam Designation: PP1D2
Type of Loading: Dynamic (cyclic)
f'_c at time of loading = 5806 Psi
Effective prestress, f_{pe} = 138.0 Ksi

Stress range in the prestressing strand = $\Delta f_{ps(max)} - \Delta f_{ps(min)}$

Stress range in the reinforcing bars = $f_{s(max)} - f_{s(min)}$

Note: See Table 8S for more details.

Number of Cycles N	Δf_{ps} at P_{min} & P_{max} (ksi)		f_s at P_{min} & P_{max} (ksi)		Deflection at P_{min} and P_{max} (in)		Crack width at P_{min} & P_{max} (mm)		Curvature at P_{min} and P_{max} x 10^{-4} (rad/in)		Remarks
	min	max	min	max	min	max	W_{min}	W_{max}	min	max	
1	15.71	28.13	25.18	43.55	0.217	0.403	0.097	0.160	1.98	3.40	
2	20.86	28.78	29.31	43.66	0.304	0.413	0.117	0.162	2.57	3.46	$\bar{\omega}$ = 0.20
3	21.14	29.07	29.41	43.75	0.309	0.416	0.118	0.162	2.61	3.48	PPR = 0.33
1000	21.67	29.76	29.98	44.33	0.316	0.425	0.120	0.163	2.66	3.53	P_{min} = 6.25 Kips
10^4	22.12	30.49	30.05	44.55	0.324	0.436	0.120	0.163	2.79	3.60	P_{max} = 9.5 Kips
$5x10^4$	22.36	31.07	29.87	44.75	0.339	0.448	0.121	0.164	2.84	3.66	
$1.5x10^5$	23.10	31.88	31.48	46.14	0.349	0.460	0.122	0.166	2.93	3.74	
$5x10^5$	22.16	30.88	31.79	46.53	0.369	0.478	0.122	0.166	3.07	3.87	
10^6	22.79	31.22	33.22	47.67	0.380	0.491	0.123	0.166	3.17	3.96	
$1.5x10^6$	22.05	27.03	34.63	49.46	0.389	0.501	0.122	0.167	3.24	4.03	
$2x10^6$	21.24	29.81	34.18	49.00	0.398	0.509	0.120	0.165	3.28	4.07	

TABLE 8D (CONTINUED)

Number of Cycles N	Δf_{ps} at P_{min} & P_{max} (ksi)		fs at P_{min} & P_{max} (ksi)		Deflection at P_{min} and P_{max} (in)		Crack width at P_{min} & P_{max} (mm)		Curvature at P_{min} and P_{max} x 10^{-4} (rad/in)		Remarks
	min	max	min	max	min	max	W_{min}	W_{max}	min	max	
$2.5x10^6$	21.27	29.46	34.67	49.19	0.404	0.515	0.124	0.165	3.34	4.12	
$3x10^6$	21.24	29.74	35.15	49.90	0.413	0.521	0.122	0.164	3.34	4.16	Beam was loaded
$3.5x10^6$	21.05	29.51	35.00	49.72	0.418	0.525	0.121	0.164	3.38	4.17	statically to
$4x10^6$	20.77	29.24	34.83	49.56	0.422	0.530	0.121	0.164	3.42	4.21	failure at
$4.5x10^6$	19.98	28.43	34.30	49.04	0.426	0.534	0.121	0.163	3.45	4.23	$5x10^6$ cycles
$5x10^6$	20.11	28.50	36.44	51.19	0.432	0.539	0.121	0.165	3.48	4.27	

TABLE 9D

Beam Designation: PP1D3
Type of Loading: Dynamic (cyclic)
f'_c at time of loading = 5998 Psi
Effective prestress, f_{pe} = 150.0 Ksi

Stress range in the prestressing strand = $\Delta f_{ps(max)} - \Delta f_{ps(min)}$

Stress range in the reinforcing bars = $f_{s(max)} - f_{s(min)}$

Note: See Table 9S for more details.

Number of Cycles N	Δf_{ps} at P_{min} & P_{max} (ksi)		f_s at P_{min} & P_{max} (ksi)		Deflection at P_{min} and P_{max} (in)		Crack width at P_{min} & P_{max} (mm)		Curvature at P_{min} and P_{max} x 10^{-4} (rad/in)		Remarks
	min	max	min	max	min	max	W_{min}	W_{max}	min	max	
1	13.45	24.57	17.86	36.76	0.213	0.397	0.082	0.138			
2	17.67	24.58	24.47	36.97	0.297	0.400	0.104	0.138			$\bar{\omega}$ = 0.3
3	17.84	24.74	24.93	37.34	0.302	0.401	0.105	0.138			PPR = 0.34
5000	16.93	24.04	24.80	37.29	0.314	0.416	0.111	0.137			P_{min} = 8.37 Kips
10^4	16.98	25.61	24.73	38.94	0.318	0.436	0.109	0.143			P_{max} = 12.55 Kips
10^5	18.07	25.52	26.24	39.11	0.338	0.442	0.113	0.144			
$2x10^5$	17.18	24.43	25.45	38.07	0.344	0.450	0.115	0.144			
$5.5x10^5$	17.42	25.00	26.44	39.29	0.362	0.465	0.113	0.146			
$7.5x10^5$	17.32	24.82	26.35	39.14	0.365	0.470	0.113	0.145			
10^6	17.07	22.92	27.13	40.91	0.389	0.501	0.120	0.157			
$1.5x10^6$	19.44	26.66	29.48	42.71	0.400	0.513	0.127	0.161			

TABLE 9D (CONTINUED)

Number of Cycles N	Δf_{ps} at P_{min} & P_{max} (ksi)		fs at P_{min} & P_{max} (ksi)		Deflection at P_{min} and P_{max} (in)		Crack width at P_{min} & P_{max} (mm)		Curvature at P_{min} and P_{max} x 10^{-4} (rad/in)		Remarks
	min	max	min	max	min	max	W_{min}	W_{max}	min	max	
$2x10^6$	18.70	26.57	31.05	42.88	0.414	0.523	0.126	0.162			
$2.5x10^6$	18.94	26.91	30.12	43.32	0.424	0.529	0.125	0.161			Beam was loaded
$3x10^6$	19.57	27.40	30.93	44.04	0.428	0.534	0.127	0.163			statically to
$3.5x10^6$	20.69	28.38	32.01	44.97	0.429	0.538	0.131	0.167			failure at
$3.85x10^6$	21.18	28.95	32.64	45.43	0.434	0.541	0.133	0.168			$5x10^6$ cycles
$4.25x10^6$	21.66	29.25	33.05	45.87	0.436	0.545	0.134	0.169			
$4.75x10^6$	19.71	27.17	31.08	43.84	0.445	0.549	0.128	0.163			
$5x10^6$	21.24	28.83	32.73	45.66	0.445	0.549	0.129	0.165			

TABLE 10D

Beam Designation: RD1
Type of Loading: Dynamic (cyclic)
f'_c at time of loading = 5940 Psi
Effective prestress, f_{pe} = ---

Stress range in the prestressing strand = $\Delta f_{ps(max)} - \Delta f_{ps(min)}$

Stress range in the reinforcing bars = $f_{s(max)} - f_{s(min)}$

Note: See Table 10S for more details.

Number of Cycles N	Δf_{ps} at P_{min} & P_{max} (ksi)		f_s at P_{min} & P_{max} (ksi)		Deflection at P_{min} and P_{max} (in)		Crack width at P_{min} & P_{max} (mm)		Curvature at P_{min} and P_{max} x 10^{-4} (rad/in)		Remarks
	min	max	min	max	min	max	W_{min}	W_{max}	min	max	
1	--	--	28.46	46.70	0.221	0.386	0.123	0.185			
2	--	--	32.53	47.45	0.281	0.395	0.135	0.188			$\bar{\omega}$ = 0.12
10^4	--	--	33.52	49.09	0.294	0.410	0.127	0.181			PPR = 0
$2.5x10^4$	--	--	34.63	50.22	0.302	0.420	0.124	0.179			P_{min} = 4.4 Kips
$5x10^4$	--	--	34.74	50.47	0.306	0.423	0.125	0.178			P_{max} = 6.8 Kips
10^5	--	--	35.64	51.41	0.306	0.426	0.127	0.180			
$1.5x10^5$	--	--	36.68	52.66	0.314	0.432	0.120	0.171			
$2x10^5$	--	--	37.43	53.30	0.315	0.435	0.117	0.171			
$5x10^5$	--	--	38.01	53.69	0.349	0.474	0.121	0.174			
$7.5x10^5$	--	--	39.16	55.02	0.350	0.474	0.120	0.173			
10^6	--	--	41.36	57.12	0.357	0.475	0.123	0.174			

TABLE 10D (CONTINUED)

Number of Cycles N	Δf_{ps} at P_{min} & P_{max} (ksi)		fs at P_{min} & P_{max} (ksi)		Deflection at P_{min} and P_{max} (in)		Crack width at P_{min} & P_{max} (mm)		Curvature at P_{min} and P_{max} x 10^{-4} (rad/in)		Remarks
	min	max	min	max	min	max	W_{min}	W_{max}	min	max	
$1.5x10^6$	--	--	43.42	58.15	0.380	0.485	0.141	0.177			
$1.75x10^6$	--	--	39.96	54.41	0.383	0.486	0.134	0.167			Beam was loaded
$2x10^6$	--	--	43.90	58.59	0.384	0.490	0.142	0.176			statically to
$2.5x10^6$	--	--	43.51	57.91	0.388	0.493	0.139	0.174			failure at
$3x10^6$	--	--	45.63	60.20	0.392	0.497	0.150	0.184			$3x10^6$ cycles

TABLE 11D

Beam Designation: RD2
Type of Loading: Dynamic (cyclic)
f'_c at time of loading = 5870 Psi
Effective prestress, f_{pe} = ---

Stress range in the prestressing strand = $\Delta f_{ps(max)} - \Delta f_{ps(min)}$

Stress range in the reinforcing bars = $f_{s(max)} - f_{s(min)}$

Note: See Table 11S for more details.

Number of Cycles N	Δf_{ps} at P_{min} & P_{max} (ksi)		f_s at P_{min} & P_{max} (ksi)		Deflection at P_{min} and P_{max} (in)		Crack width at P_{min} & P_{max} (mm)		Curvature at P_{min} and P_{max} x 10^{-4} (rad/in)		Remarks
	min	max	min	max	min	max	W_{min}	W_{max}	min	max	
1	--	--	25.81	41.87	0.263	0.422	0.092	0.137			$\bar{\omega}$ = 0.20 PPR = 0 P_{min} = 7.27 Kips P_{max} = 10.8 Kips
2	--	--	31.06	42.59	0.312	0.430	0.105	0.137			
3	--	--	31.74	43.00	0.330	0.434	0.106	0.138			
10^4	--	--	32.82	45.04	0.350	0.455	0.108	0.135			
$2.5x10^4$	--	--	33.35	45.04	0.356	0.460	0.109	0.135			
$5x10^4$	--	--	33.51	45.53	0.360	0.464	0.110	0.135			
10^5	--	--	33.63	45.71	0.366	0.470	0.111	0.136			
$2x10^5$	--	--	33.93	46.11	0.375	0.477	0.111	0.136			
$5x10^5$	--	--	31.12	43.27	0.376	0.485	0.104	0.131			
$7.5x10^5$	--	--	32.31	44.23	0.387	0.492	0.107	0.141			
10^6	--	--	30.96	42.81	0.391	0.497	0.106	0.140			

TABLE 11D (CONTINUED)

Number of Cycles N	Δf_{ps} at P_{min} & P_{max} (ksi)		fs at P_{min} & P_{max} (ksi)		Deflection at P_{min} and P_{max} (in)		Crack width at P_{min} & P_{max} (mm)		Curvature at P_{min} and P_{max} x 10^{-4} (rad/in)		Remarks
	min	max	min	max	min	max	W_{min}	W_{max}	min	max	
$1.6x10^6$	--	--	29.32	41.76	0.402	0.505	0.104	0.138			
$2x10^6$	--	--	34.47	46.65	0.405	0.509	0.115	0.149			Beam was loaded
$2.3x10^6$	--	--	32.31	43.68	0.410	0.515	0.112	0.146			statically to
$2.5x10^6$	--	--	34.27	46.19	0.411	0.516	0.115	0.150			failure at
$3x10^6$	--	--	32.37	44.27	0.420	0.525	0.112	0.145			$5x10^6$ cycles
$3.5x10^6$	--	--	35.04	46.90	0.423	0.527	0.119	0.153			
$4x10^6$	--	--	32.51	43.97	0.430	0.534	0.118	0.152			
$4.5x10^6$	--	--	34.41	46.30	0.435	0.539	0.117	0.151			
$5x10^6$	--	--	34.93	46.89	0.440	0.540	0.117	0.151			

TABLE 12D

Beam Designation: RD3
Type of Loading: Dynamic (cyclic)
f'c at time of loading = 5553 Psi
Effective prestress, f_{pe} = ---

Stress range in the prestressing strand = $\Delta f_{ps(max)} - \Delta f_{ps(min)}$

Stress range in the reinforcing bars = $f_{s(max)} - f_{s(min)}$

Note: See Table 12S for more details.

Number of Cycles N	Δf_{ps} at P_{min} & P_{max} (ksi)		f_s at P_{min} & P_{max} (ksi)		Deflection at P_{min} and P_{max} (in)		Crack width at P_{min} & P_{max} (mm)		Curvature at P_{min} and P_{max} x 10^{-4} (rad/in)		Remarks
	min	max	min	max	min	max	W_{min}	W_{max}	min	max	
1	--	--	24.92	38.64	0.252	0.405	0.095	0.136	1.93	2.99	
2	--	--	28.43	39.12	0.314	0.411	0.106	0.139	2.23	3.02	$\bar{\omega}$ = 0.29
3	--	--	28.95	39.35	0.319	0.415	0.108	0.139	2.36	3.04	PPR = 0
2500	--	--	29.71	40.45	0.330	0.428	0.110	0.142	2.41	3.09	P_{min} = 10.0 Kips
10^4	--	--	30.19	40.74	0.334	0.433	0.113	0.143	2.43	3.12	P_{max} = 15.0 Kips
$5x10^4$	--	--	32.00	43.02	0.347	0.443	0.115	0.147	2.46	3.17	
10^5	--	--	33.03	43.96	0.352	0.447	0.118	0.150	2.50	3.20	
$2.5x10^5$	--	--	32.83	43.97	0.358	0.456	0.118	0.152	2.55	3.26	
$6x10^5$	--	--	29.18	39.50	0.369	0.467	0.102	0.136	2.57	3.28	
$7.5x10^5$	--	--	28.98	40.09	0.374	0.471	0.096	0.132	2.59	3.30	
$1.25x10^6$	--	--	28.56	39.80	0.382	0.479	0.093	0.129	2.63	3.35	

TABLE 12D (CONTINUED)

Number of Cycles N	Δf_{ps} at P_{min} & P_{max} (ksi)		fs at P_{min} & P_{max} (ksi)		Deflection at P_{min} and P_{max} (in)		Crack width at P_{min} & P_{max} (mm)		Curvature at P_{min} and P_{max} x 10^{-4} (rad/in)		Remarks
	min	max	min	max	min	max	W_{min}	W_{max}	min	max	
$1.5x10^6$	--	--	29.42	40.50	0.384	0.482	0.095	0.130	2.66	3.38	
$2x10^6$	--	--	27.37	38.28	0.389	0.487	0.088	0.123	2.68	3.40	Beam was loaded
$2.5x10^6$	--	--	28.27	39.50	0.394	0.492	0.089	0.125	2.71	3.43	statically to
$3x10^6$	--	--	28.53	39.61	0.396	0.495	0.091	0.125	2.74	3.45	failure at
$3.5x10^6$	--	--	29.82	41.00	0.400	0.498	0.095	0.130	2.76	3.48	$5x10^6$ cycles
$3.75x10^6$	--	--	30.77	41.92	0.401	0.499	0.099	0.133	2.78	3.50	
$4.25x10^6$	--	--	31.04	41.80	0.401	0.501	0.102	0.136	2.81	3.52	
$4.5x10^6$	--	--	32.10	43.09	0.402	0.502	0.103	0.139	2.81	3.54	
$5x10^6$	--	--	28.13	39.22	0.406	0.506	0.085	0.120	2.82	3.54	